Measurement of Energy-dependent Inclusive Muon Neutrino Charged-Current Cross Section at MicroBooNE

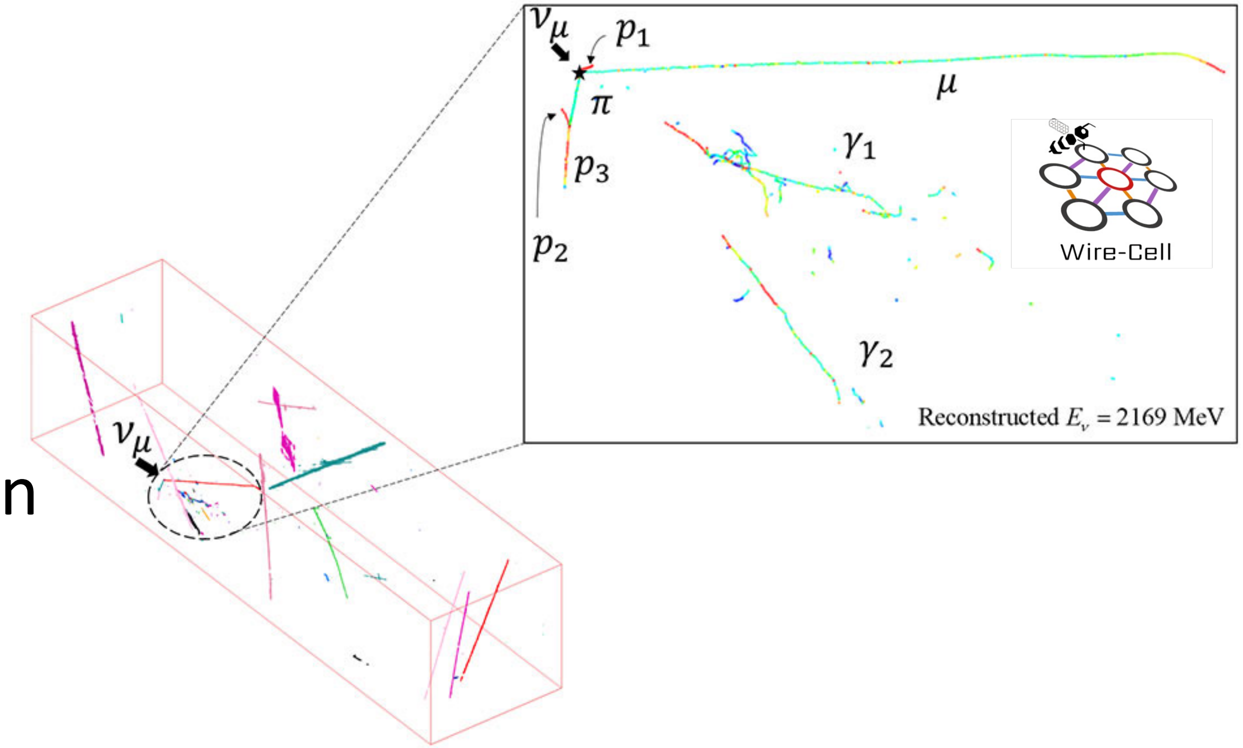

Wenqiang Gu (BNL)

On behalf of MicroBooNE collaboration

Fermilab　μBooNE　Brookhaven National Laboratory

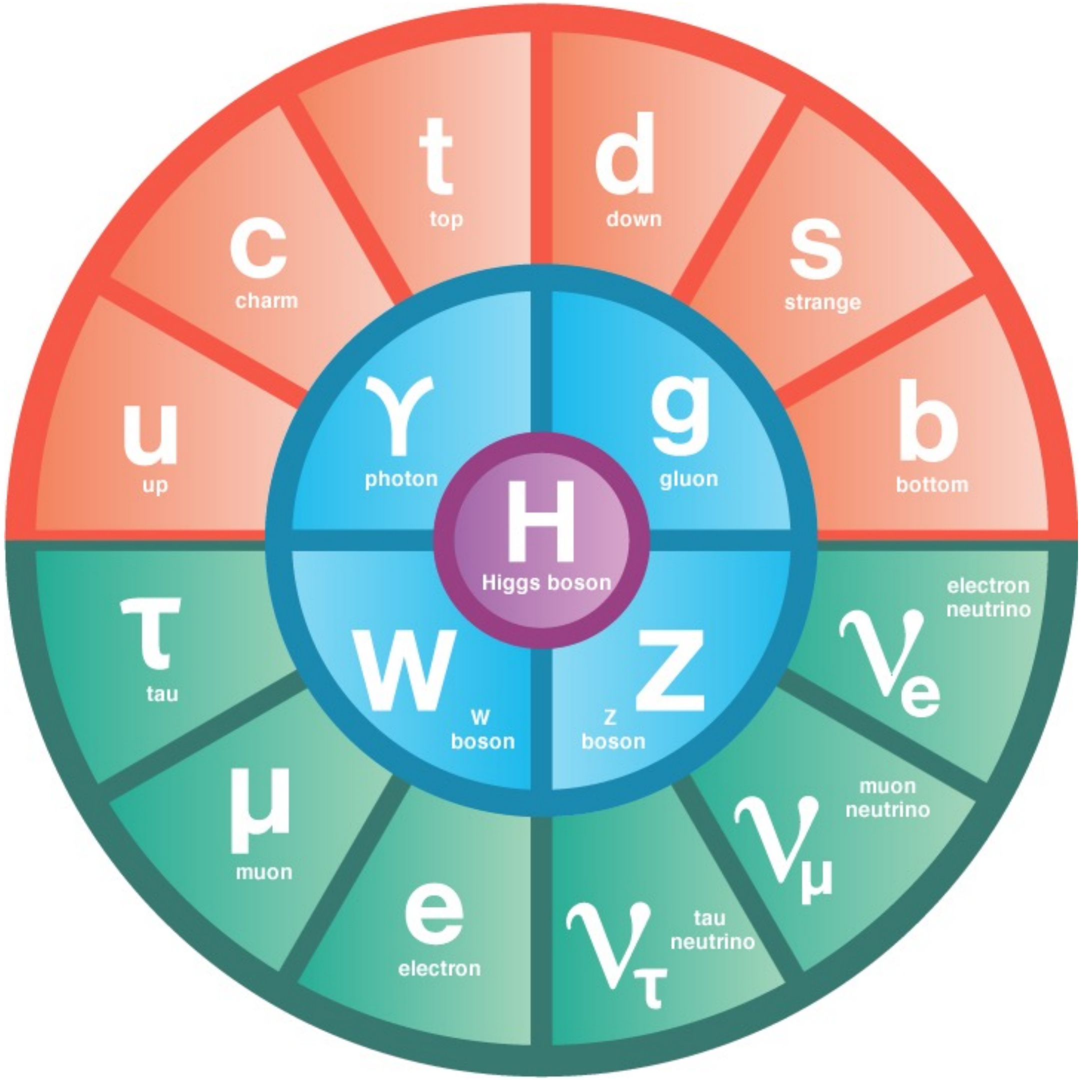

Neutrino Oscillation

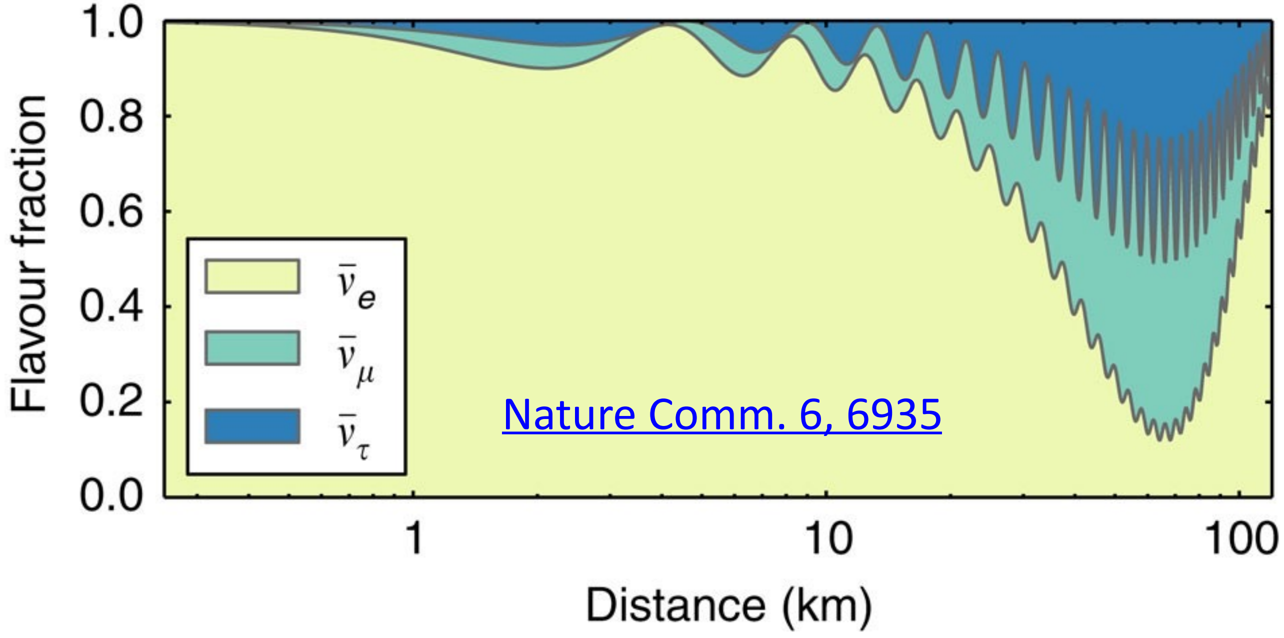

$$P(\nu_\alpha \rightarrow \nu_\beta)^* \sim \sin^2 2\theta \cdot \sin^2\left(1.27 \cdot \Delta m_{21}^2 \left[eV^2\right] \frac{L[km]}{E_\nu [GeV]}\right)$$

* Two neutrino flavor, for simplicity

Neutrino oscillation experiments have provided the first evidence for physics beyond the Standard Model of particle physics

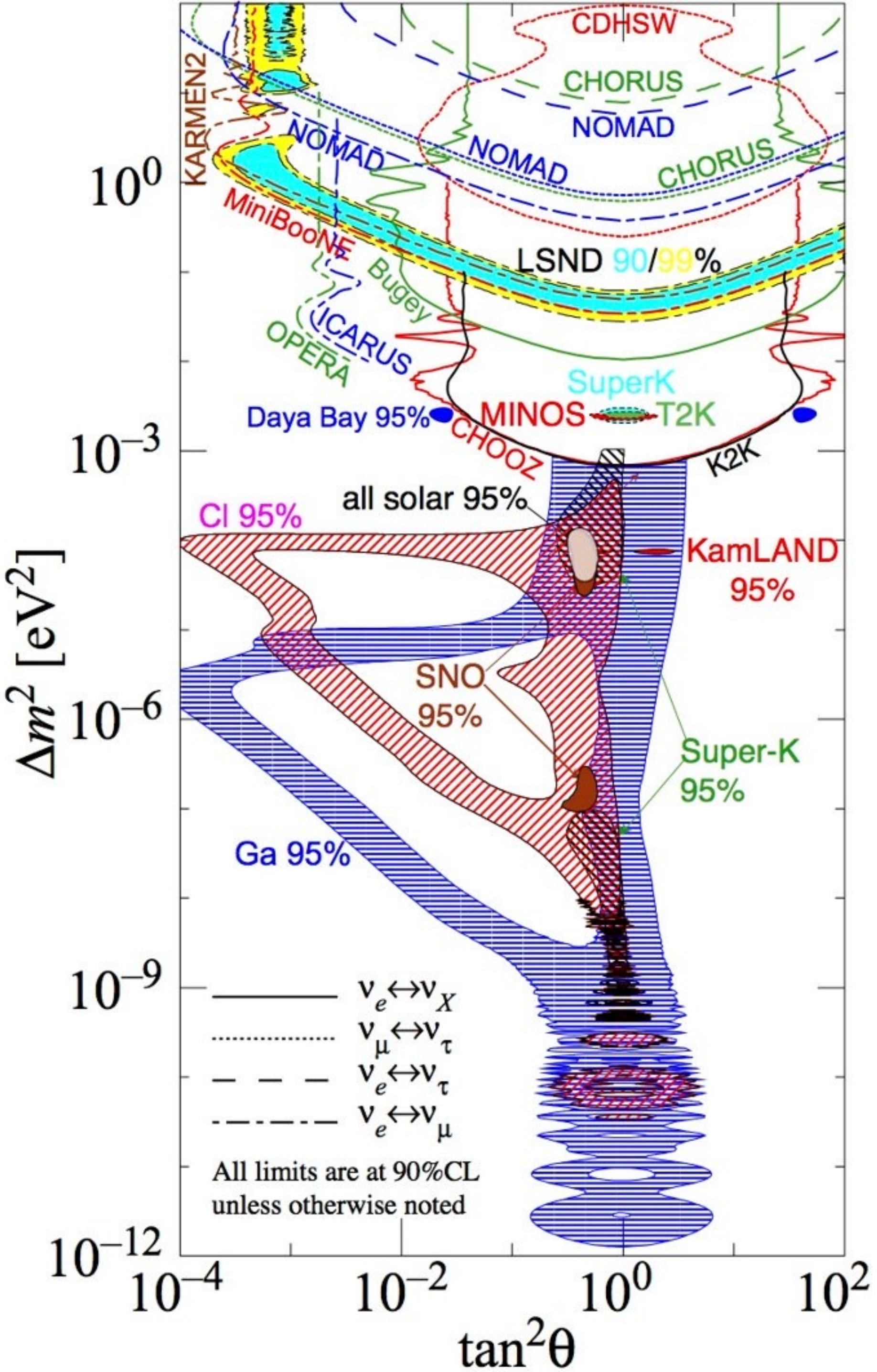

Neutrino Oscillation Experiments

- > 50 years
- > 30 experiments
- > Phase space over tens of orders of magnitude

Courtesy: Hitoshi Murayama

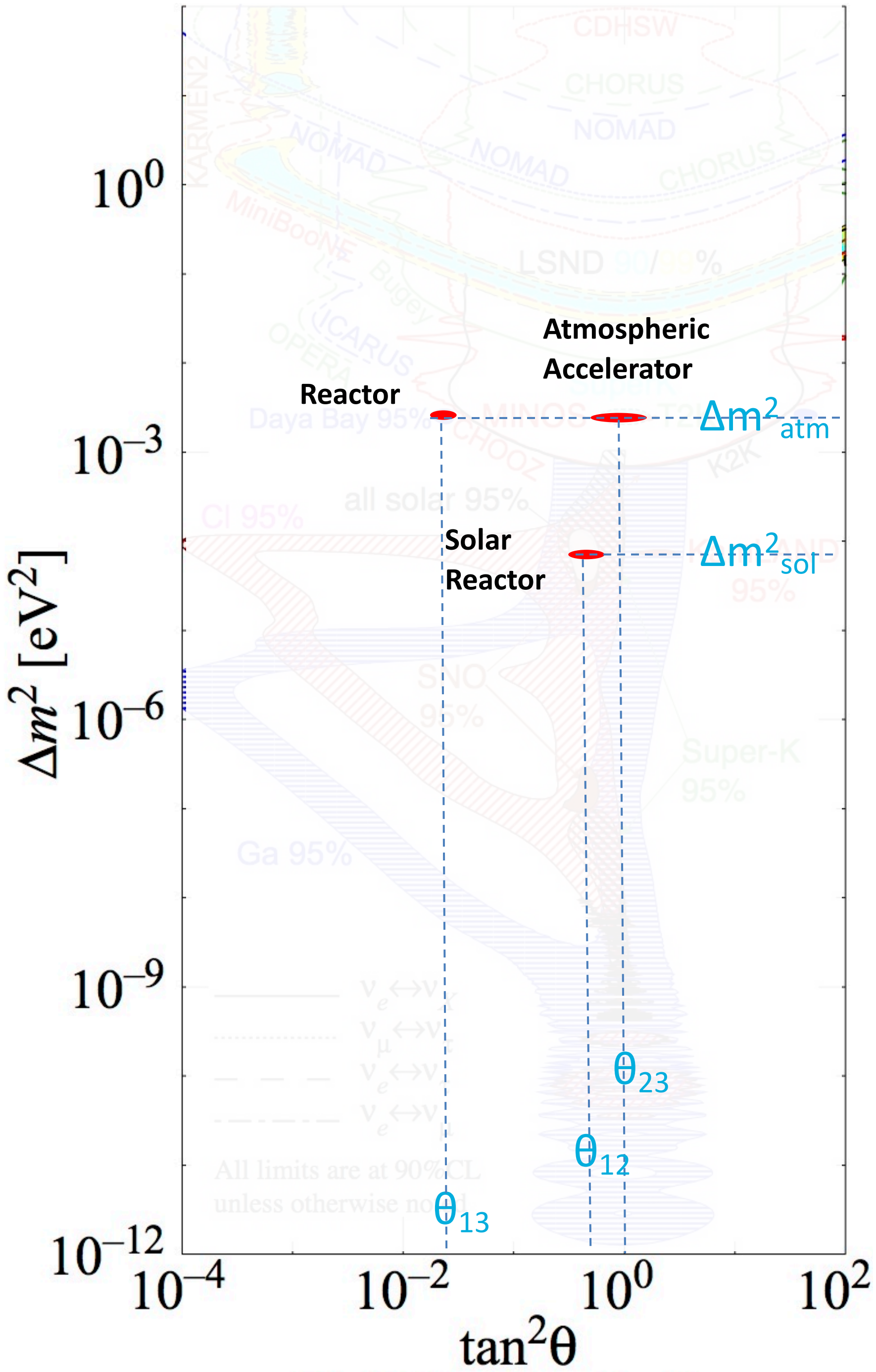

Three-ν Paradigm

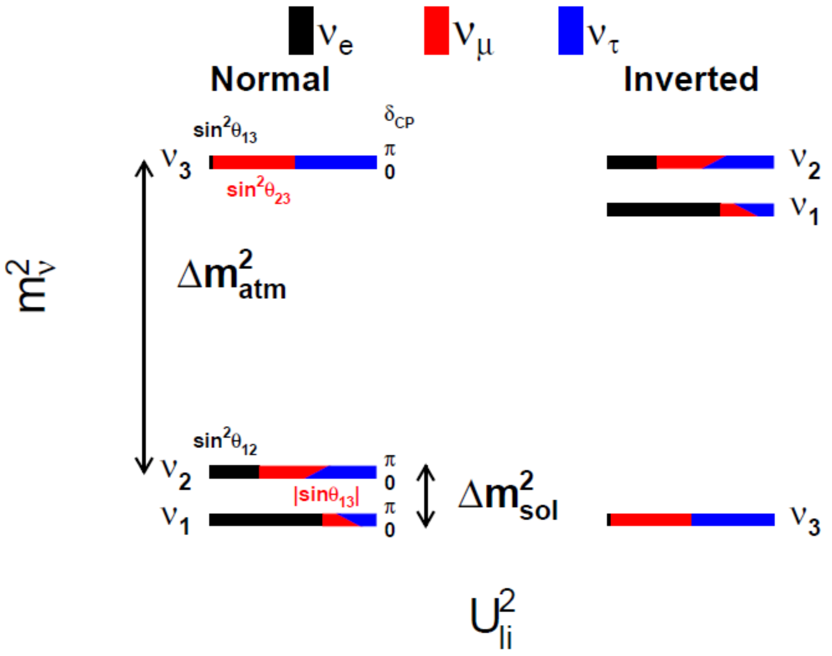

Unknowns: CP phase? Normal or inverted mass ordering? …

2015 Nobel Prize
Takaaki Kajita &
Arthur B. McDonald

Quests for CP Phase and Neutrino Mass Ordering

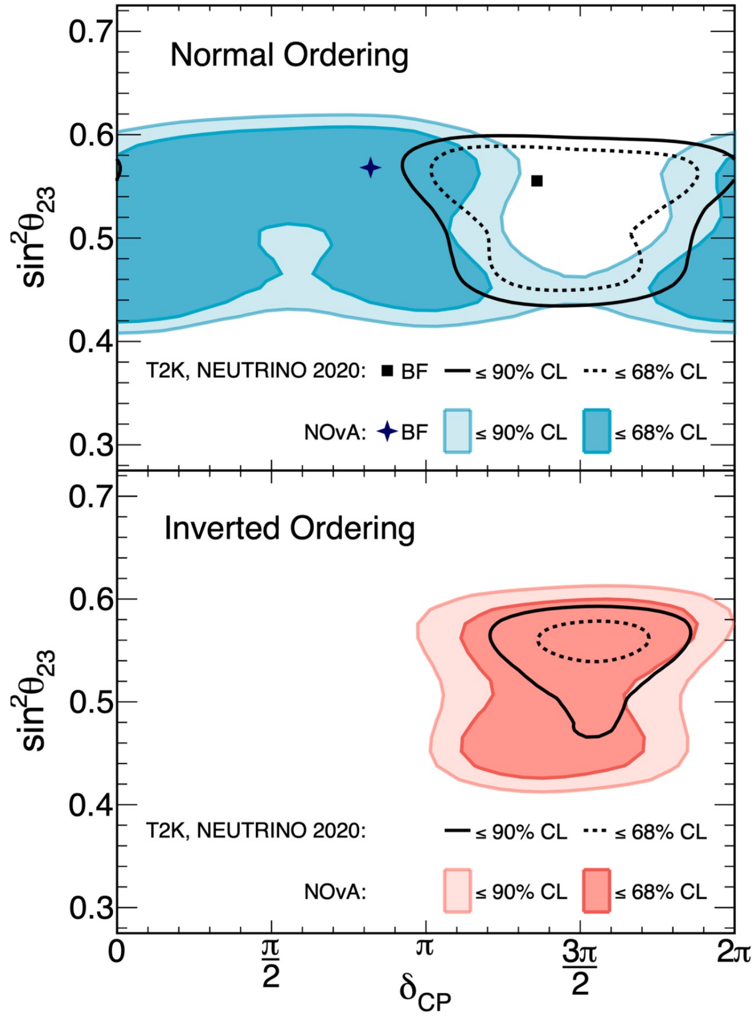

[Jeff Hartnell (Neutrino 2022)]

Accelerator neutrino experiments:

NOvA → **DUNE**

T2K → **Hyper-K**

Non-accelerator experiments:

Also JUNO, KM3NeT, …

CP violation sensitivity

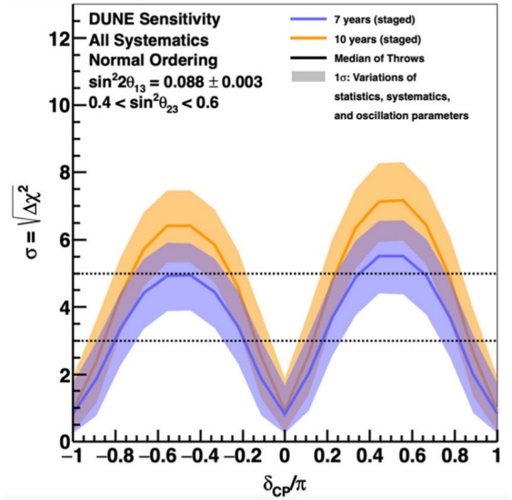

[Eur.Phys.J.C 80 (2020) 10, 978]

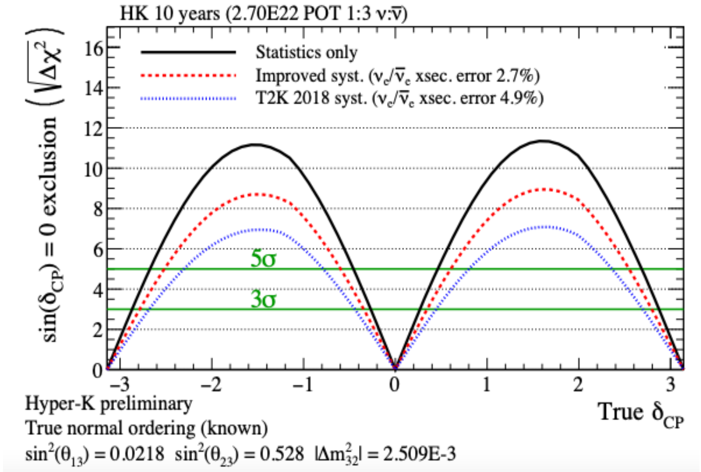

[Jeanne Wilson (Neutrino 2022)]

Deep Underground Neutrino Experiment (DUNE)

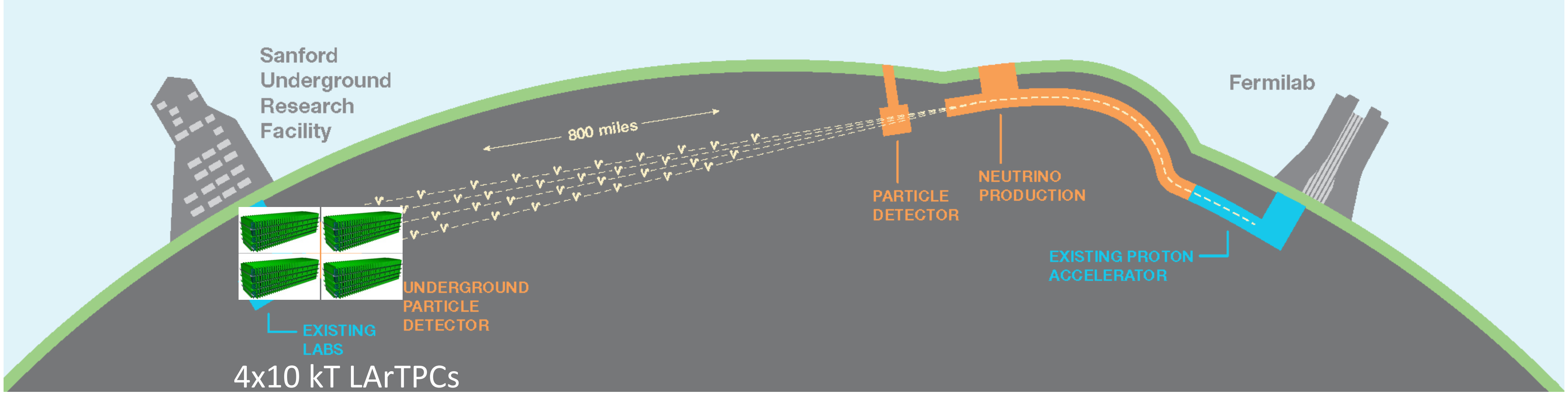

- Search for new CP violation and determine the mass ordering through precision measurement of $\boldsymbol{\nu_\mu(\bar{\nu}_\mu) \rightarrow \nu_e(\bar{\nu}_e)}$ **oscillation**
  - Also search for proton decay and detection of supernova neutrinos
- Four 10 kT LArTPC detectors (each 20 x 20 x 70 m^3)

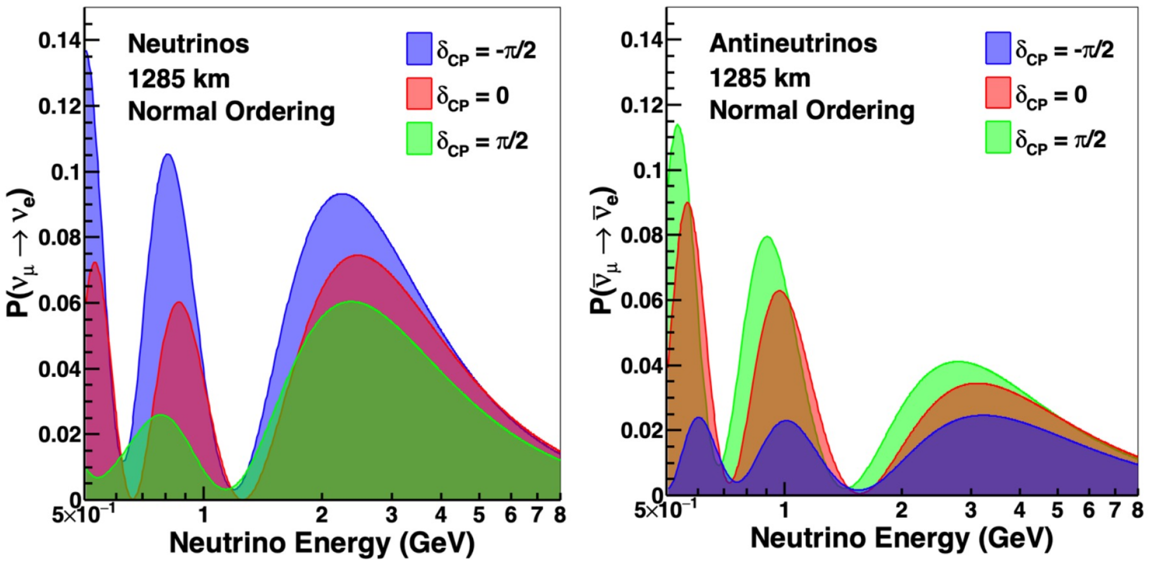

EPJC 80, 978

Systematic Budget

- Cross section uncertainty is one major systematic for accelerator oscillation experiments

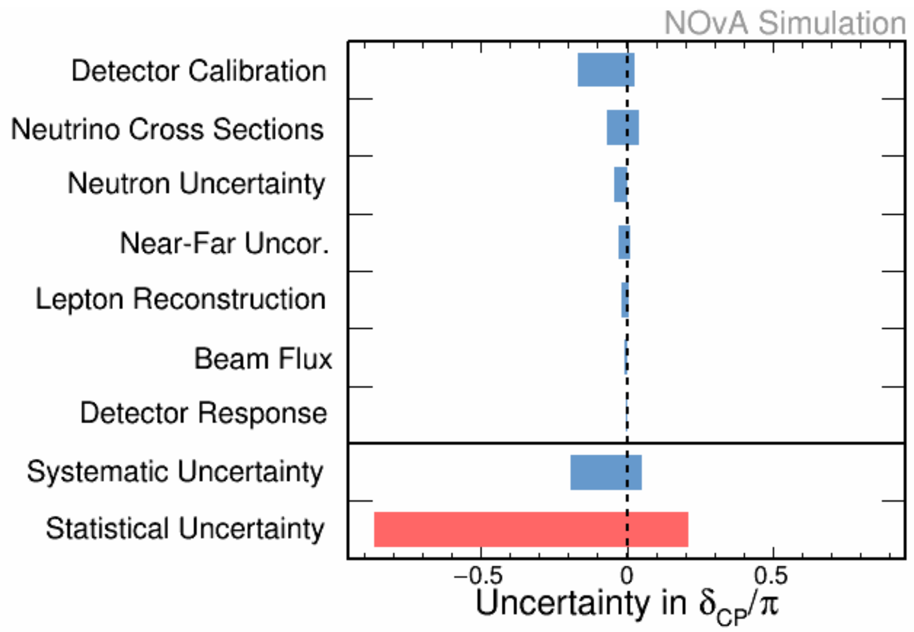

$$\frac{N^{far}(E_{reco}) = \int \Phi(E_\nu, L) \times \sigma(E_\nu) \times \epsilon(E_\nu) \times \mathbf{D}(E_\nu \rightarrow E_{reco}) dE_\nu}{N^{near}(E_{reco}) = \int \Phi(E_\nu, 0) \times \sigma(E_\nu) \times \epsilon(E_\nu) \times \mathbf{D}(E_\nu \rightarrow E_{reco}) dE_\nu}$$

2108.08219 [hep-ex]

- It's important to understand
  - Energy dependence of the inclusive cross section: $\boldsymbol{\sigma(E_\nu)}$
  - Mapping: $\mathbf{D}(\boldsymbol{E_\nu} \rightarrow \boldsymbol{E_{reco}})$

} focus of this talk

Charged-Current (CC) Interactions

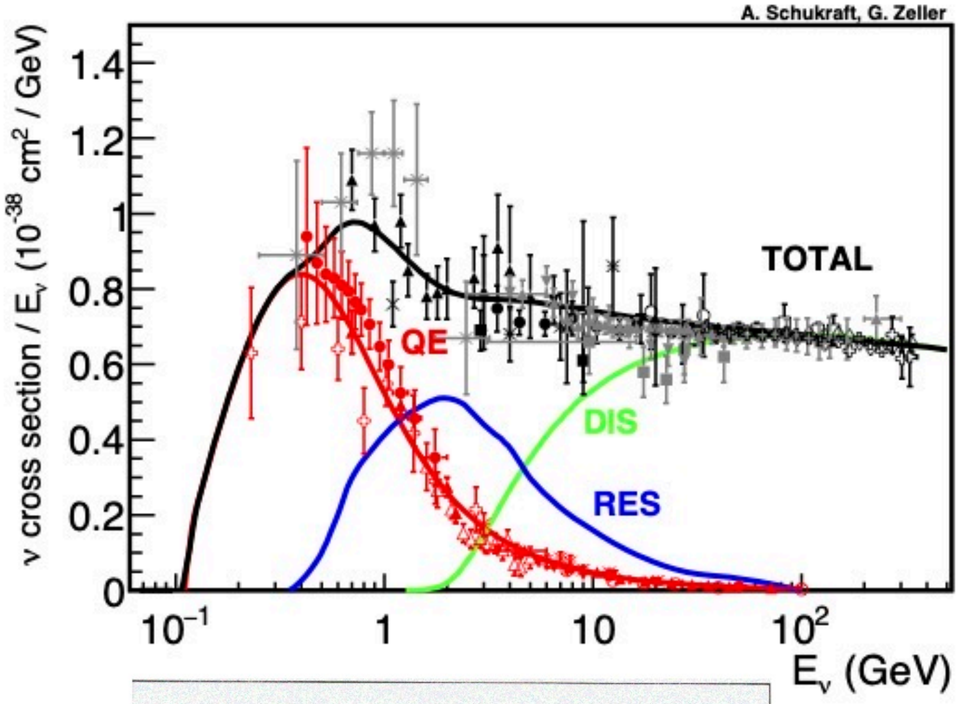

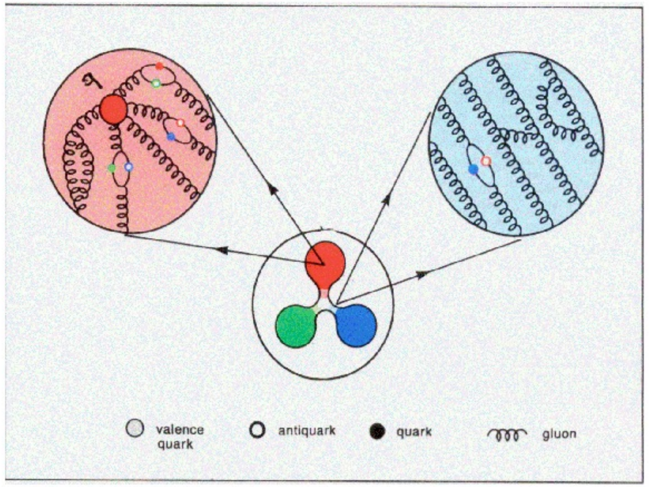

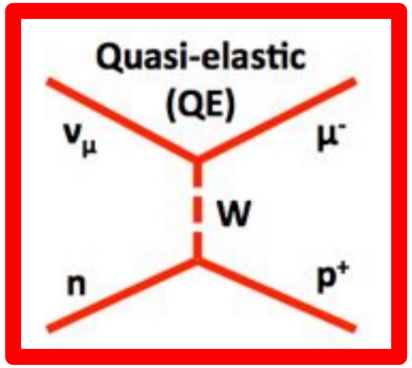

Scattering off single nucleon

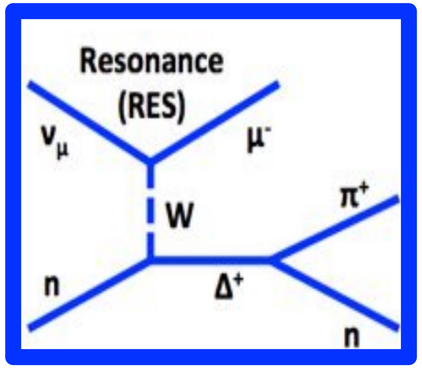

Inelastic scattering: Excites the nucleon

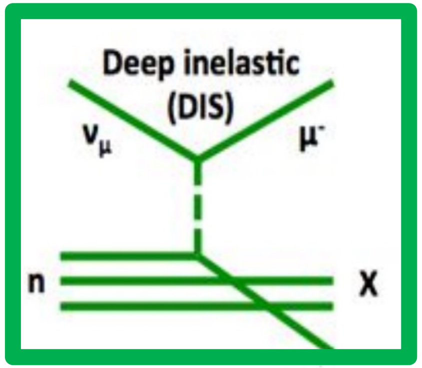

Breaks up nucleon

- Charged-current neutrino-nucleus interaction, allowing to tag neutrino flavor, is the major channel for oscillation experiments
- Understanding the QCD in the confinement region is at the frontier of nuclear physics research

Complicated Nuclear Effects

- Even the “simple” QE scattering is not so simple (2p2h, RPA, etc.)
  - Short range nucleon-nucleon correlations
  - 2p2h (medium range)
  - Long range nucleon-nucleon correlations: suppression on low Q^2
- Also, Final State Interactions (FSI)

Lack of a first-principle description of the neutrino-nucleus interaction → measurements and development of event generators are important

GiBUU NuWro GENIE NEUT

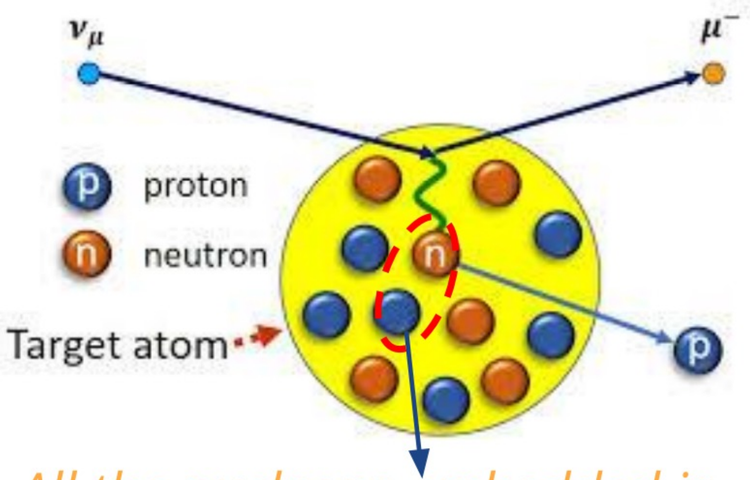

All the nucleons embedded in nucleus

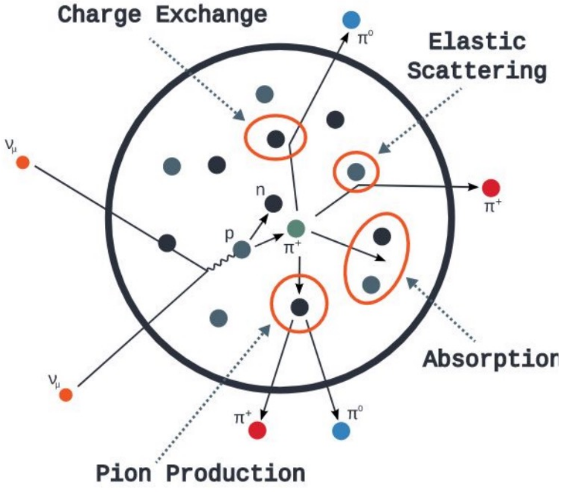

FSI

Credit: T. Golan

In the Old Days

- Historical accelerator-based neutrino experiments often reported E_ν-dependent cross sections: $\boldsymbol{\sigma(E_\nu)}$

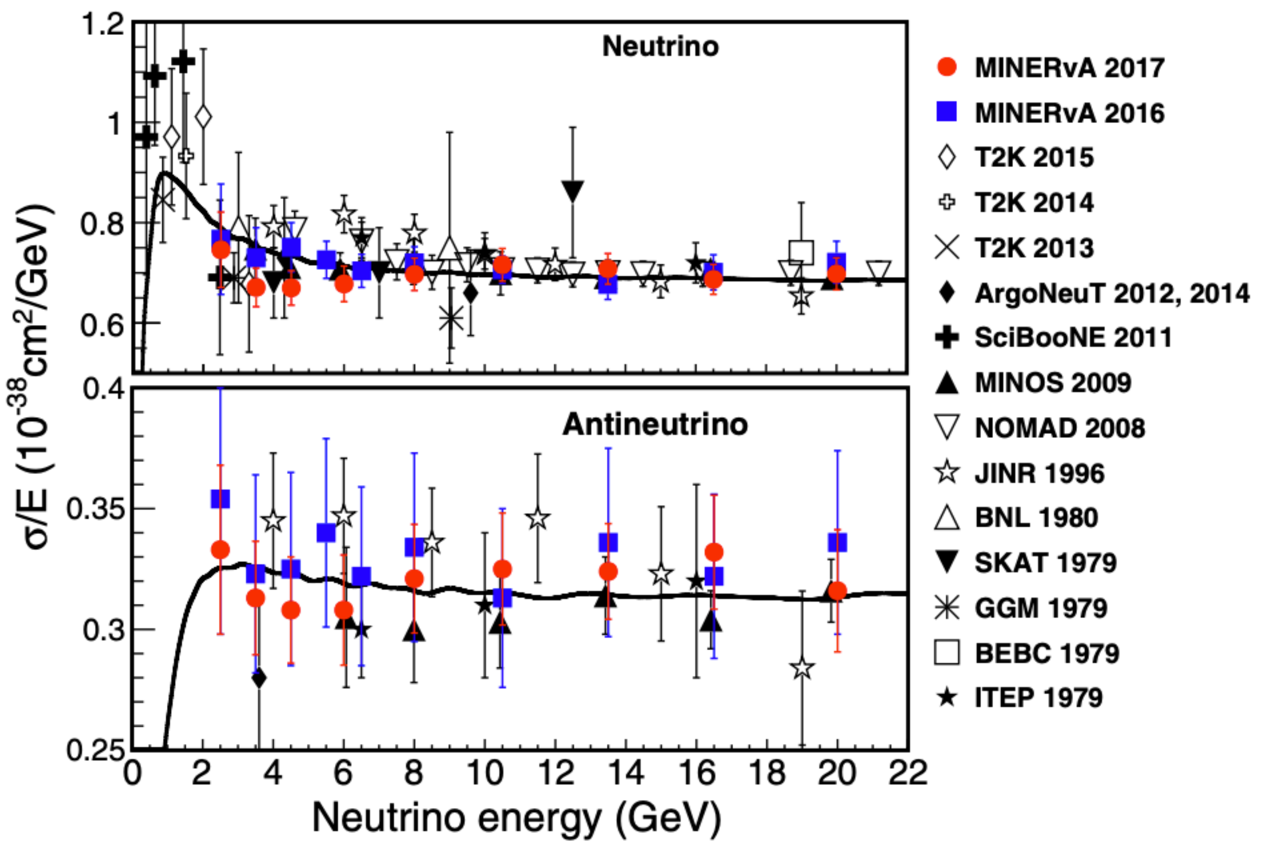

Phys. Rev. D **95**, 072009

Recent Years

- "Industry standard" now ≈ measure flux-averaged <dσ/dx> as a function of (directly visible) final state particle kinematics

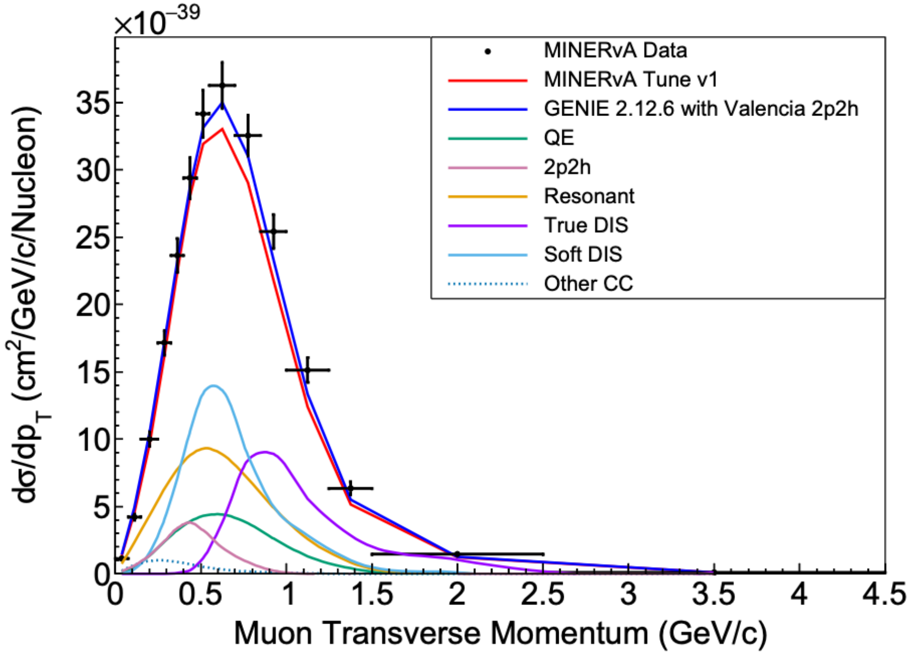

MINERvA: Phys. Rev. D **104**, 092007 (2021)

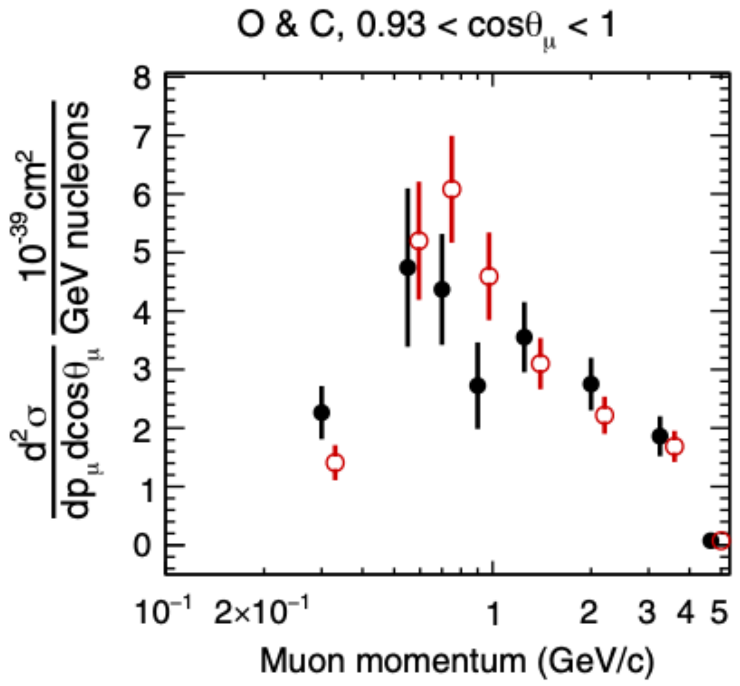

T2K CC0π: Phys. Rev. D **101**, 112004 (2020)

Why Is There a Shift in the "Industry Standard"?

- Do not trust $\mathbf{D}(E_\nu \rightarrow E_{reco})$!

$$N^{near}(E_{reco}) = \int \Phi(E_\nu, 0) \times \boldsymbol{\sigma}(E_\nu) \times \epsilon(E_\nu) \times \mathbf{D}(E_\nu \rightarrow E_{reco})\, dE_\nu$$

- $\mathbf{D}(E_\nu \rightarrow E_{reco})$ depends on the invisible final state particles, broadband beam flux ⇒ no mono-energetic beam to calibrate such response

- However, the inclusive cross section $\boldsymbol{\sigma}(E_\nu)$ is essential for oscillation search

O. Benhar: "The interpretation of the nuclear cross sections measured using accelerator neutrino beams involve **severe difficulties**, arising primarily from the **average over the incoming neutrino flux**. The broad energy distribution of the beam particles hampers the determination of the **energy transfer to the nuclear target**, the knowledge of which is needed to pin down the dominant reaction mechanism."

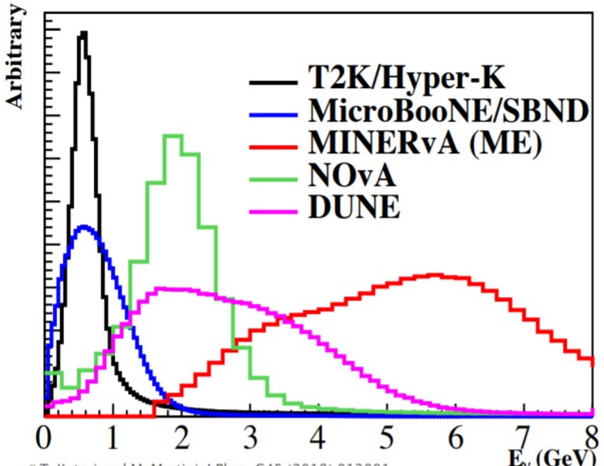

T. Katori and M. Martini, J.Phys. G45 (2018) 013001

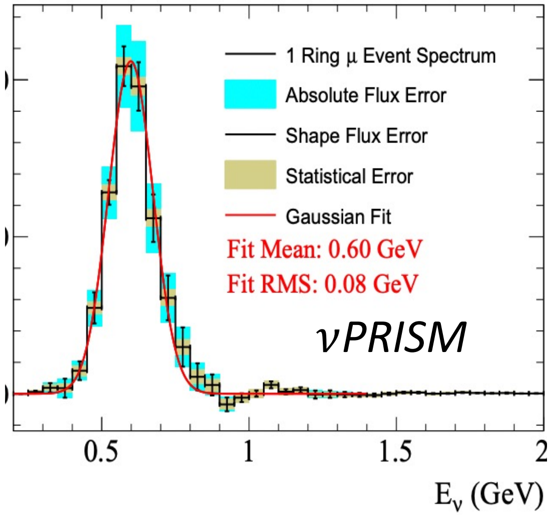

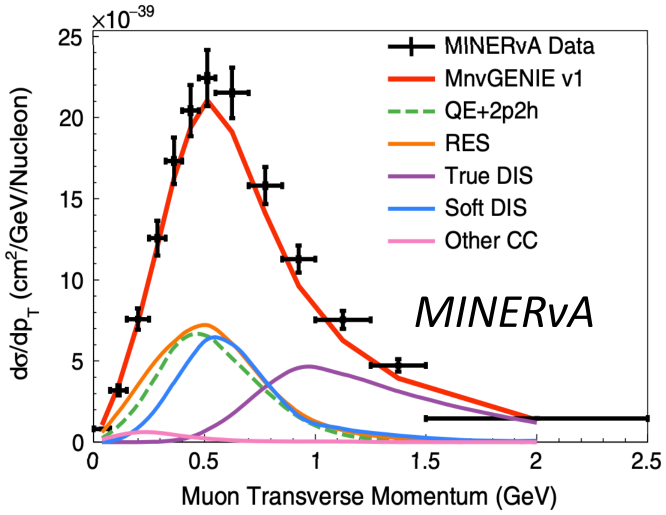

PRD **101**, 112007

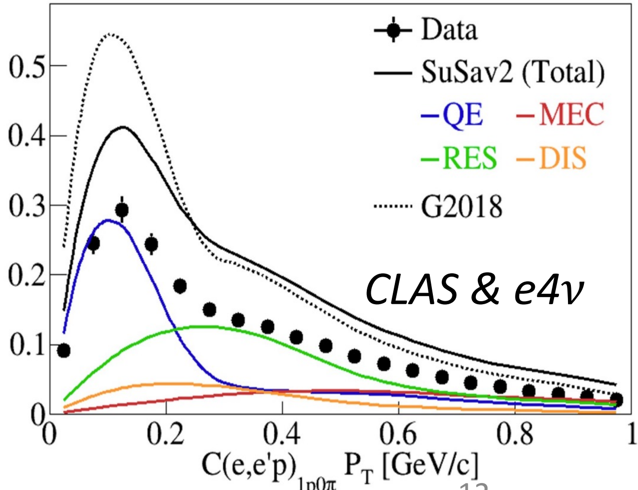

Nature **599**, 565 (2021)

Inclusive ν_μCC Cross Section on Argon at MicroBooNE

Validate $\mathbf{D}(E_\nu \ \rightarrow E_{reco})$

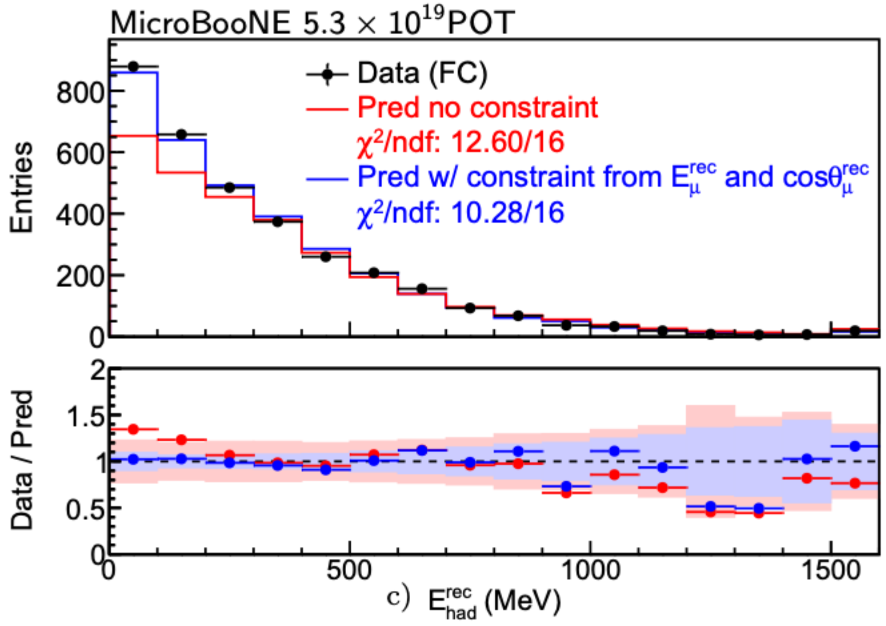

Measure $\sigma(E_\nu)$

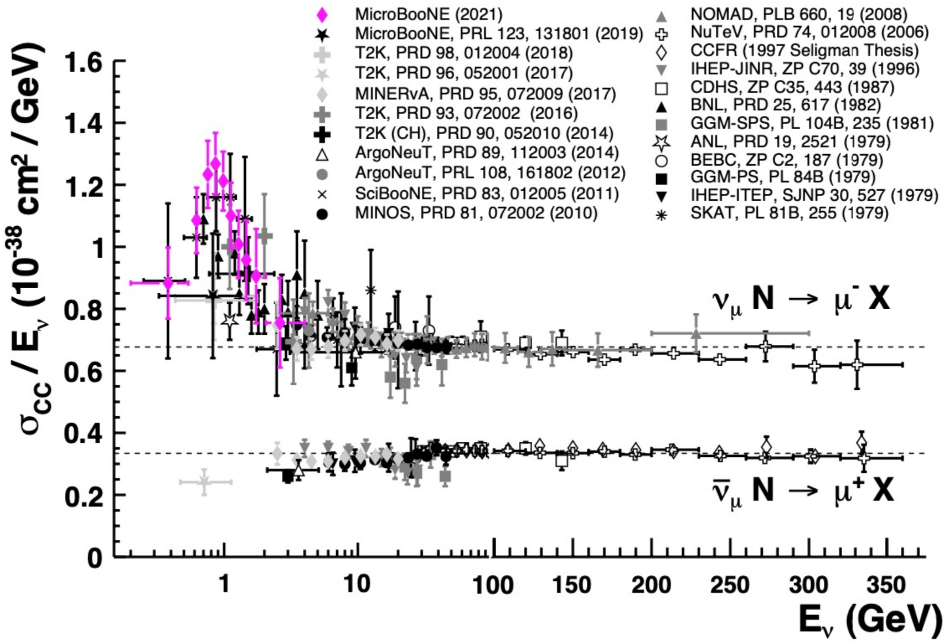

- Good basis for the study of various exclusive interaction processes
- Important for improving ν-Ar cross-section model in DUNE


201 collaborators, 36 institutions, 5 countries
MicroBooNE collaboration @ 2022

Booster Neutrino Beamline

BNB @ MicroBooNE

Mean Neutrino Energy 0.8 GeV

Over 99% $\nu_\mu/\bar{\nu}_\mu$

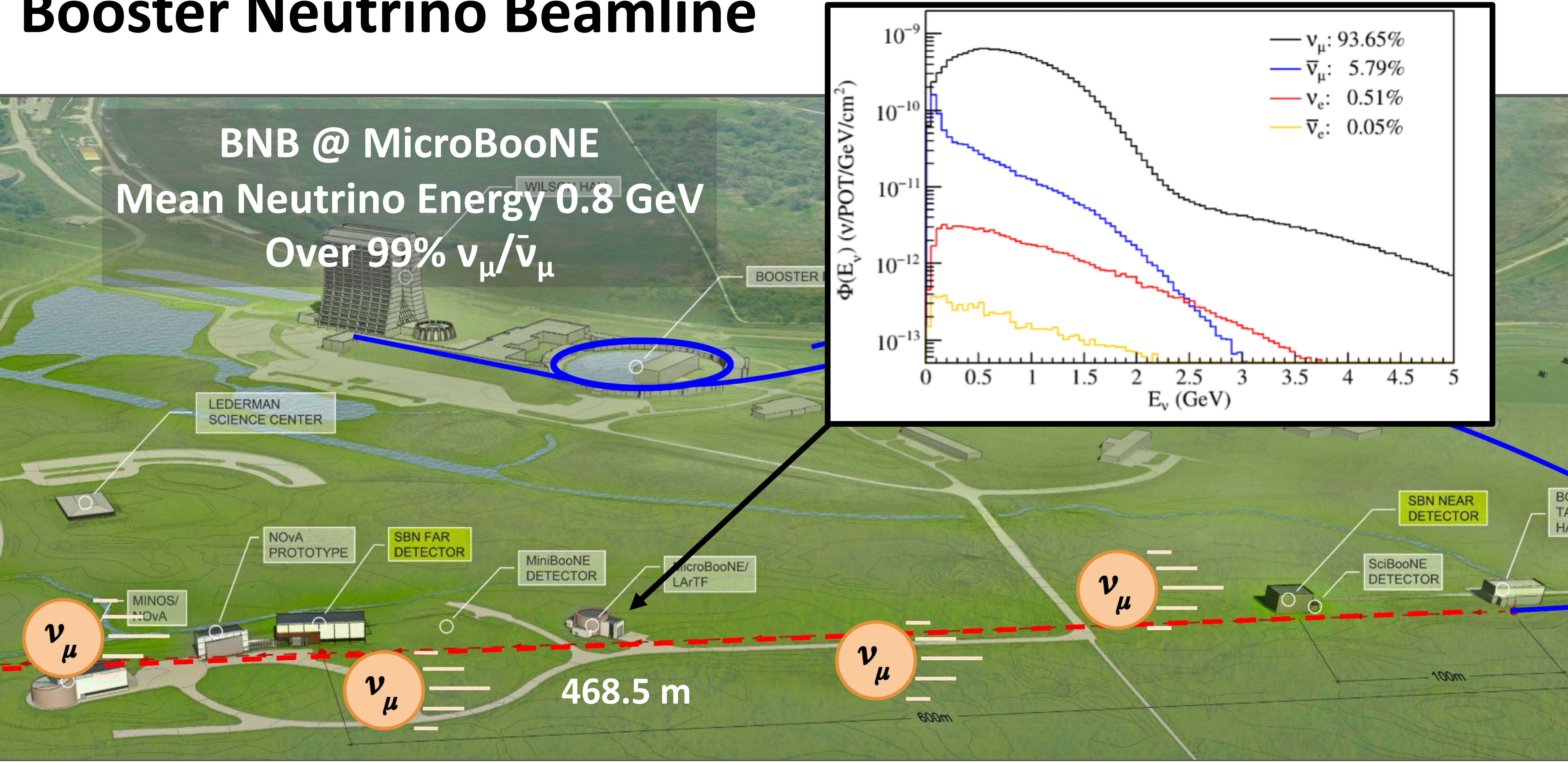

MicroBooNE Detector: An 85-tonne LArTPC

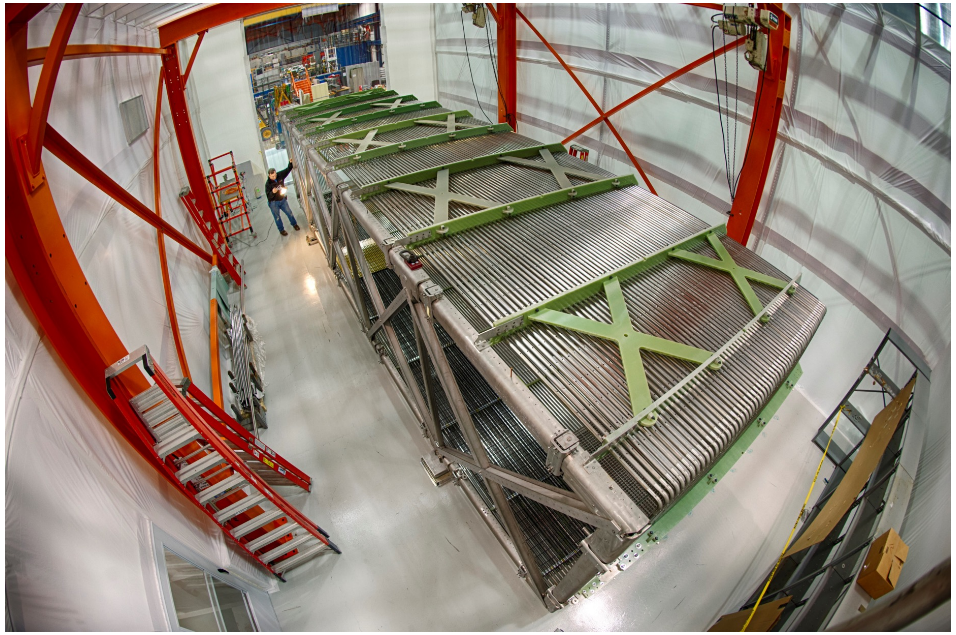

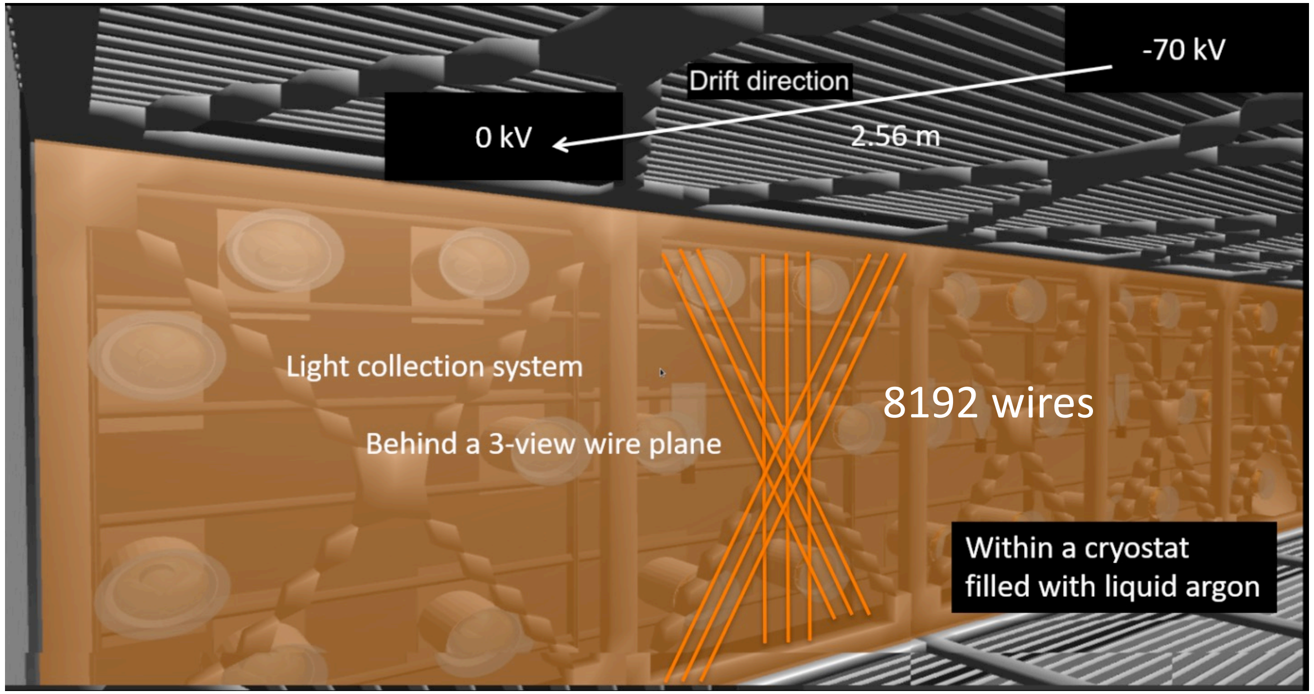

Principle of Single-Phase Liquid Argon Time Projection Chamber (LArTPC)

- ~mm scale position resolution with multiple 1D wire readouts
- Particle identification (PID) with energy depositions and topologies

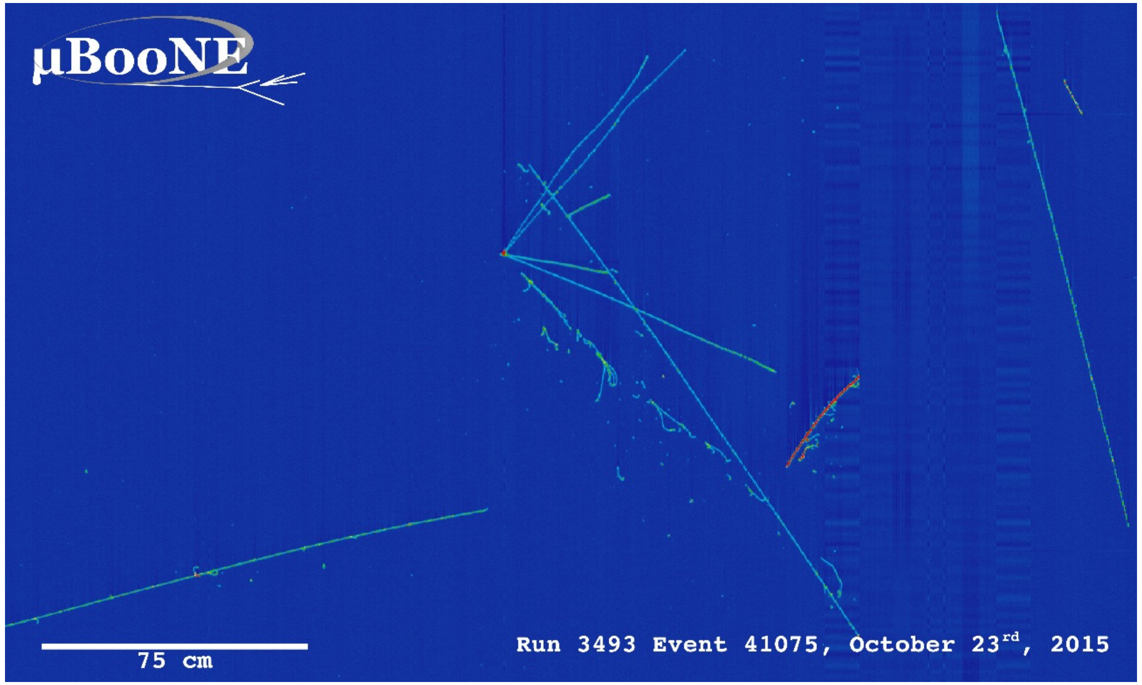

Made by Bo Yu (BNL)

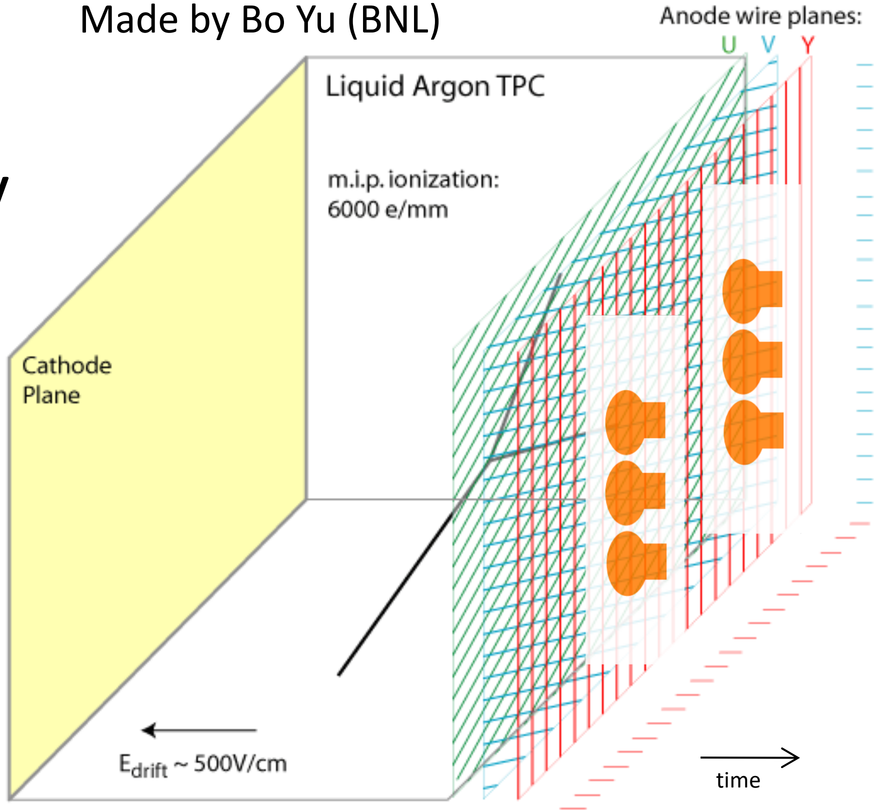

Drift velocity 1.6 km/s → several ms drift time

Evolution of LArTPC Programs in the US

- MicroBooNE is the critical path towards next generation LArTPC programs

* not a complete list

Yale TPC (2007)

Material Test Stand (2008)

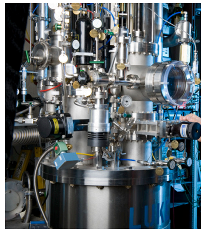

ArgoNeuT (2008)

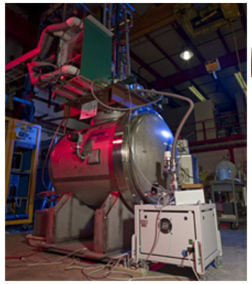

MicroBooNE (2015)

SBN (2015 - ?)

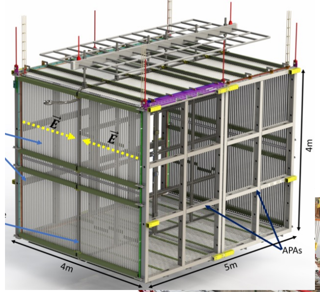

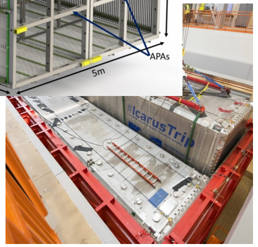

DUNE FD (202?)

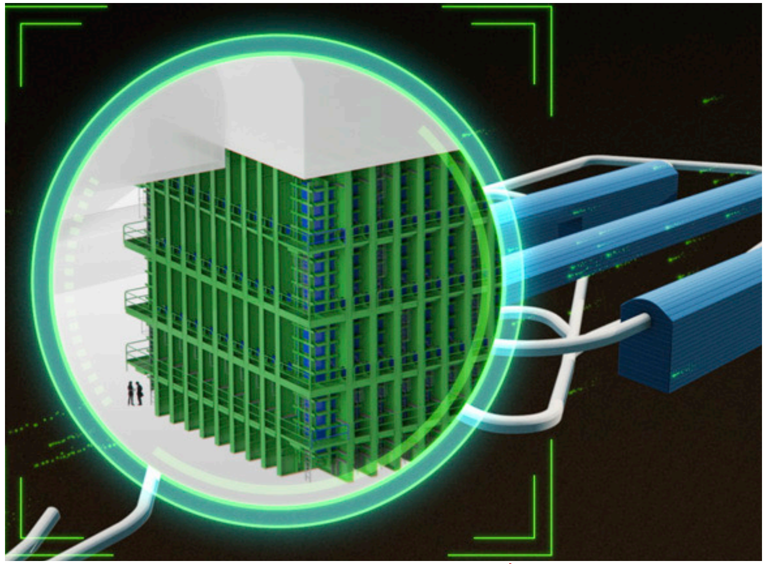

R&D → **Physics**

Hardware & software

LArTPC design, cryostat, cold electronics ...

Noise filtering, TPC signal processing, detector physics, event reconstruction

Precision physics

Low energy excess

ν-Ar interactions

Beyond-SM physics

Even more physics

ν oscillation (mass ordering, CP violation)

Nucleon decay, supernova, …

MicroBooNE Science Output

2017 | 2018 | 2019 | 2020 | 2021 | 2022

- Strong track record of publications
  - >40 papers
    - ~1/2 JINST, ~1/2 Phys Rev, EPJC
  - >70 public notes
    - Sharing with the community as we go

Observation of radon mitigation in MicroBooNE by a liquid argon filtration system
Cosmic ray muon clustering for the MicroBooNE liquid argon time projection chamber using sMask-RCNN
Novel approach for evaluating detector-related uncertainties in a LArTPC using MicroBooNE data
First measurement of energy-dependent inclusive muon neutrino charged-current cross sections on argon with the MicroBooNE detector
Search for an anomalous excess of inclusive charged-current ν_e interactions without pions in the final state with the MicroBooNE experiment
Search for an anomalous excess of charged-current quasi-elastic ve interactions with the MicroBooNE experiment using deep-learning-based reconstruction
New theory-driven GENIE tune for MicroBooNE
Search for an anomalous excess of inclusive charged-current ν_e interactions in the MicroBooNE experiment using Wire-Cell reconstruction
Search for an excess of electron neutrino interactions in MicroBooNE using multiple final state topologies
Wire-Cell 3D pattern recognition techniques for neutrino event reconstruction in large LArTPCs
Electromagnetic shower reconstruction and energy validation with Michel electrons and π^0 samples for the deep-learning-based analyses in MicroBooNE
Search for neutrino-induced NC Δ radiative decay in MicroBooNE and a first test of the MiniBooNE low-energy excess under a single-photon hypothesis
First measurement of inclusive electron-neutrino and antineutrino charged current differential cross sections in charged lepton energy on argon in MicroBooNE
Calorimetric classification of track-like signatures in liquid argon TPCs using MicroBooNE data
Search for a Higgs Portal Scalar Decaying to Electron-Positron Pairs in the MicroBooNE Detector
Measurement of the Longitudinal Diffusion of Ionization Electrons in the Detector
Cosmic Ray Background Rejection with Wire-Cell LAr TPC Event Reconstruction in the MicroBooNE Detector
Measurement of the Flux-Averaged Inclusive Charged Current Electron Neutrino and Antineutrino Cross Section on Argon using the NuMI Beam in MicroBooNE
Measurement of the Atmospheric Muon Rate with the MicroBooNE Liquid Argon TPC
Semantic Segmentation with a Sparse Convolutional Neural Network for Event Reconstruction in MicroBooNE
High-performance Generic Neutrino Detection in a LAr TPC near the Earth's Surface with the MicroBooNE Detector
Neutrino Event Selection in the MicroBooNE LAr TPC using Wire-Cell 3D Imaging, Clustering, and Charge-Light Matching
A Convolutional Neural Network for Multiple Particle Identification in the MicroBooNE Liquid Argon Time Projection Chamber
Vertex-Finding and Reconstruction of Contained Two-track Neutrino Events in the MicroBooNE Detector
The Continuous Readout Stream of the MicroBooNE Liquid Argon Time Projection Chamber for Detection of Supernova Burst Neutrinos
Measurement of Differential Cross Sections for Muon Neutrino CC Interactions on Argon with Protons and No Pions in the Final State
Measurement of Space Charge Effects in the MicroBooNE LAr TPC Using Cosmic Muons
First Measurement of Differential Charged Current Quasi-Elastic-Like Muon Neutrino Argon Scattering Cross Sections with the MicroBooNE Detector
Search for heavy neutral leptons decaying into muon-pion pairs in the MicroBooNE detector
Reconstruction and Measurement of O(100) MeV Electromagnetic Activity from Neutral Pion to Gamma Gamma Decays in the MicroBooNE LArTPC
A Method to Determine the Electric Field of Liquid Argon Time Projection Chambers Using a UV Laser System and its Application in MicroBooNE
Calibration of the Charge and Energy Response of the MicroBooNE Liquid Argon Time Projection Chamber Using Muons and Protons
First Measurement of Inclusive Muon Neutrino Charged Current Differential Cross Sections on Argon at Enu ~0.8 GeV with the MicroBooNE Detector
Design and Construction of the MicroBooNE Cosmic Ray Tagger System
Rejecting Cosmic Background for Exclusive Neutrino Interaction Studies with Liquid Argon TPCs: A Case Study with the MicroBooNE Detector
First Measurement of Muon Neutrino Charged Current Neutral Pion Production on Argon with the MicroBooNE detector
A Deep Neural Network for Pixel-Level Electromagnetic Particle Identification in the MicroBooNE Liquid Argon Time Projection Chamber
Comparison of Muon-Neutrino-Argon Multiplicity Distributions Observed by MicroBooNE to GENIE Model Predictions
Ionization Electron Signal Processing in Single Phase LArTPCs II: Data/Simulation Comparison and Performance in MicroBooNE
Ionization Electron Signal Processing in Single Phase LArTPCs I: Algorithm Description and Quantitative Evaluation with MicroBooNE Simulation
The Pandora Multi-Algorithm Approach to Automated Pattern Recognition of Cosmic Ray Muon and Neutrino Events in the MicroBooNE Detector
Measurement of Cosmic Ray Reconstruction Efficiencies in the MicroBooNE LAr TPC Using a Small External Cosmic Ray Counter
Noise Characterization and Filtering in the MicroBooNE Liquid Argon TPC
Michel Electron Reconstruction Using Cosmic Ray Data from the MicroBooNE LAr TPC
Determination of Muon Momentum in the MicroBooNE LAr TPC Using an Improved Model of Multiple Coulomb Scattering
Convolutional Neural Networks Applied to Neutrino Events in a Liquid Argon Time Projection Chamber
Design and Construction of the MicroBooNE Detector

- https://microboone.fnal.gov/documents-publications/
- https://microboone.fnal.gov/public-notes/

Highlights of MicroBooNE's Cross Section Results (Flux-Avg.)

PRL **123**, 131801 (2019)

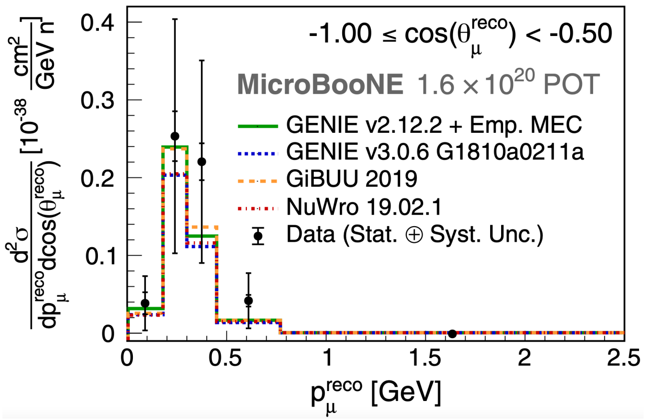

PRD **104**, 052002 (2021)

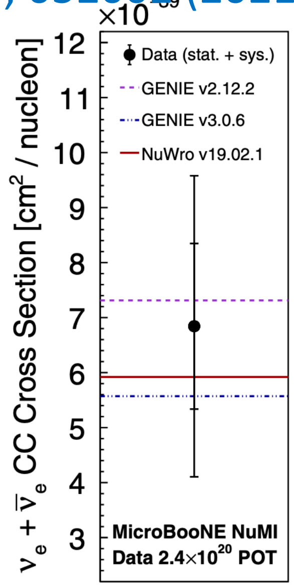

PRD **99**, 091102 (2019)

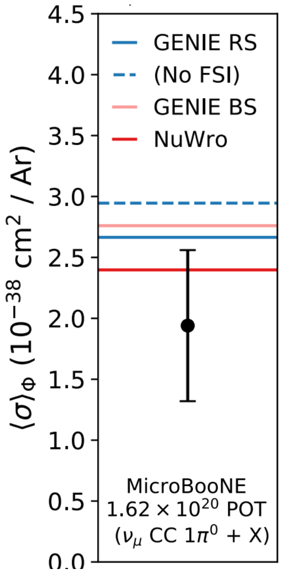

PRL **125**, 201803 (2020)

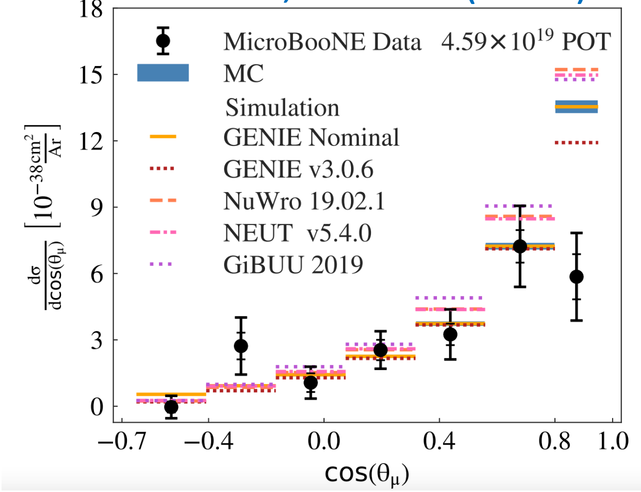

PRD **102**, 112013 (2020)

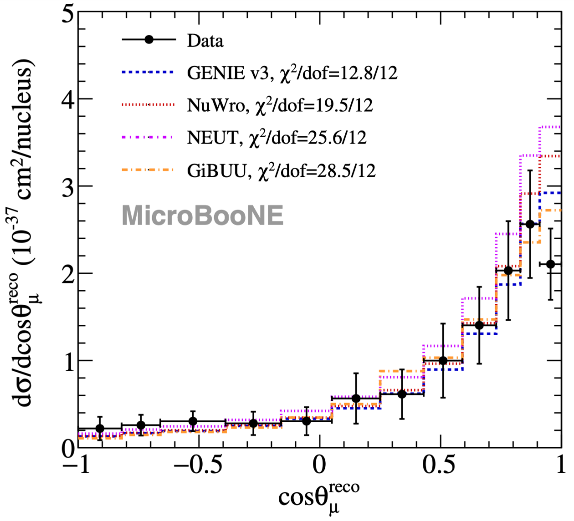

ν_μ CC inclusive

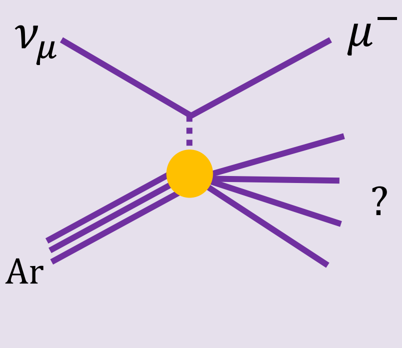

$\nu_e(\bar{\nu}_e)$ CC inclusive

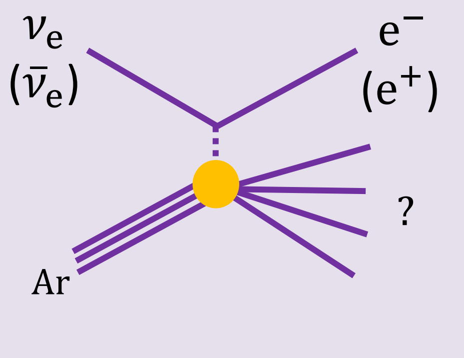

CC $1\pi^0$X

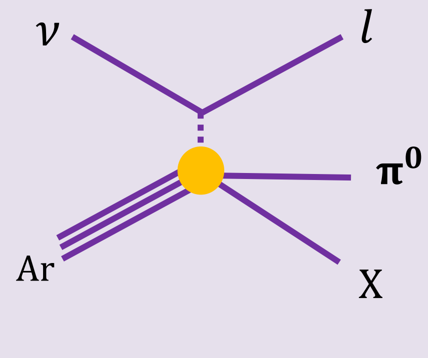

CC Quasi-Elastic (QE)-Like

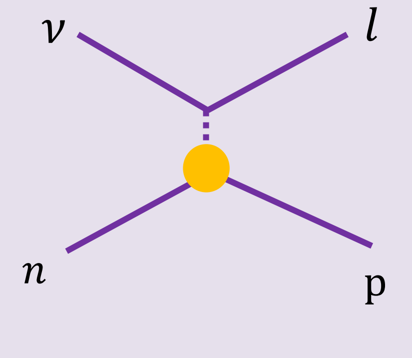

CC 0πNp

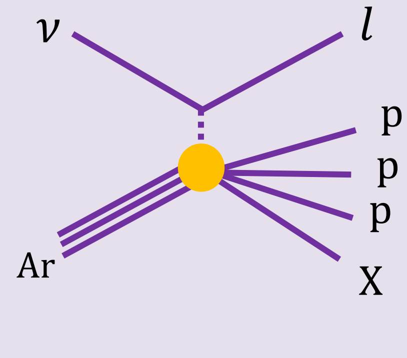

Challenge for MicroBooNE's Neutrino Studies

- Cosmic-ray muon background rejection
  - ~1 ν interaction per 600 beam spills
  - Near surface operation of LArTPC (slow readout detector) leads to 20-30 cosmic muons per trigger

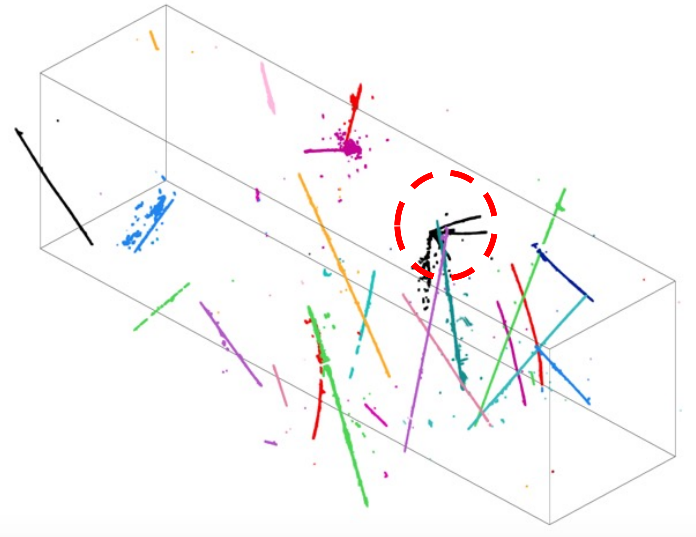

- Event reconstruction
  - Pattern recognition given complicated event topology: Tracks, showers, decays
  - Three paradigms used: Pandora, Deep Learning (DL), Wire-Cell

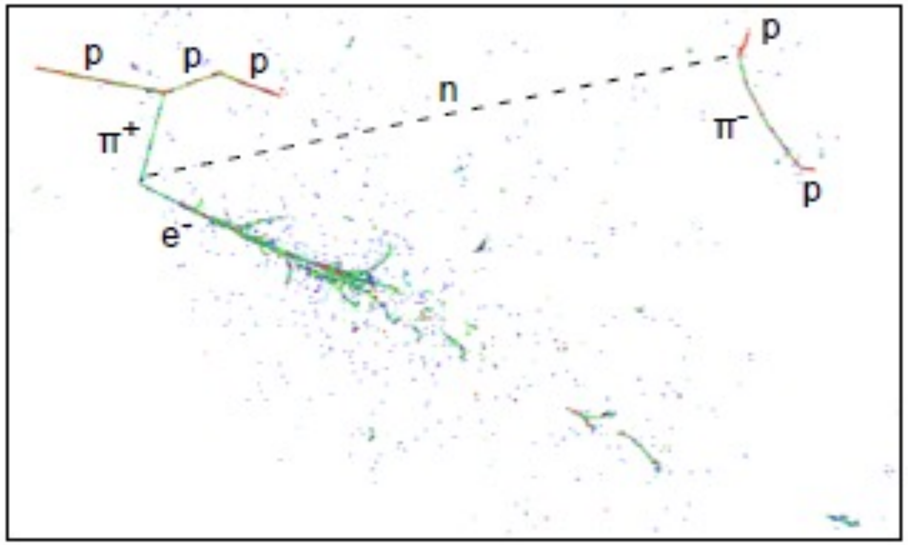

Wire-Cell Event Reconstruction

TPC simulation noise filtering signal processing	3D imaging clustering charge-light matching	3D trajectory & dQ/dx fitting cosmic muon tagger	multi-track fitting DL-3D vertexing particle identification

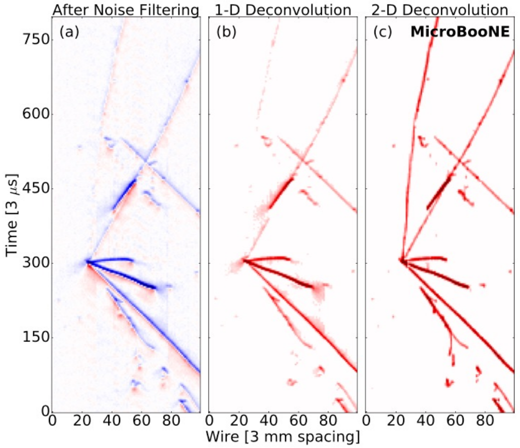

JINST 12 P08003 (2017)
JINST 13 P07006 (2018)
JINST 13 P07007 (2018)
JINST 16 P01036 (2020)

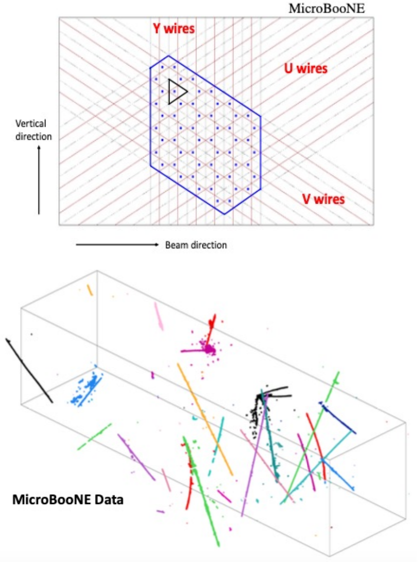

JINST 13 P05032 (2018)
JINST 16 P06043 (2021)

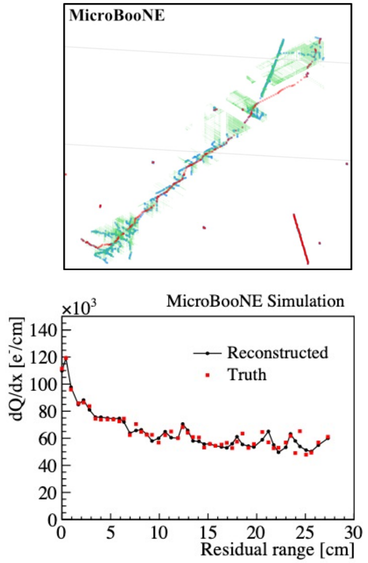

Phys. Rev. Applied 15 064071 (2021)
arXiv:2012.07928

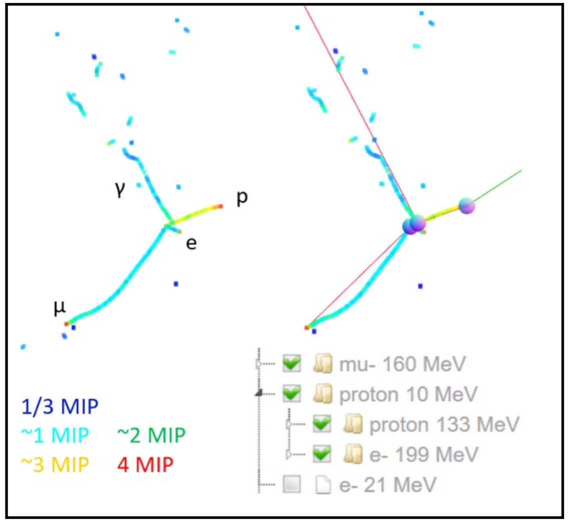

JINST 17 (2022) P01037

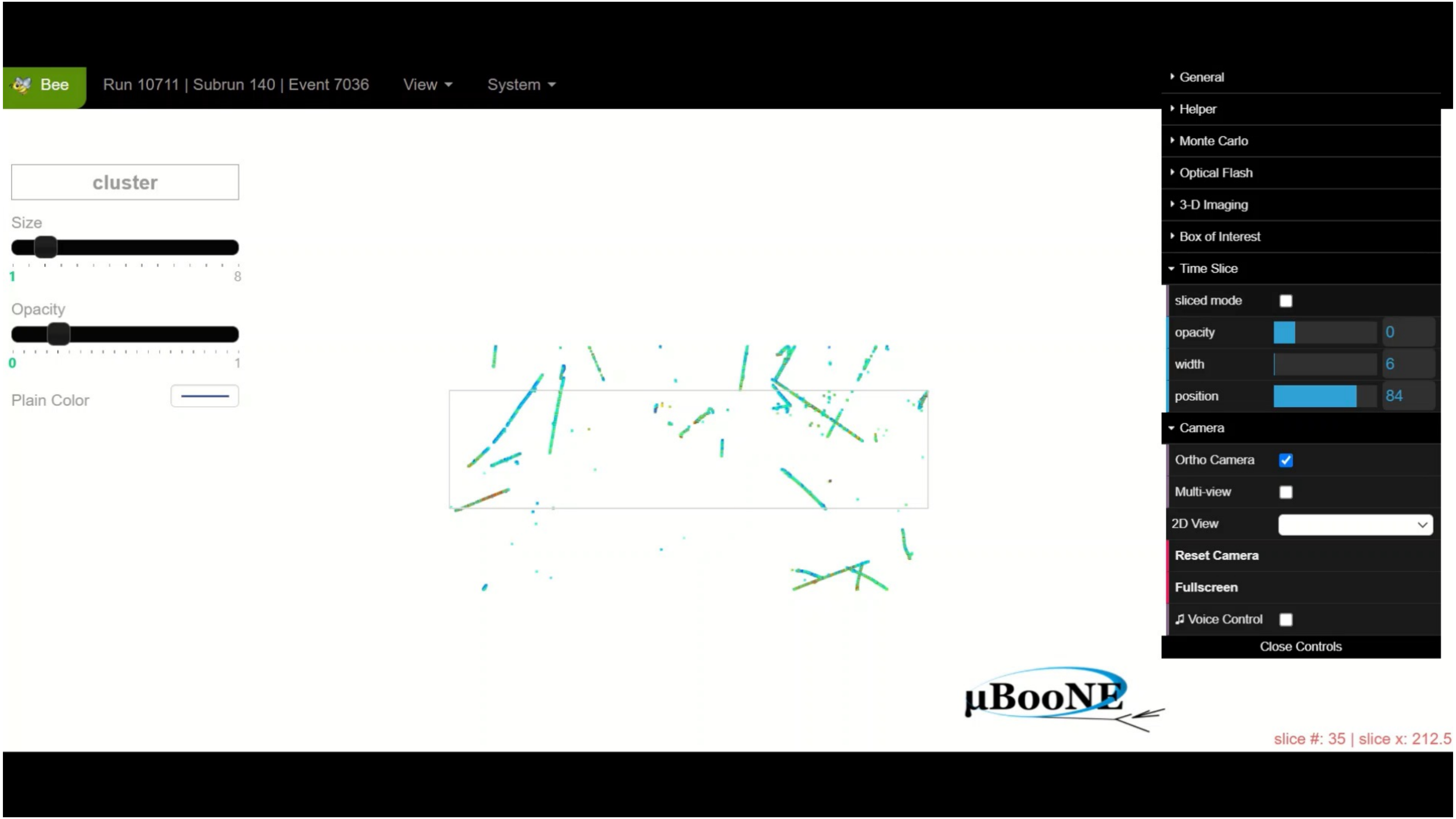

Bee
Run 10711 | Subrun 140 | Event 7036
View
System
cluster
Size
1
8
Opacity
0
1
Plain Color
General
Helper
Monte Carlo
Optical Flash
3-D Imaging
Box of Interest
Time Slice
sliced mode
opacity
0
width
6
position
84
Camera
Ortho Camera
Multi-view
2D View
Reset Camera
Fullscreen
Voice Control
Close Controls
µBooNE
slice #: 35 | slice x: 212.5

The First **Many-to-Many** Charge-Light Matching

JINST **16** P06043

3D imaging, clustering

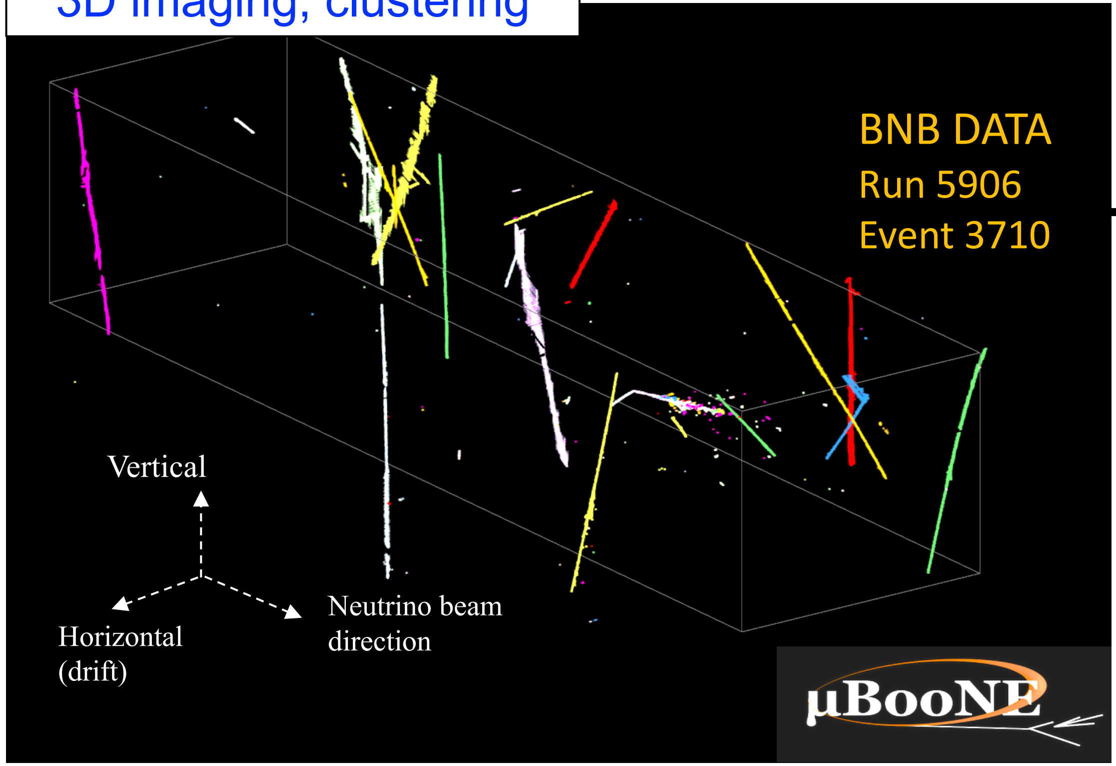

Charge-light matching

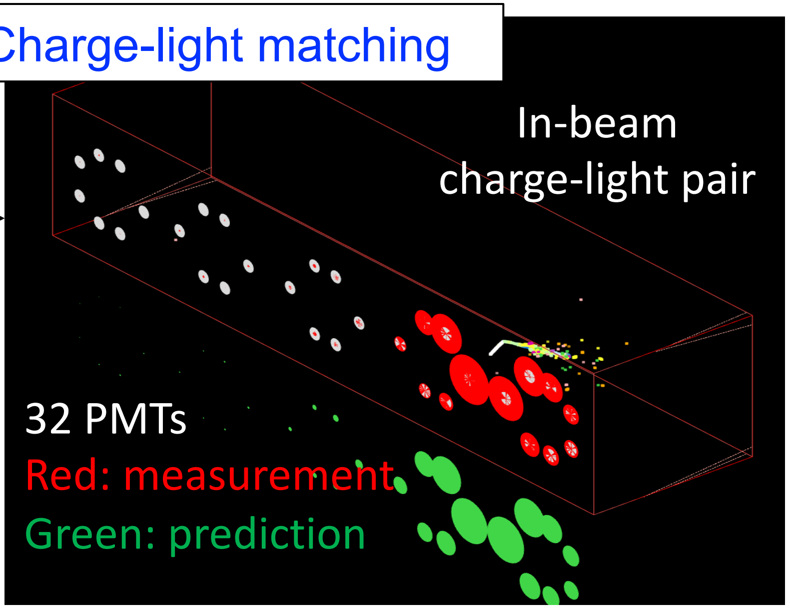

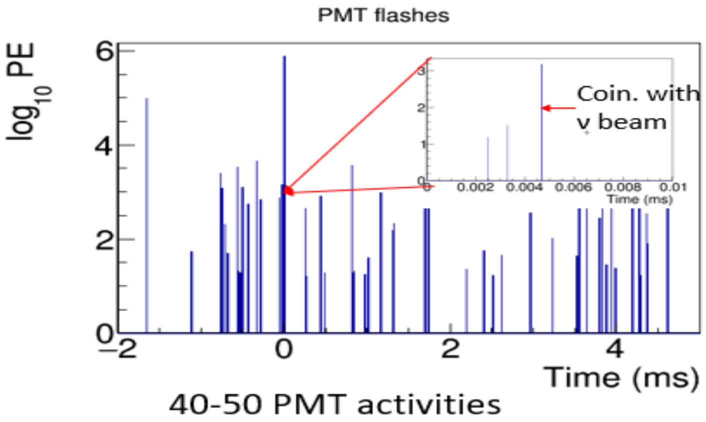

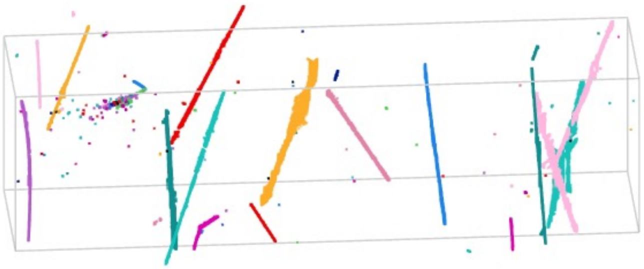

Rejecting Random Coincident Cosmic-Ray Muons

Through-going muon (TGM)

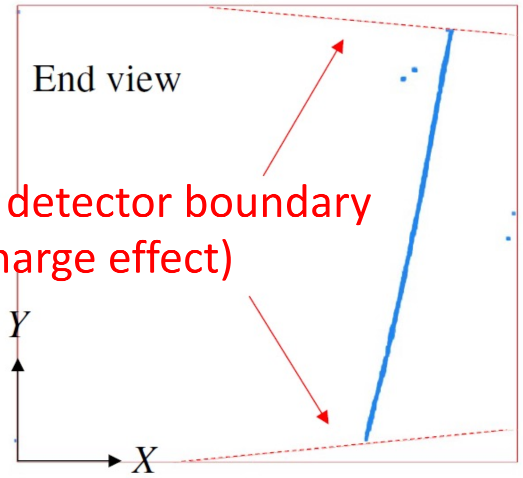

Stopping muon (STM)

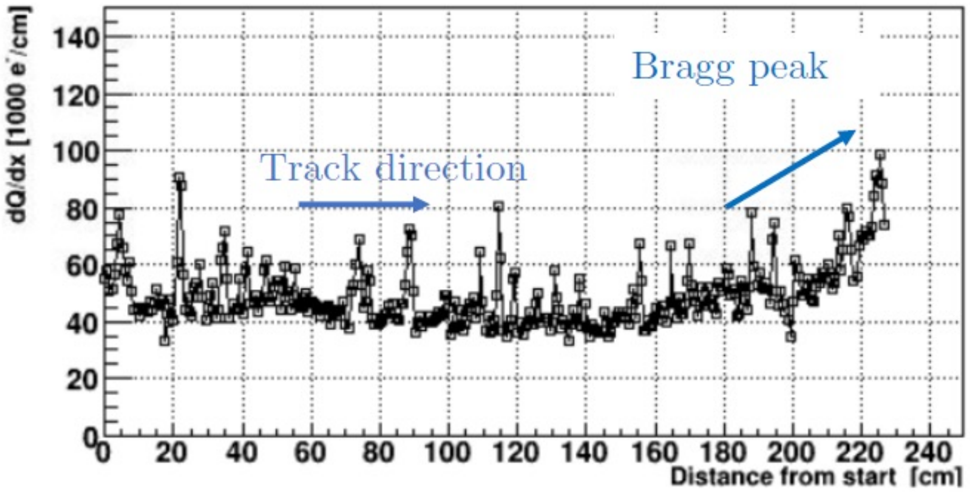

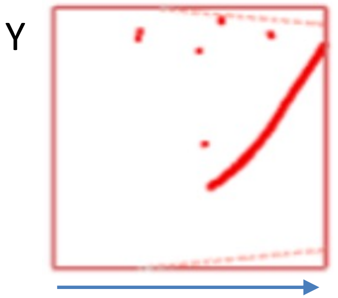

	Neutrino:Cosmic-ray	
Charge-light matching	1 : 6.4	Improved by factor of >6
TGM rejection	1 : 0.91	
STM rejection	1 : 0.36	Improved by factor of ~3
Additional Cuts	1 : 0.20	

Preselection

- Generic neutrino detection powered by many-to-many charge light matching and additional cosmic taggers to reject in-time coincidence cosmic-ray muons

  – 99.999% cosmic-ray muon background rejected
    - Start with 1:20,000 neutrinos to cosmics
    - End with 5.2:1 neutrinos to cosmics

  – 80% efficiency for ν_μCC

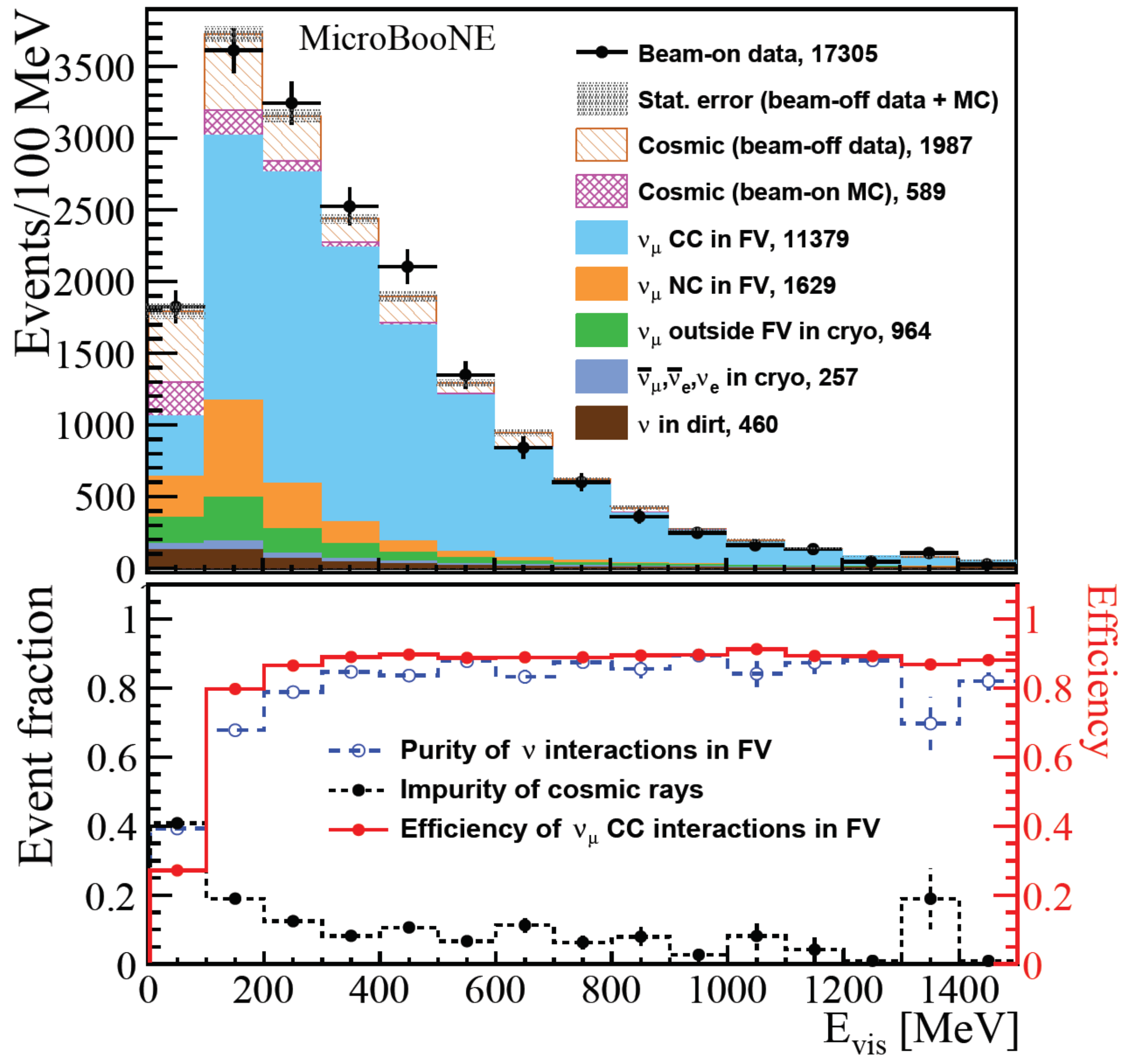

Phys. Rev. Applied 15, 064071

Wire-Cell 3D Pattern Recognition

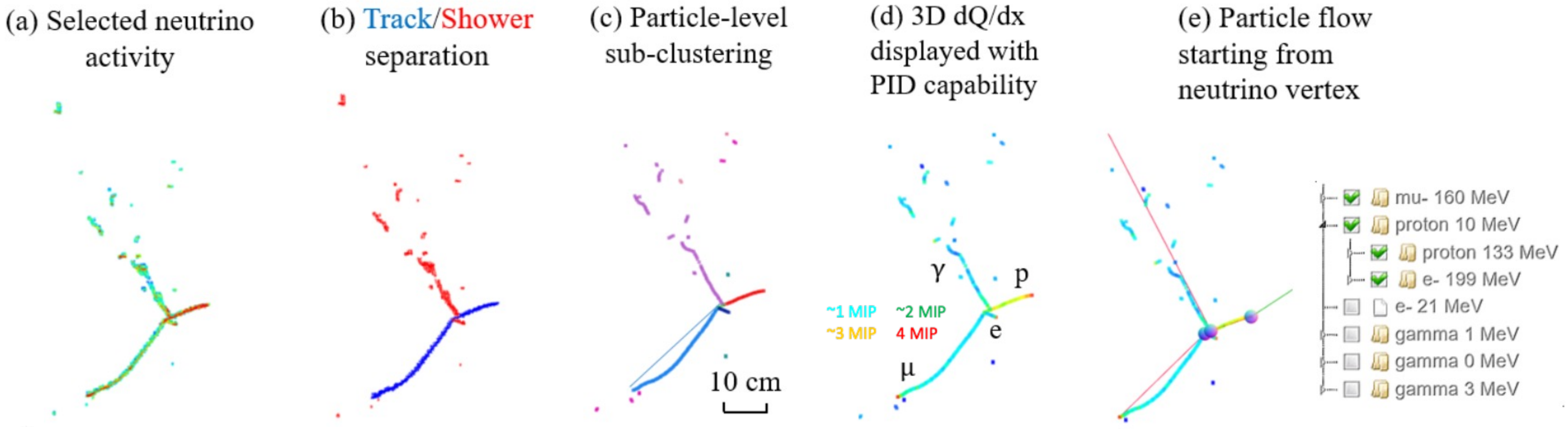

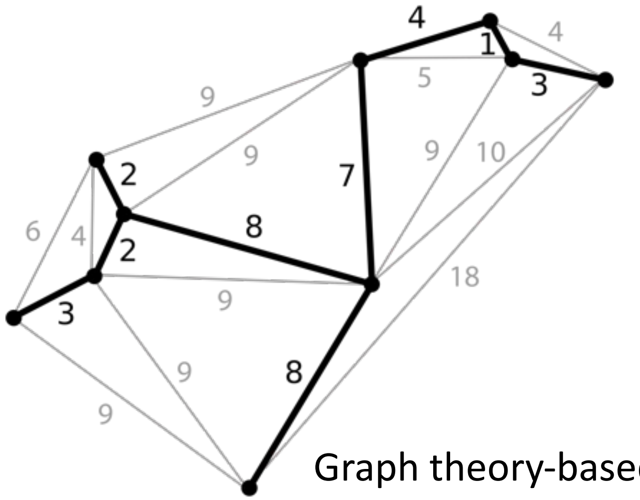

Graph theory-based multi-track fitting (e.g., Steiner tree)

Hybrid of Traditional and Deep-Learning based approaches

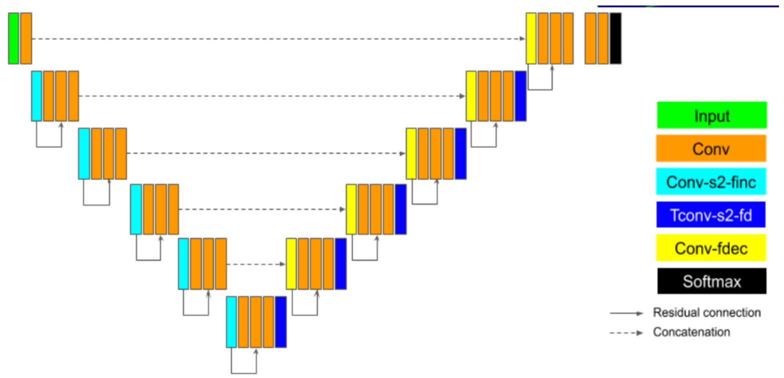

Deep-learning neural network for neutrino vertex identification

Neutrino Energy Reconstruction

- Calorimetry energy reconstruction with particle mass and binding energy included if PID can be done
  - Track: Range, dQ/dx → dE/dx correction
    - Calibrated by stopped muons/protons
  - EM shower: scaling of charge
    - Calibrated by π^0 invariant mass

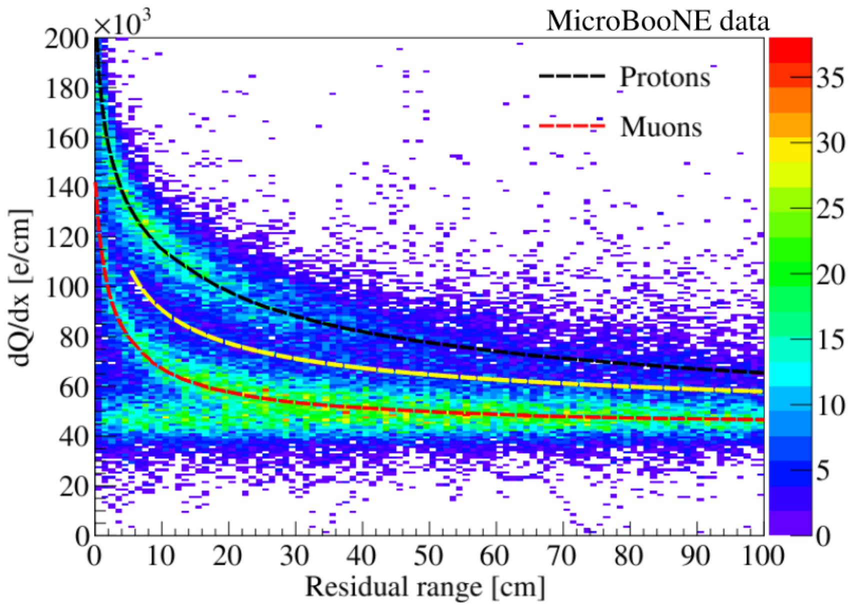

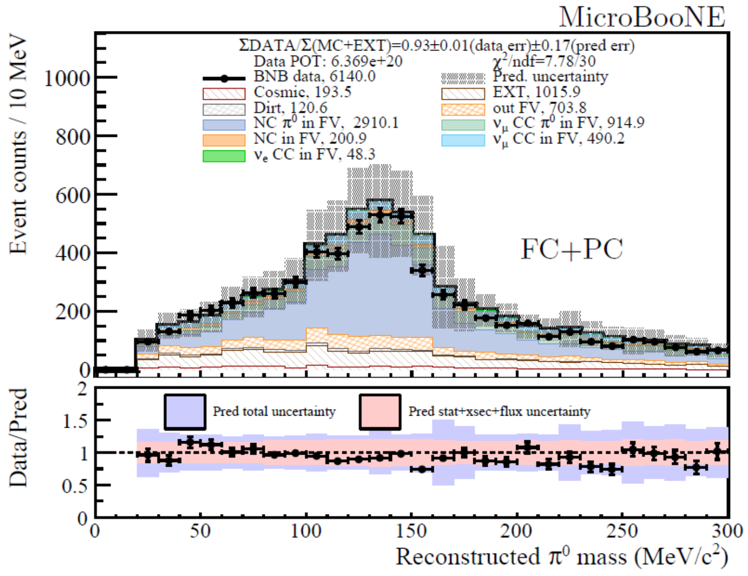

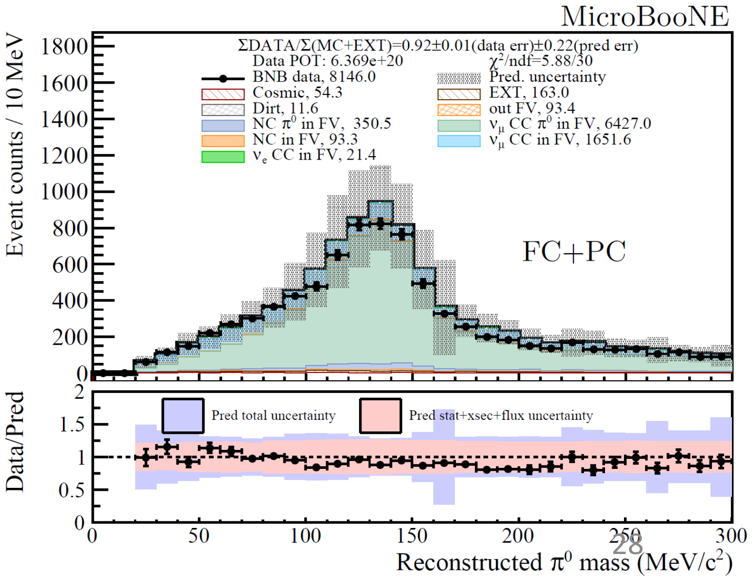

JINST 17 (2022) P01037

Neutrino Energy Reconstruction

- Calorimetry energy reconstruction with particle mass and binding energy included if PID can be done
  - Track: Range, dQ/dx → dE/dx correction
    - Calibrated by stopped muons/protons
  - EM shower: scaling of charge
    - Calibrated by π^0 invariant mass
- Fully contained events

ν_μCC 15-20% energy resolution ~10% bias

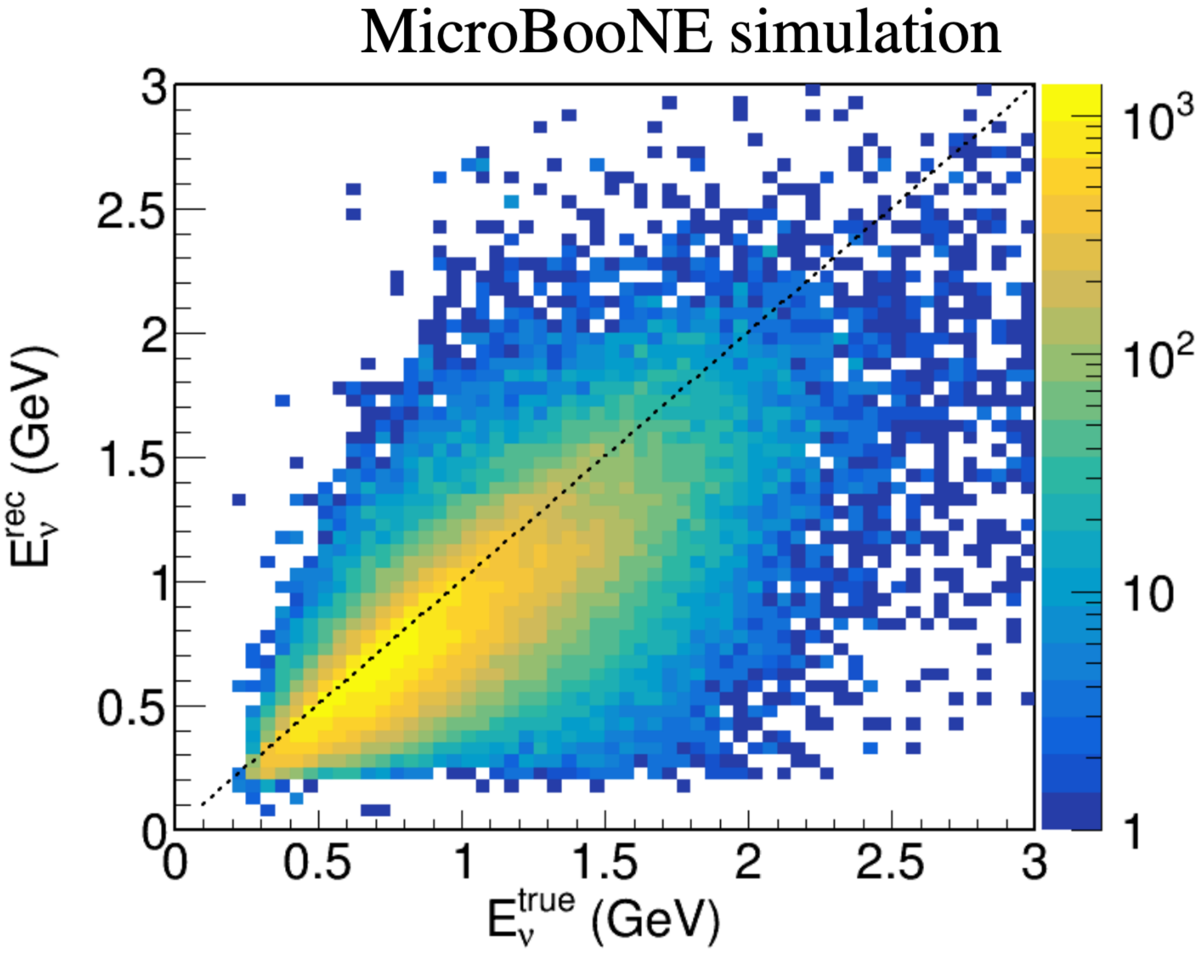

Fully contained ν_μCC

[JINST 17 (2022) P01037](#)

ν_μ CC Selection through XGBoost BDT

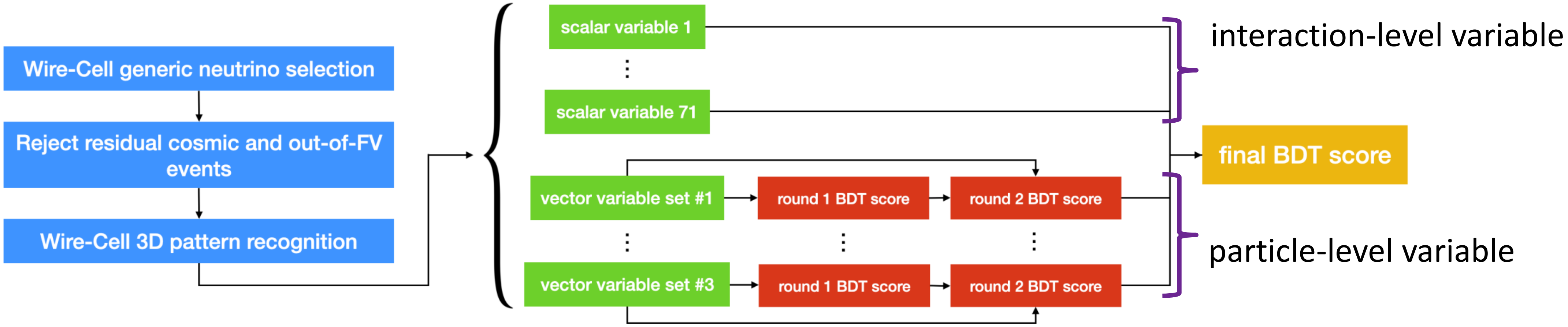

Human feature engineering

+

Machine learning algorithm:

XGBOOST: extreme Gradient Boosting

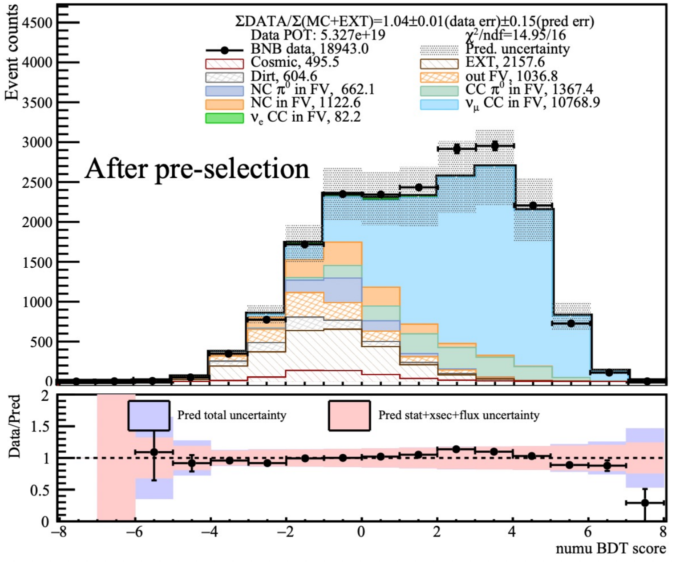

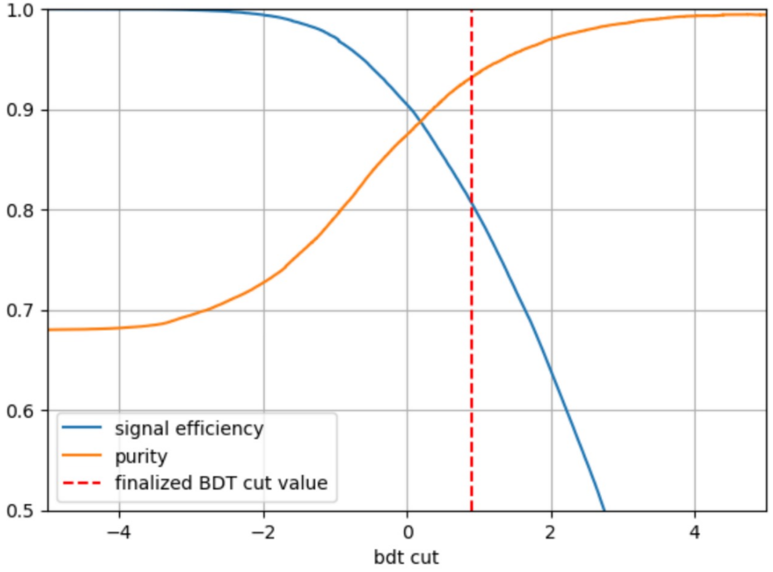

Selection of Inclusive ν_μCC Interactions

	Efficiency	Purity	Cosmic-μ rejection
Trigger	1	5e-5	1
Cosmic-ray rejection	80%	65%	7e-6
ν_μCC with pattern recognition **(Fully & Partially Contained)**	**68%**	**92%**	7e-7

- Achieved excellent cosmic-μ rejection
  - Wire-Cell reconstruction: JINST 16 (2021) 06, P06043
  - Cosmic-ray rejection:
    - arXiv:2012.07928, Phys. Rev. Applied 15, 064071 (2021)
- **High-statistics** event selection allows for precision cross-section measurements
  - Demonstration of good performance of LArTPC for next-generation programs

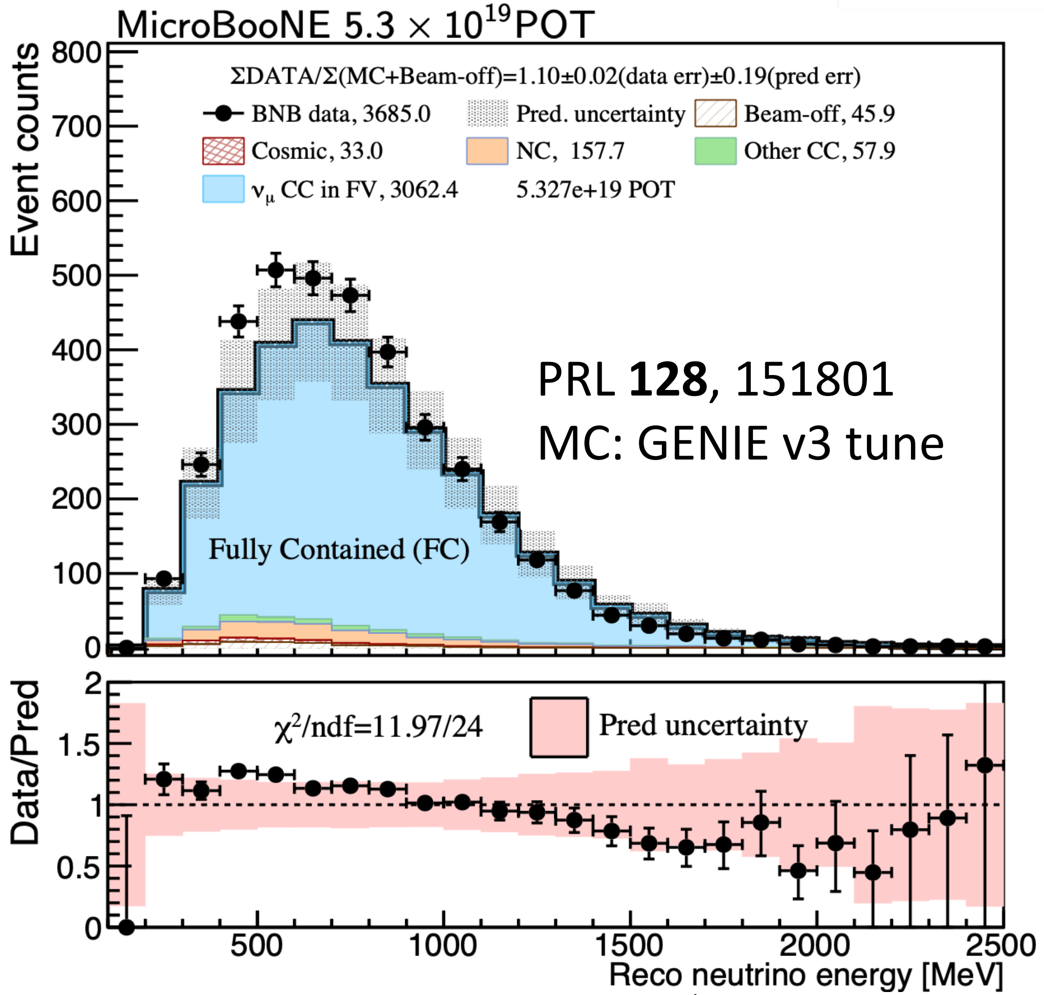

PRL **128**, 151801
MC: GENIE v3 tune

Calorimetric energy:

$$\mathbf{E_{\nu}^{rec} = E_{\mu}^{rec} + E_{had}^{rec}}$$

Evolved Neutrino Interaction Model

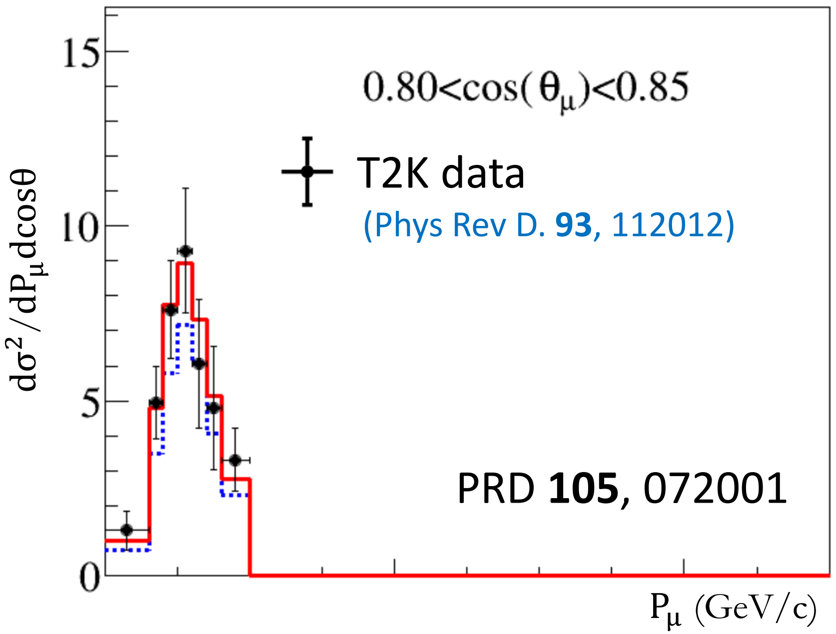

Generic neutrino preselection

Before tuning

After tuning

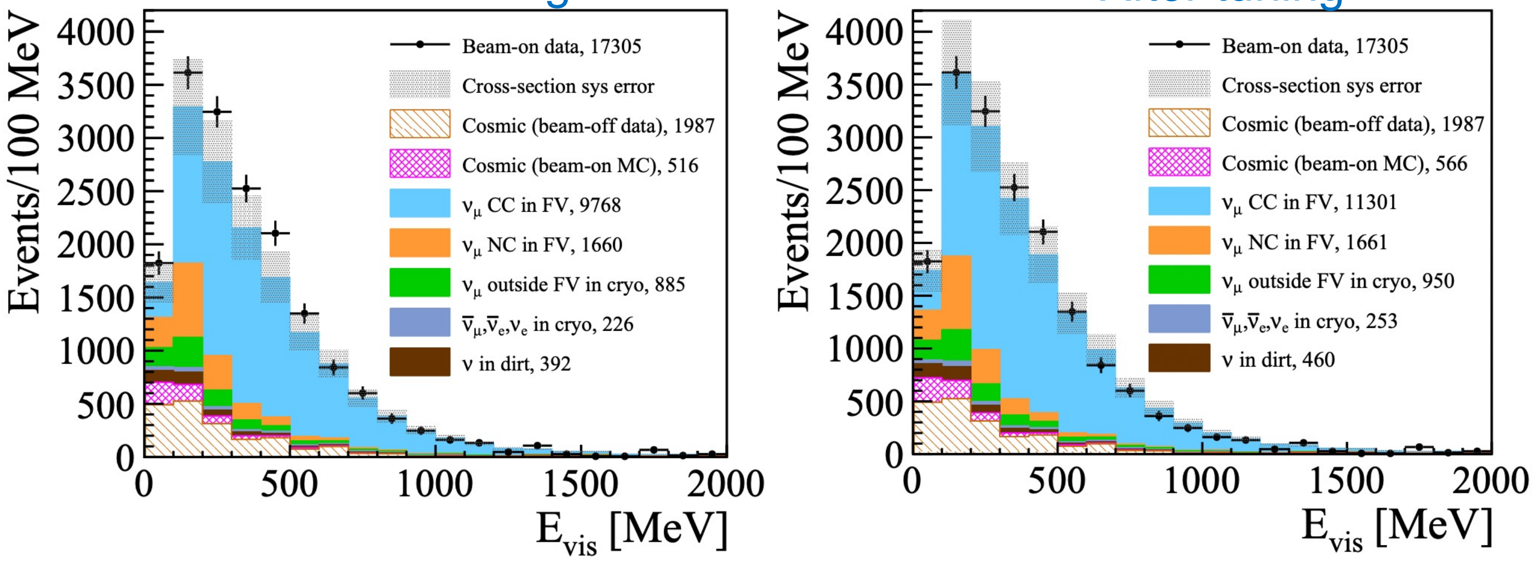

- MicroBooNE's interaction model evolved from GENIE v2 to GENIE v3
- New model is tuned through fitting to T2K's ν_μ CC0π data (CH) at similar beam energy
  - ➡ Tune 4 key parameters related to CCQE and 2p2h models
  - ➡ No additional fit to MicroBooNE data (Ar)

	MaCCQE (GeV)	CC2p2h Norm.	CCQE RPA Strength	CC2p2h Shape
Untuned	0.961242	1	100%	0
Tuned	1.10 ± 0.07	1.66 ± 0.19	(85 ± 20) %	$1^{+0}_{-0.74}$

Systematic Uncertainties

- BNB neutrino flux uncertainty
  - MiniBooNE: Phys. Rev. D **79**, 072002 (2009)
- Neutrino cross section uncertainty
  - GENIE-v3 with the MicroBooNE tune: Phys. Rev. D **105**, 072001 (2022)
- Detector systematics
  - TPC, Light, Space Charge, Recombination: *Eur.Phys.J.C* **82** (2022) 5, 454
  - Bootstrapping approach
- Hadron-argon interaction uncertainty
  - GEANT4 reweight: *JINST* 16 (2021) 08, P08042
- MC statistical uncertainty
  - Bayesian approach
- Dirt systematics
  - Materials outside the cryostat

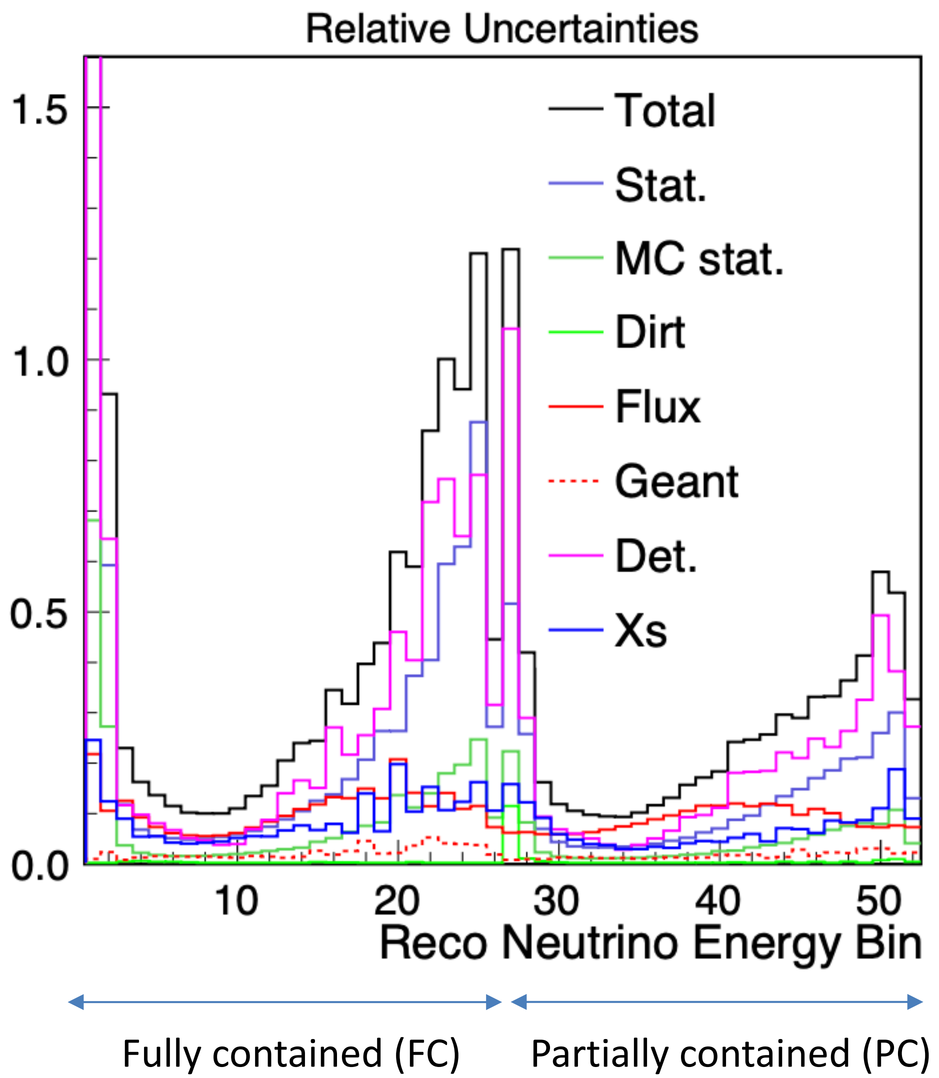

Cross Section Extraction: Unfolding

- We measure $\sigma(E)$, $\mathrm{d}\sigma/\mathrm{d}E_\mu$, $\mathrm{d}\sigma/\mathrm{d}\nu$ using Wiener-SVD unfolding

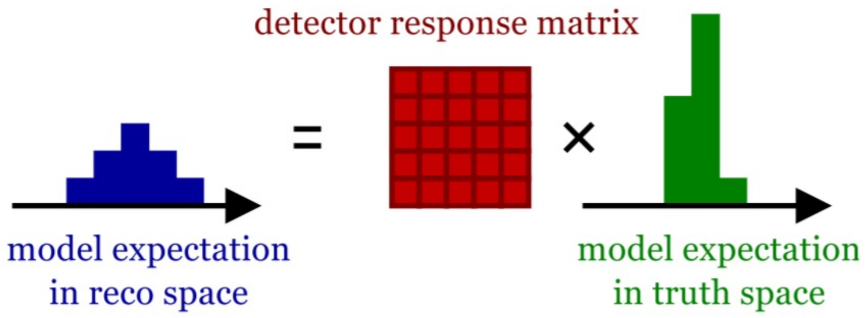

Wiener-SVD unfolding: JINST 12 (2017) 10, P10002

$$\boldsymbol{M_i = \sum_j R_{ij} \cdot S_j + B_i}$$

M_i (B_i): # of candidate (bkgd) in reco bin i
R_{ij}: response (smearing) matrix
S_j: cross section to be extracted in **true bin j**

Prerequisites: data well-described by model predictions within uncertainties

Overall Model Validation: Goodness-of-Fit Test

- χ^2**/ndf** calculated from the full systematics (flux, Xs, detector, MC statistics) and statistics

$$\chi^2 = (M-P)^T \times Cov_{full}^{-1}(M,P) \times (M-P)$$

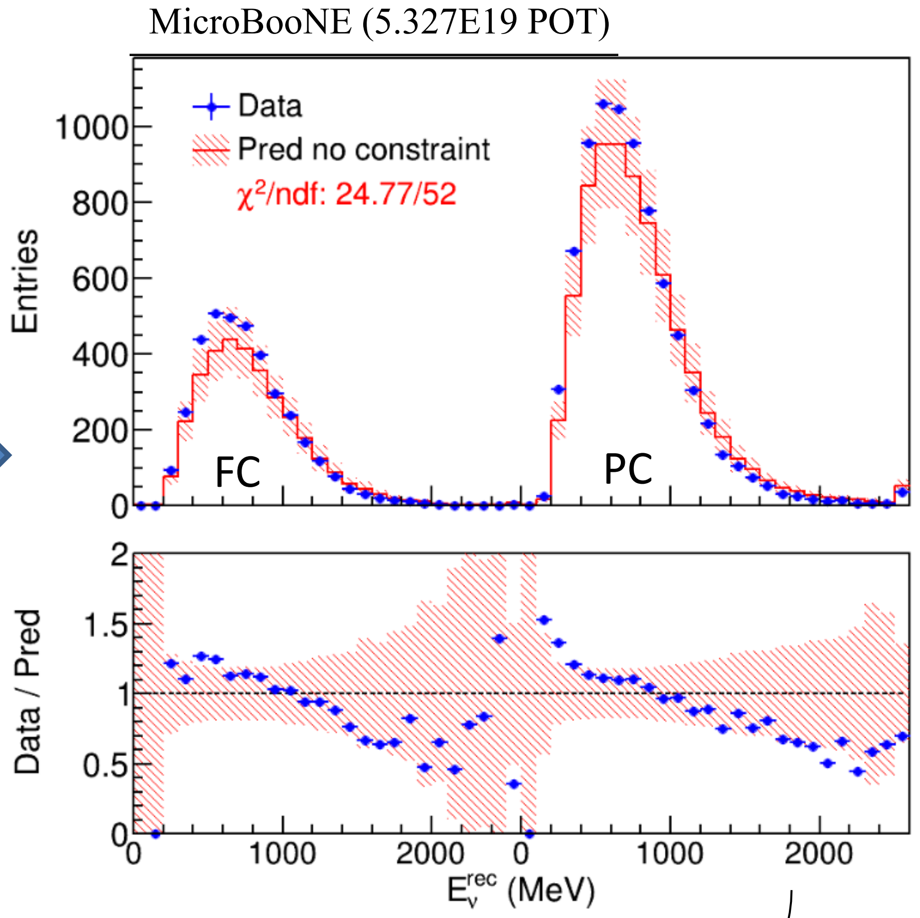

Calorimetric energy:

$$\mathbf{E_\nu^{rec} = E_\mu^{rec} + E_{had}^{rec}}$$

- What if conservative estimates of some types of uncertainty hide potential biases in others?
  - Can be tested with conditional constraining procedure as introduced shortly

Model validation of E_{μ}^{rec} : Meas. vs. Pred.

$$E_\nu = E_\mu + E_{had,vis} + E_{had,missing}$$

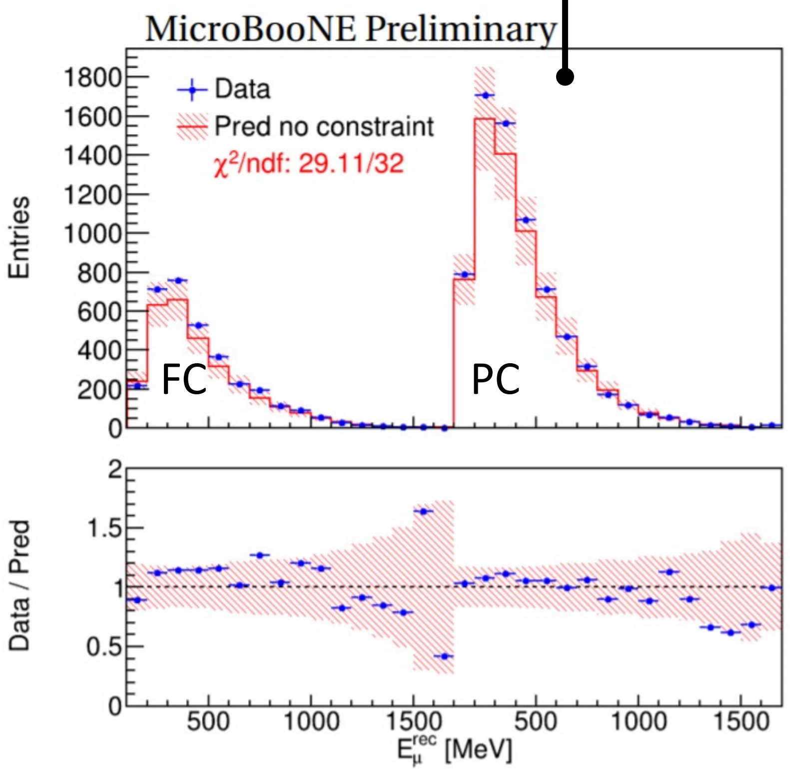

FC: fully-contained events in the fiducial volume (FV)
PC: partially contained events in the FV
Goodness-of-fit test:
$\chi^2 = (M - \mu)^T \cdot \Sigma^{-1} \cdot (M - \mu)$

- Good agreement within model uncertainty given that χ^2/ndf = 29.11/32

Model validation: $M(E_{had}^{rec})$ vs. $\mu(E_{had}^{rec})$

$$\mathbf{E_\nu = E_\mu + E_{had,vis} + E_{had,missing}}$$

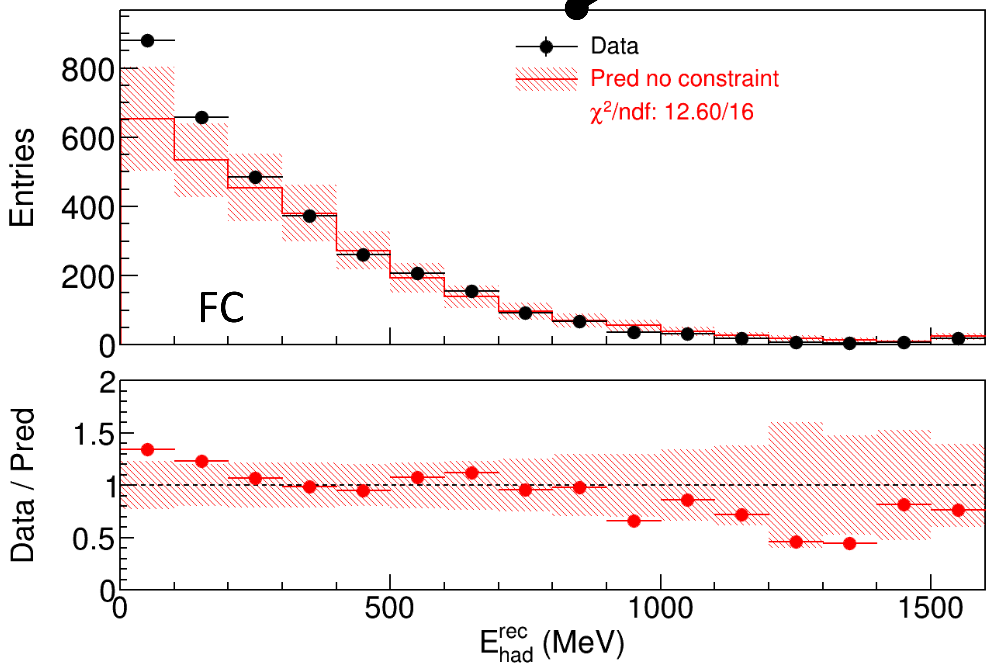

- Excess at low hadronic energy
- Mis-modeling of hadronic missing energy given neutrino flux reasonably well known?
  - $\mathbf{D}(E_\nu \to E_{reco})$!
- χ^2/ndf is reasonable but large uncertainty could hide the potential bias

Challenge in Validating Energy Model $\mathbf{D}(E_\nu \rightarrow E_{reco})$

- How to verify the modeling of the undetected **missing hadronic energy**?
  - ➥ Mapping of $E_\nu \rightarrow \mathbf{E}_\nu^{\mathbf{rec}}$

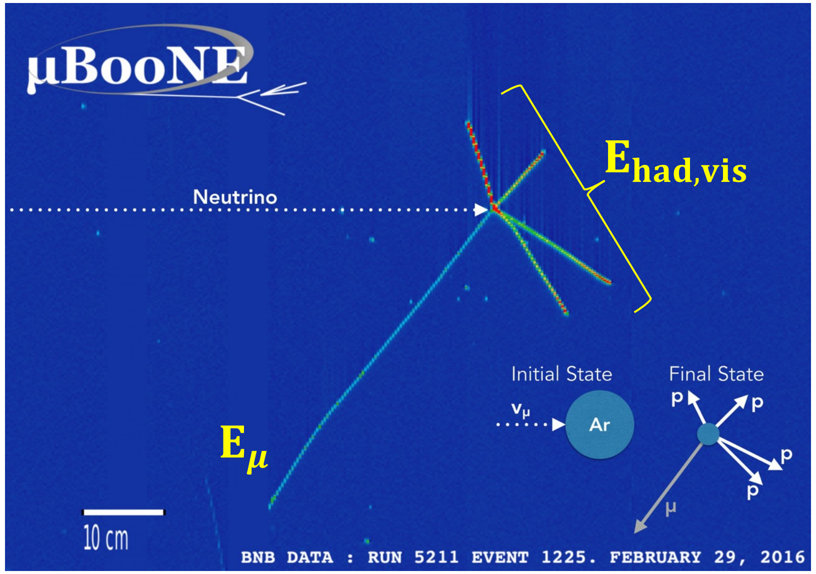

True energy components:

$$\mathbf{E}_\nu = \mathbf{E}_\mu + \mathbf{E}_{\mathbf{had,vis}} + \mathbf{E}_{\mathbf{had,missing}}$$

Calorimetric energy reconstruction:

$$\mathbf{E}_\nu^{\mathbf{rec}} = \mathbf{E}_\mu^{\mathbf{rec}} + \mathbf{E}_{\mathbf{had,vis}}^{\mathbf{rec}}$$

Conditional Constraining Procedure

- Overcome the challenge by leveraging LArTPC's simultaneous measurements of **lepton energy** and **visible hadronic energy**

Conditional expectation & covariance

$$\boldsymbol{\mu}_{X,Y} = \begin{pmatrix} \boldsymbol{\mu}_X \\ \boldsymbol{\mu}_Y \end{pmatrix}, \qquad \boldsymbol{\Sigma}_{X,Y} = \begin{pmatrix} \boldsymbol{\Sigma}_{XX} & \boldsymbol{\Sigma}_{XY} \\ \boldsymbol{\Sigma}_{YX} & \boldsymbol{\Sigma}_{YY} \end{pmatrix}$$

$$\mu_{Y|X} = \mu_Y + \Sigma_{YX}\Sigma_{XX}^{-1}(X - \mu_X)$$

$$\boldsymbol{\Sigma}_{Y|X} = \boldsymbol{\Sigma}_{YY} - \boldsymbol{\Sigma}_{YX}\boldsymbol{\Sigma}_{XX}^{-1}\boldsymbol{\Sigma}_{XY}$$

* A variant of Gaussian Process Regression

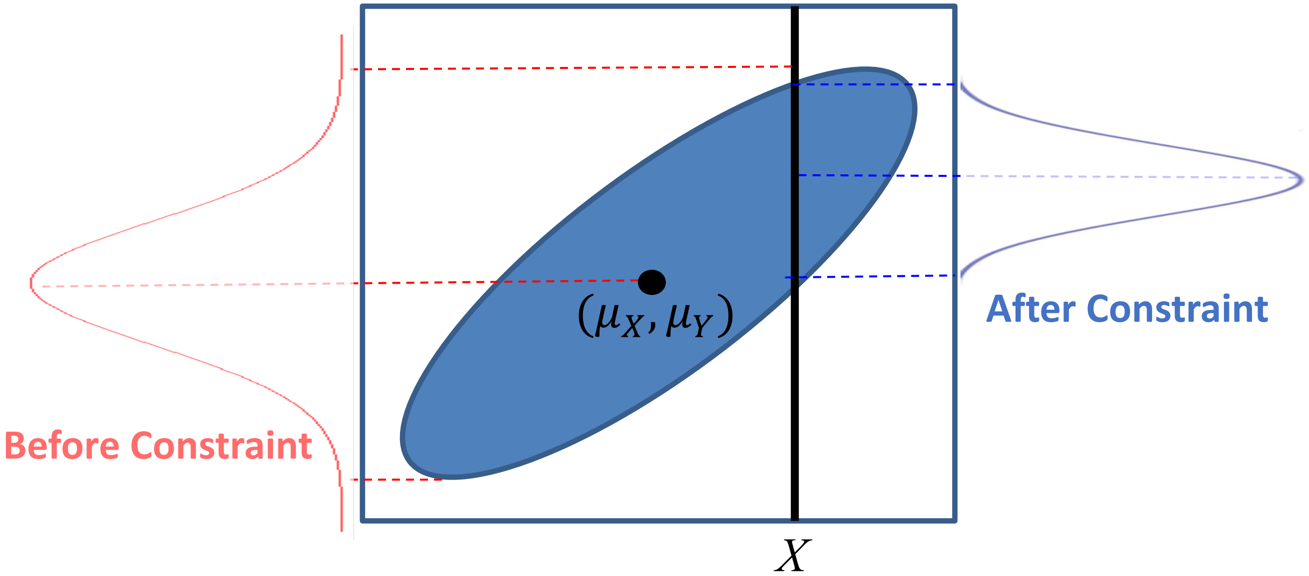

* Estimate correlated statistical uncertainty with bootstrapping (sampling w/ replacement)

$$\begin{matrix} \mu(E^{rec}_{had}) \\ \Sigma(E^{rec}_{had}) \end{matrix} + M(\mathbf{E}^{rec}_{\mu}) = \begin{matrix} \mu(E^{rec}_{had} \mid \mathbf{E}^{rec}_{\mu}, \mathbf{E}_{\nu}) \\ \Sigma(E^{rec}_{had} \mid \mathbf{E}^{rec}_{\mu}, E_{\nu}) \end{matrix}$$

Prior model Sideband Posterior model

$$\mathbf{E}_{\nu} = \mathbf{E}_{\mu} + \mathbf{E}_{\mathbf{had,vis}} + \mathbf{E}_{\mathbf{had,missing}}$$

Another Perspective of Conditional Constraining

* jusr for illustration

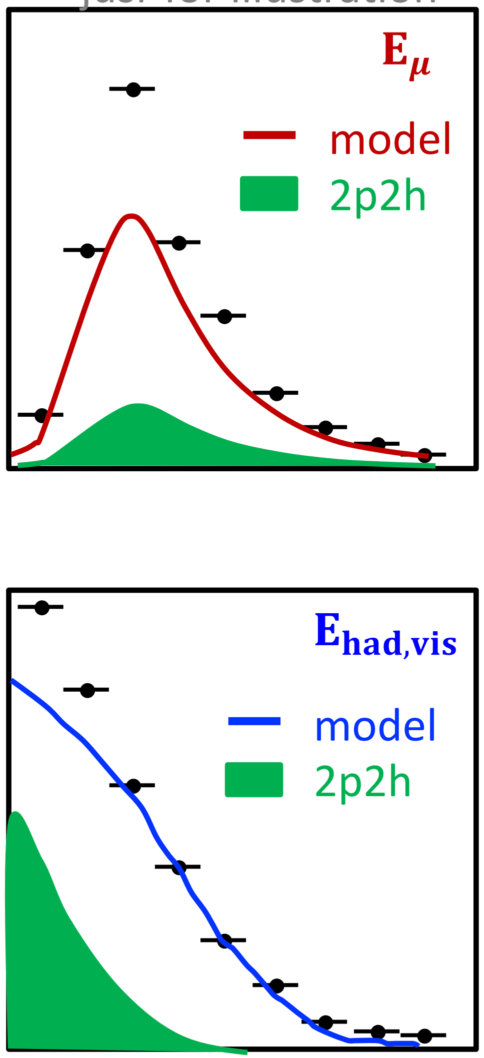

conditional constraining

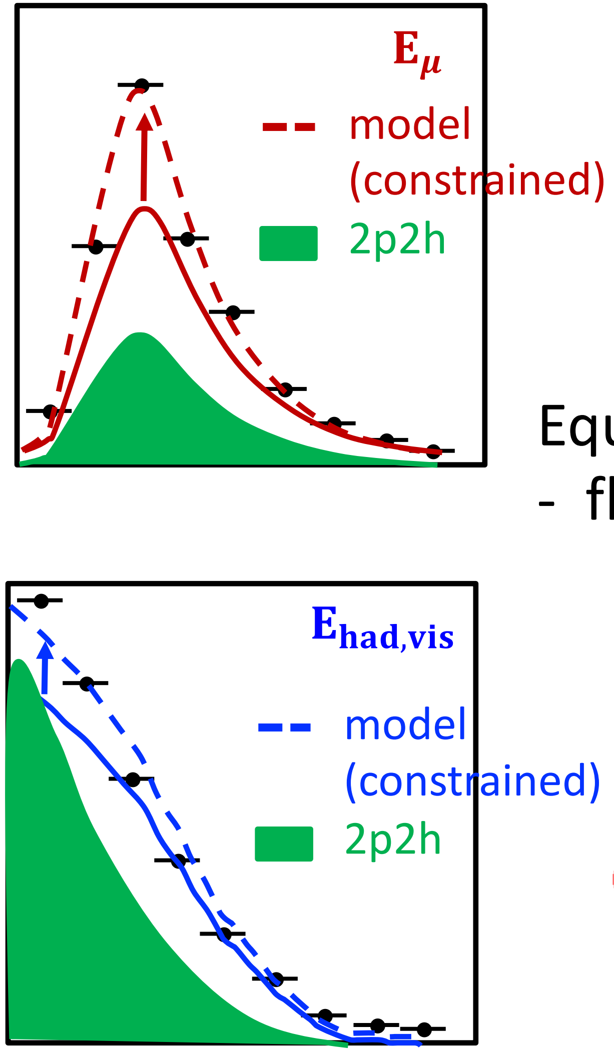

Conditional constraining

+

Muon “sidebands”

Equivalent tuning for overall model
- flux, cross section, detector effects

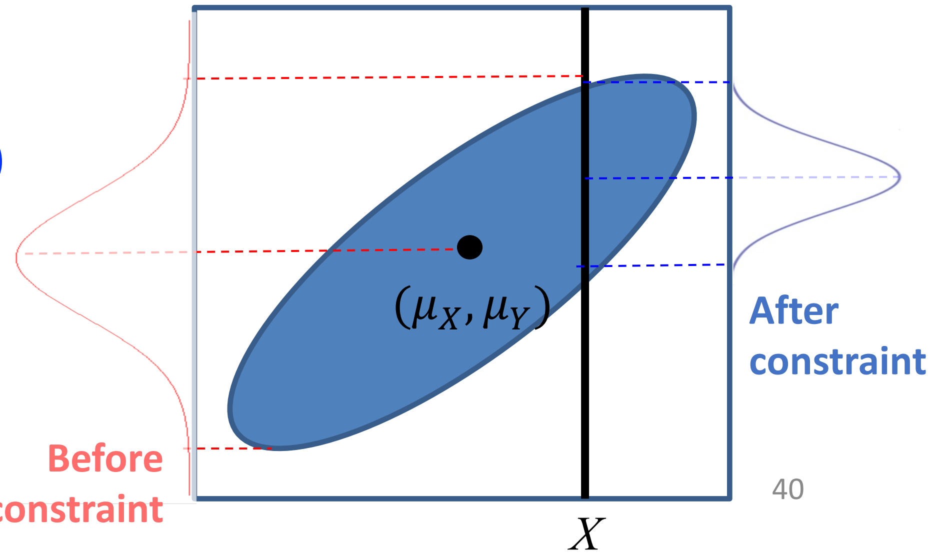

Model Validation: $M(E_{had}^{rec})$ vs. $\mu(E_{had}^{rec} \mid E_{\nu}, E_{\mu}^{rec})$

Neutrino flux modeling

Measurement of muon kinematics

- New method to validate modeling of neutrino energy reconstruction given separated lepton and hadronic energy measurements in LArTPC

$$E_{\nu} = E_{\mu} + E_{had,vis} + E_{had,missing}$$

Before Constraint

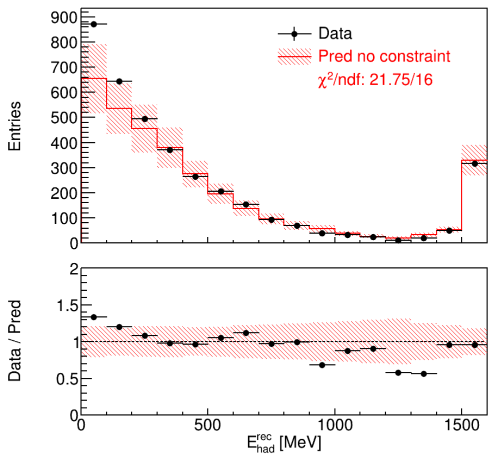

Excess at low hadronic energy indicates mis-modeling of missing energy?

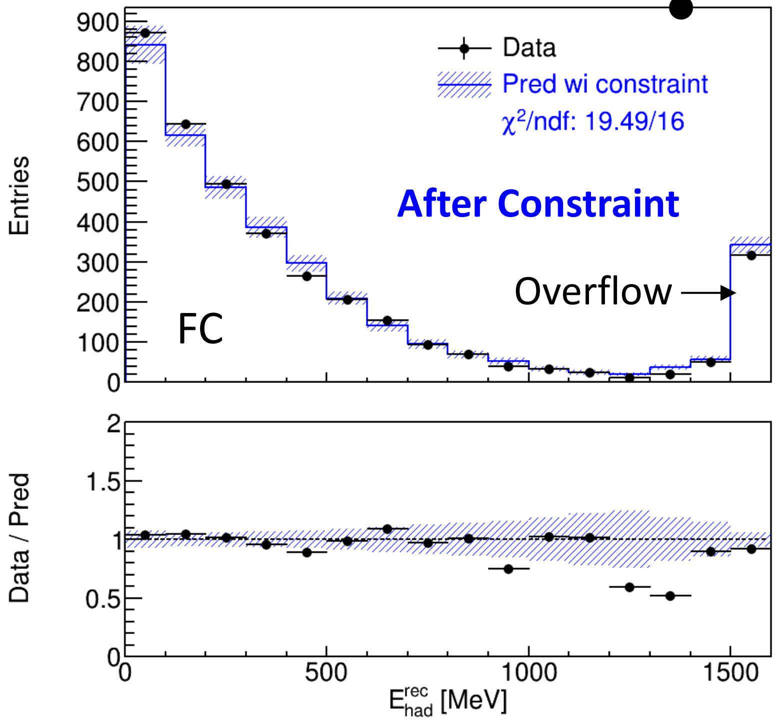

Measured muon kinematics are used to constrain the overall model (flux, cross section, etc.) for hadronic energy

- Systematic uncertainties 20% → 5% in performing model validation
- No sign of mis-modeling of the **missing hadronic energy**
  - $D(E_{\nu} \rightarrow E_{reco})$ is good!

Is the New Method Really Working?

Fake data 1: model (constrained) comparison of $E_{\text{had}}^{\text{rec}}$

Proton energy scaling	χ^2 (ndf=32)	P-value
0.95	5.34	~ 1
0.9	21.05	0.93
0.85	**47.01**	**0.04**
0.8	80.60	~ 0

- χ^2/ndf has a significant increase with a shift of ~15% in the hadronic energy fraction allocated to protons (mimicking a variation of the proton-inelastic cross section)

The conditional constraint approach is sensitive to the underlying model differences

Fake data II

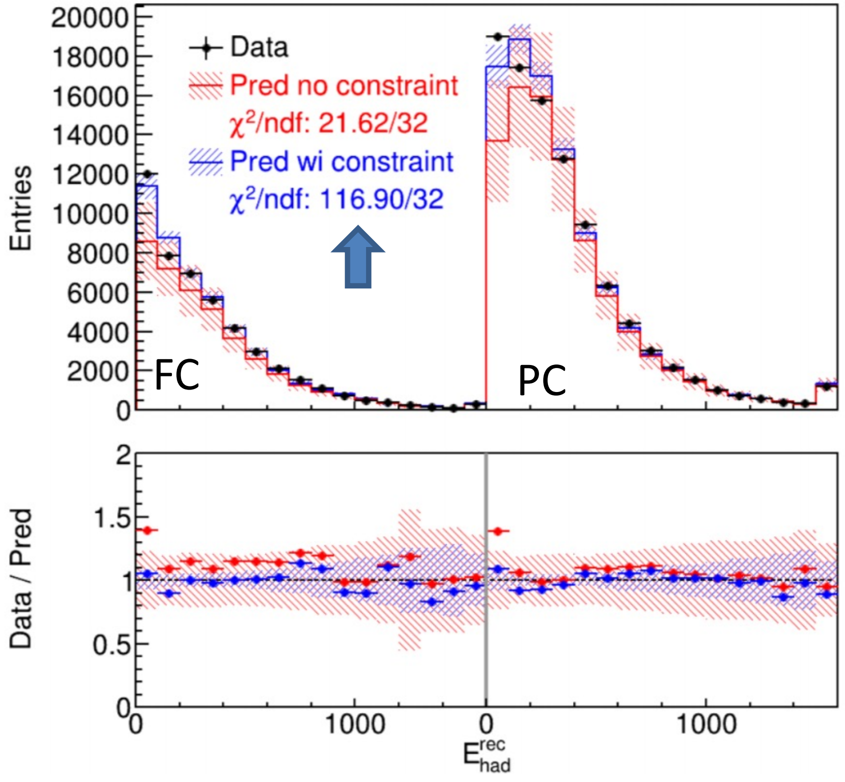

- Fake data (GENIE v2) shows a poor χ^2/ndf for $E_{\text{had}}^{\text{rec}}$ after constraint of muon kinematics

Equation For Unfolding $\sigma(E_\nu)$

Measurements — Flux — Cross section — Detector response — Selection efficiency — Background

$$M(E_{rec}) = POT \cdot T \cdot \int F(E_\nu) \cdot \sigma(E_\nu) \cdot \boldsymbol{D}(\boldsymbol{E_\nu} \rightarrow \boldsymbol{E_{rec}}) \cdot \varepsilon(E_\nu, E_{rec}) \cdot dE_\nu + B(E_{rec})$$

$$\boldsymbol{M_i = \sum_j R_{ij} \cdot S_j + B_i}$$

$$\tilde{\Delta}_{ij} = \frac{POT \cdot T \cdot \int_j F\left(E_{\nu\,\mathrm{j}}\right) \cdot \sigma\left(E_{\nu\,\mathrm{j}}\right) \cdot D\left(E_{\nu\,\mathrm{j}}, E_{rec\,i}\right) \cdot \varepsilon\left(E_{\nu\,\mathrm{j}}, E_{rec\,i}\right) \cdot dE_{\nu\,\mathrm{j}}}{POT \cdot T \cdot \int_j \overline{F}\left(E_{\nu\,\mathrm{j}}\right) \cdot \sigma\left(E_{\nu\,\mathrm{j}}\right) \cdot dE_{\nu\,\mathrm{j}}}$$

➡ a MC ratio, less sensitive to Xs uncertainty

$$R_{ij} = \tilde{\Delta}_{ij} \cdot \tilde{F}_j$$

$$\tilde{F}_j = POT \cdot T \cdot \int_j \overline{F}\left(E_{\nu\,\mathrm{j}}\right) \cdot dE_{\nu\,\mathrm{j}}$$

$$S_j = \frac{\int_j \overline{F}\left(E_{\nu\,\mathrm{j}}\right) \cdot \sigma\left(E_{\nu\,\mathrm{j}}\right) \cdot dE_{\nu\,\mathrm{j}}}{\int_j \overline{F}\left(E_{\nu\,\mathrm{j}}\right) \cdot dE_{\nu\,\mathrm{j}}}$$

} Not subject to prior knowledge of the Xs uncertainty

Benefit Of the S_j Definition

- Define the flux-averaged cross section using the nominal flux $\overline{F}$, thus can be easily compared with any model prediction based on the nominal flux

$$S_j = \frac{\int_j \overline{F}\left(E_{\nu\,\mathrm{j}}\right) \cdot \sigma\left(E_{\nu\,\mathrm{j}}\right) \cdot dE_{\nu\,\mathrm{j}}}{\int_j \overline{F}\left(E_{\nu\,\mathrm{j}}\right) \cdot dE_{\nu\,\mathrm{j}}}$$

- The uncertainty calculation is simpler and mathematically precise
  - Flux uncertainty only appears in numerator of $\widetilde{\Delta}_{ij}$
  - Switch $\overline{F}$ *to F* would bring up complicated systematic correlation

$$R_{ij} = \widetilde{\Delta}_{ij} \cdot \tilde{F}_j$$

$$\widetilde{\Delta}_{ij} = \frac{POT \cdot T \cdot \int_j F\left(E_{\nu\,\mathrm{j}}\right) \cdot \sigma\left(E_{\nu\,\mathrm{j}}\right) \cdot D\left(E_{\nu\,\mathrm{j}}, E_{rec\,i}\right) \cdot \varepsilon\left(E_{\nu\,\mathrm{j}}, E_{rec\,i}\right) \cdot dE_{\nu\,\mathrm{j}}}{POT \cdot T \cdot \int_j \overline{F}\left(E_{\nu\,\mathrm{j}}\right) \cdot \sigma\left(E_{\nu\,\mathrm{j}}\right) \cdot dE_{\nu\,\mathrm{j}}}$$

$$\tilde{F}_j = POT \cdot T \cdot \int_j \overline{F}\left(E_{\nu\,\mathrm{j}}\right) \cdot dE_{\nu\,\mathrm{j}}$$

- Proper treatment of flux shape uncertainty: PRD **102** 113012

JINST 12, P10002 (2017)

Wiener-SVD unfolding

- An unfolding technique that maximize the S/N ratio with a "Wiener" regularization → a simplified unfolding procedure

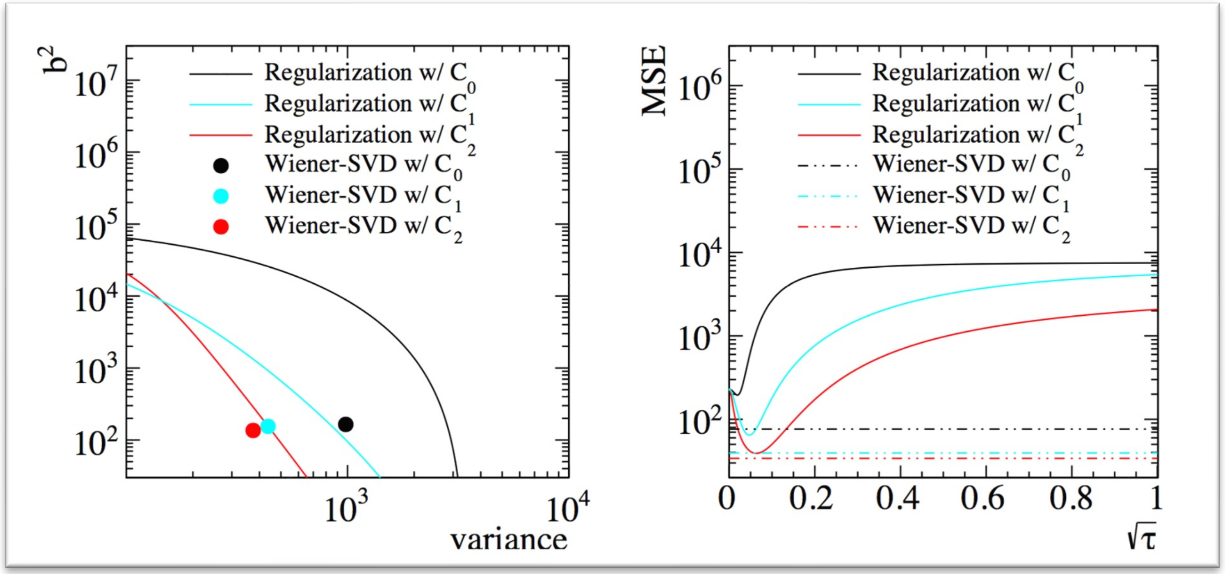

- The regularization introduce an equivalent smearing matrix **A_c**

  → an improved data/model comparison

$$M = R \cdot S \quad \Rightarrow \quad \hat{s} = A_C \cdot (R^T R)^{-1} \cdot R^T \cdot M$$

Neutrino energy distribution and $\sigma(E_\nu)/\langle E_\nu \rangle$

- Reco space

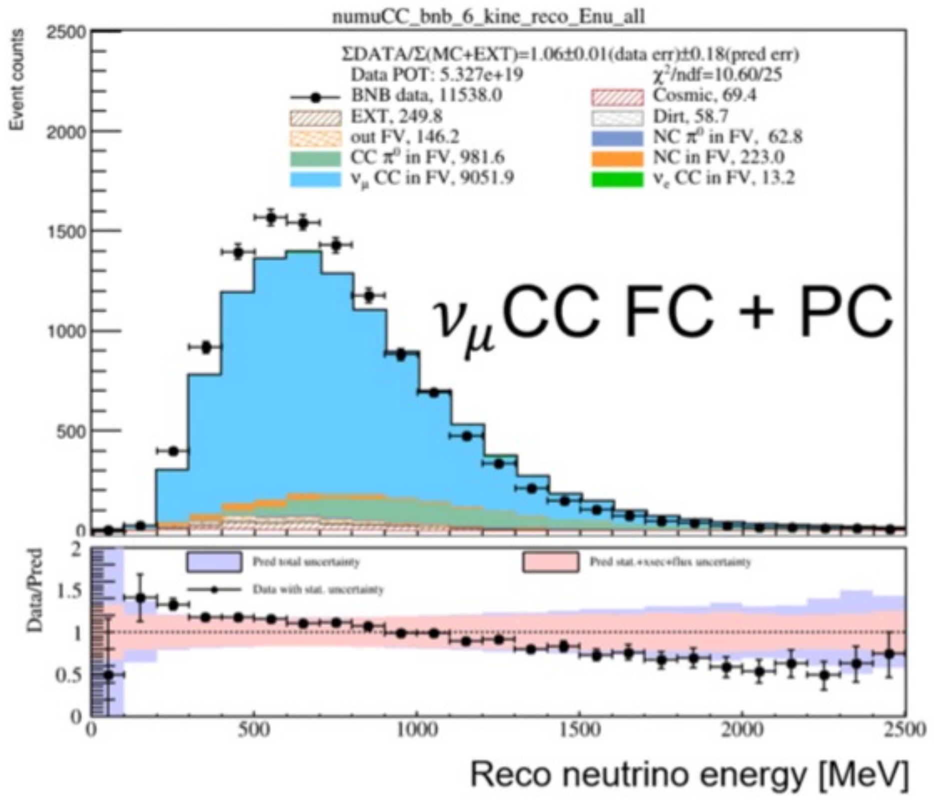

- Response matrix

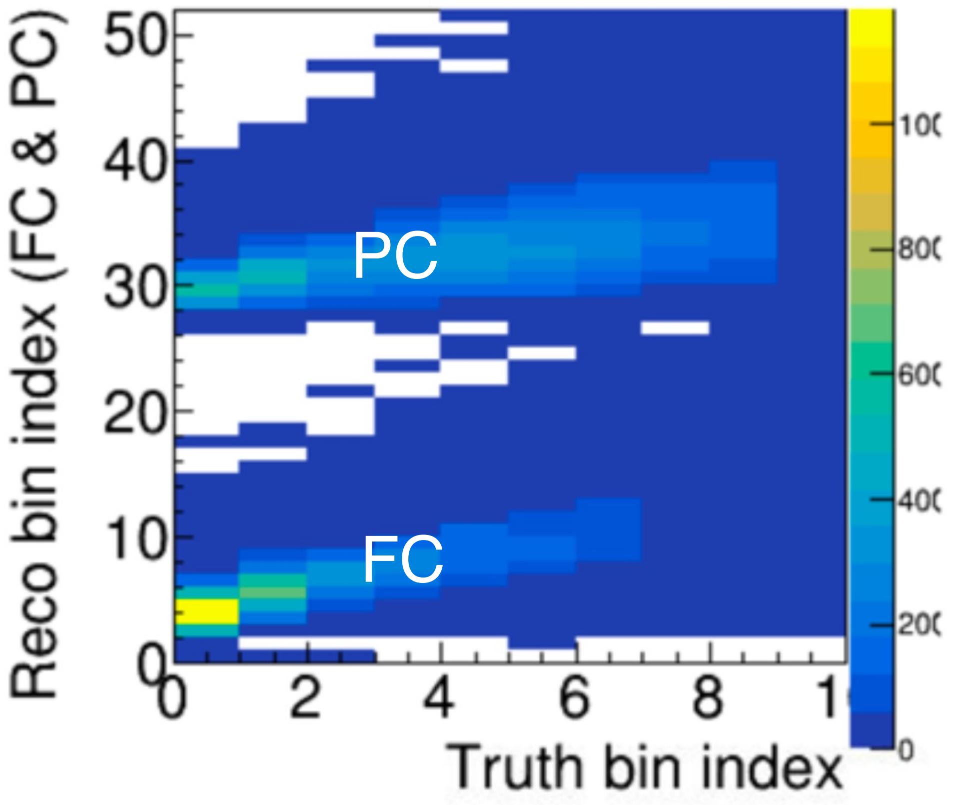

Neutrino energy distribution and $\sigma(E_\nu)/\langle E_\nu \rangle$

- Reco space

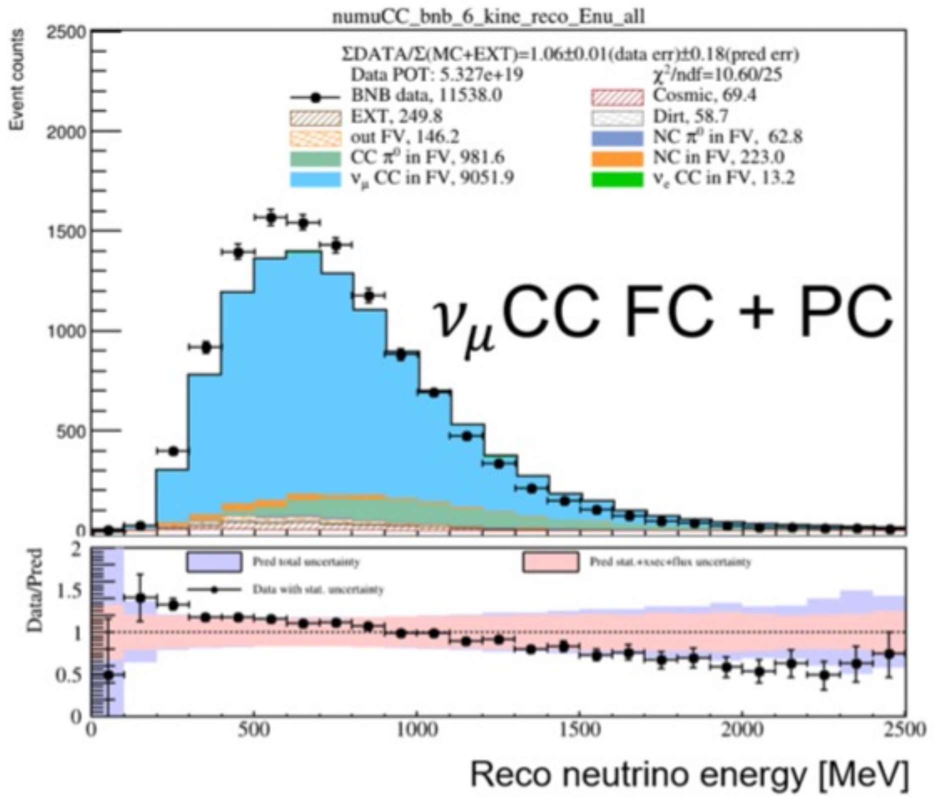

- Unfolded space

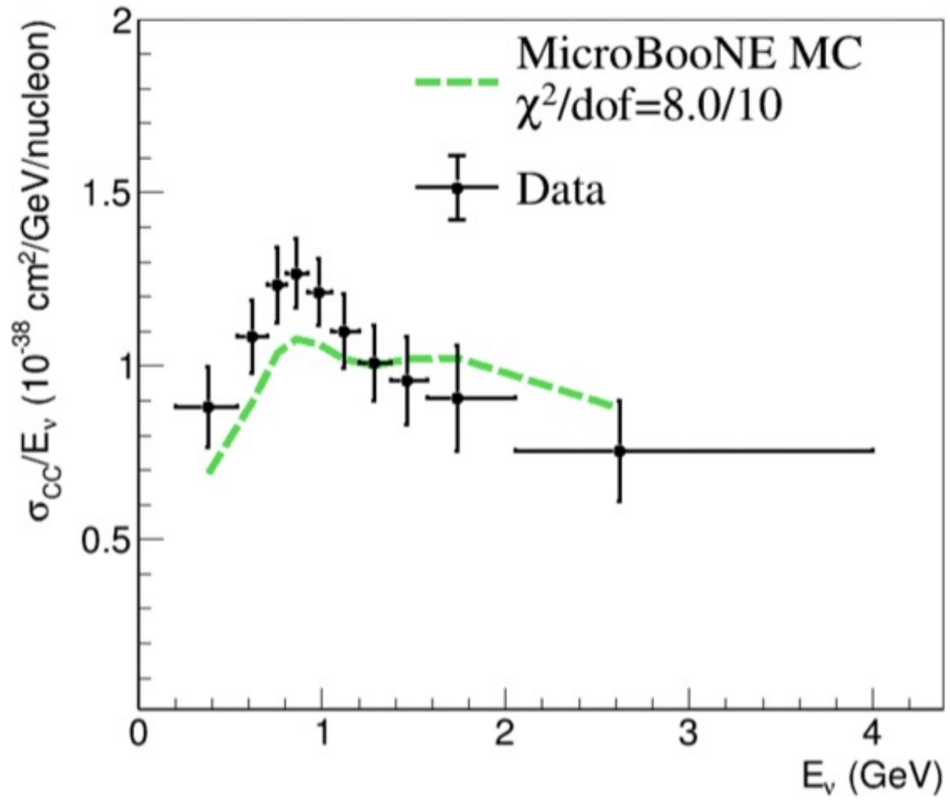

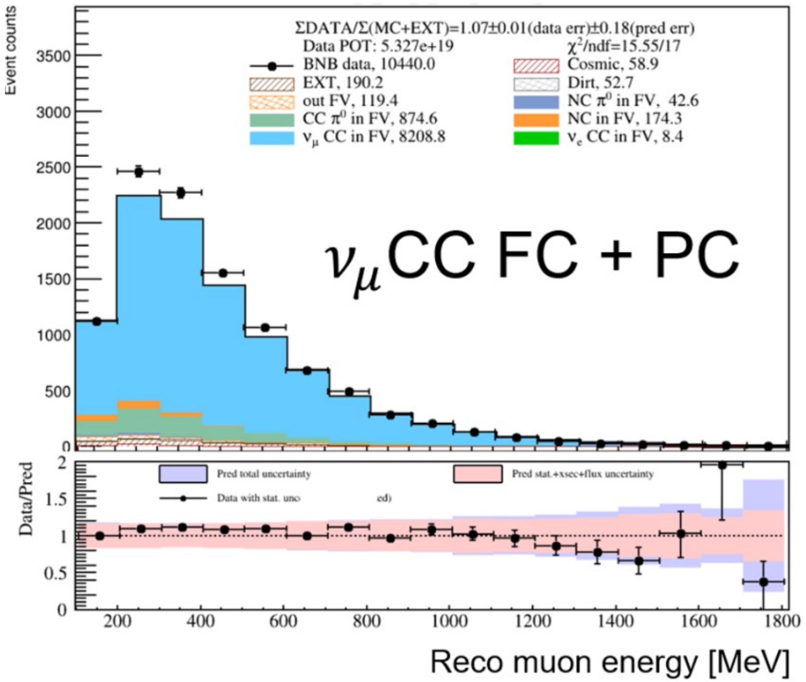
ΣDATA/Σ(MC+EXT)=1.07±0.01(data err)±0.18(pred err)
Data POT: 5.327e+19
χ^2/ndf=15.55/17
BNB data, 10440.0
Cosmic, 58.9
EXT, 190.2
Dirt, 52.7
out FV, 119.4
NC π^0 in FV, 42.6
CC π^0 in FV, 874.6
NC in FV, 174.3
ν_μ CC in FV, 8208.8
ν_e CC in FV, 8.4
ν_μCC FC + PC
Event counts
Data/Pred
Pred total uncertainty
Pred stat.+xsec+flux uncertainty
Reco muon energy [MeV]

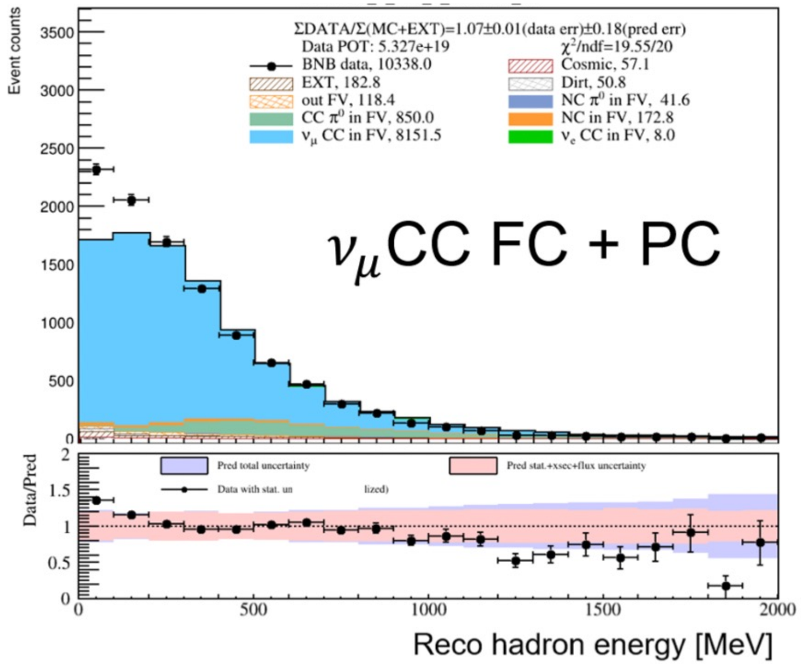
ΣDATA/Σ(MC+EXT)=1.07±0.01(data err)±0.18(pred err)
Data POT: 5.327e+19
χ^2/ndf=19.55/20
BNB data, 10338.0
Cosmic, 57.1
EXT, 182.8
Dirt, 50.8
out FV, 118.4
NC π^0 in FV, 41.6
CC π^0 in FV, 850.0
NC in FV, 172.8
ν_μ CC in FV, 8151.5
ν_e CC in FV, 8.0
ν_μCC FC + PC
Event counts
Data/Pred
Pred total uncertainty
Pred stat.+xsec+flux uncertainty
Reco hadron energy [MeV]

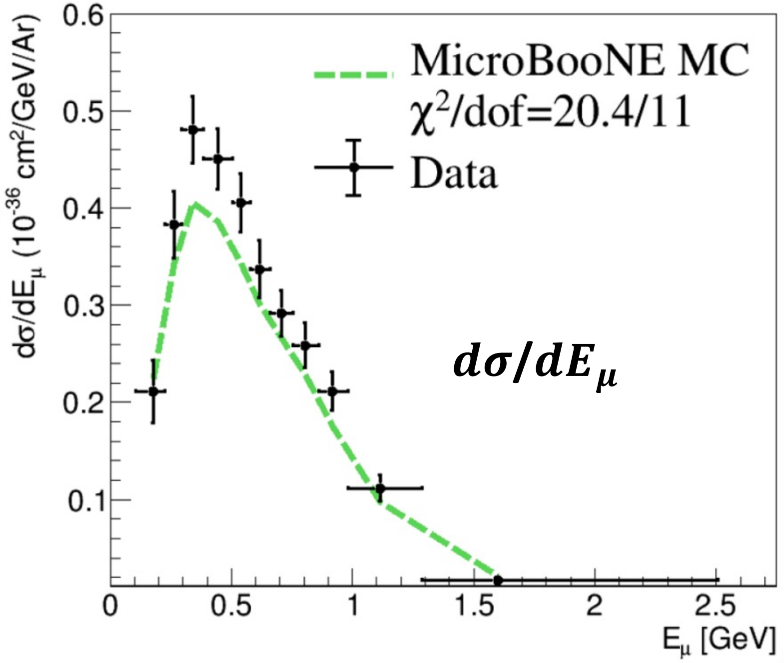
MicroBooNE MC
χ^2/dof=20.4/11
Data
$d\sigma/dE_\mu$
$d\sigma/dE_\mu$ (10^{-36} cm^2/GeV/Ar)
E_μ [GeV]

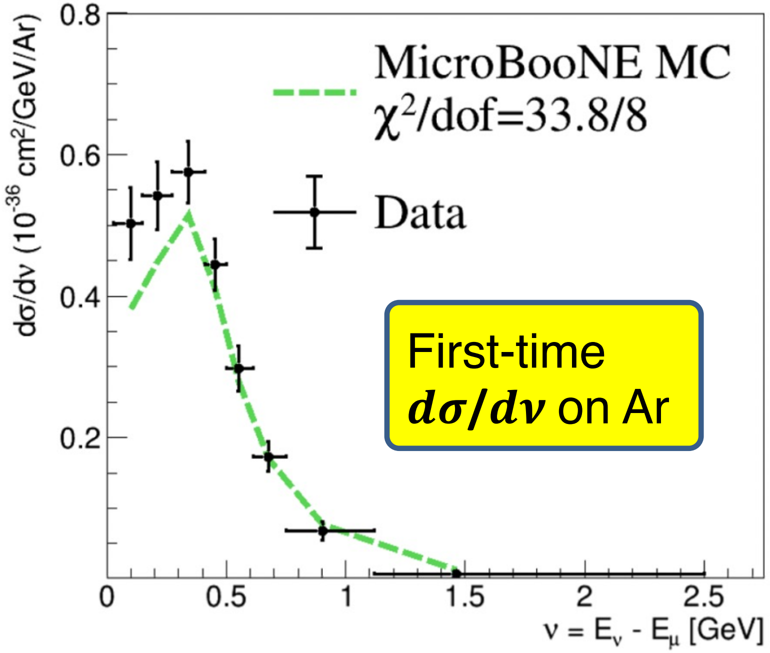
MicroBooNE MC
χ^2/dof=33.8/8
Data
First-time
$d\sigma/d\nu$ on Ar
$d\sigma/d\nu$ (10^{-36} cm^2/GeV/Ar)
$\nu = E_\nu - E_\mu$ [GeV]

Cross-section results and model comparison

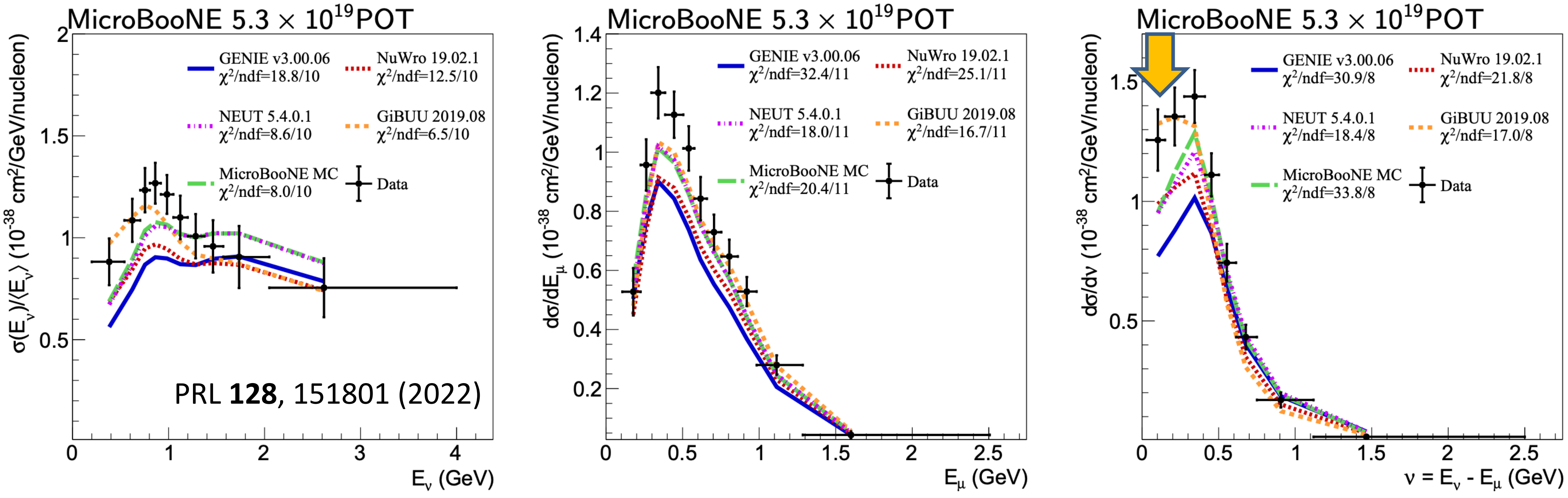

- Good separation power of model predictions from different generators
- GiBUU's central prediction gives best agreement at low energy transfer
  - Relative to other models, GiBUU predicts larger cross section for 2p2h at low ν

Next: 3-D inclusive cross section with $6.4{\times}10^{20}$ POT

- The model validation of missing energy will be extended to involve more dimension (muon polar angle)

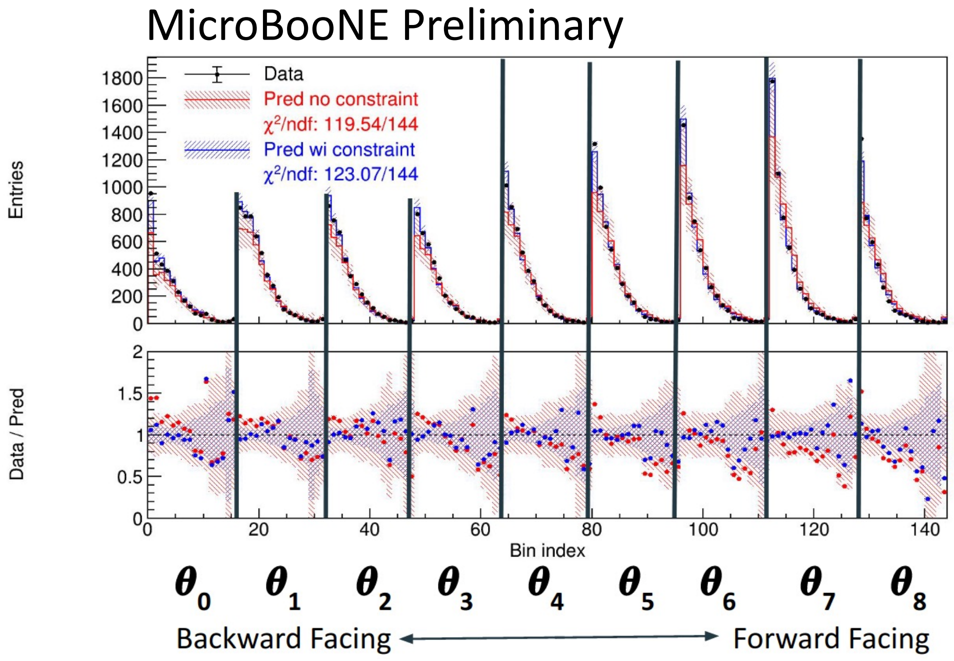

- First 3-D cross-section measurement for ν-Ar using unfolding

$$d^2\sigma/dP_\mu d\cos\theta_\mu\,(E_\nu)$$

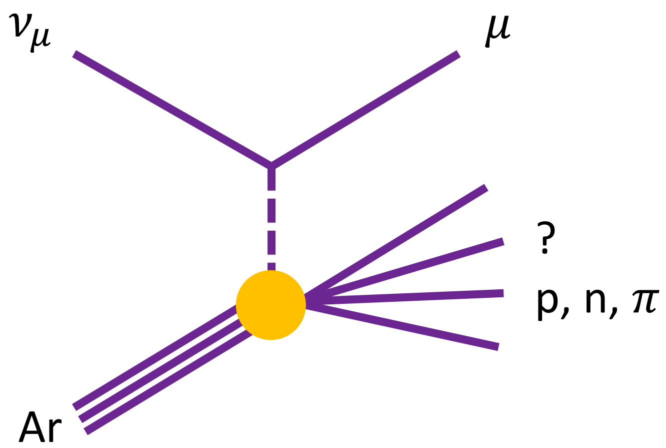

Summary

- Continuous improvement on the neutrino cross section modeling and measurement from data are important for precision accelerator-based neutrino oscillation measurements
  - Examples on argon include ArgoNeuT, MicroBooNE and SBN

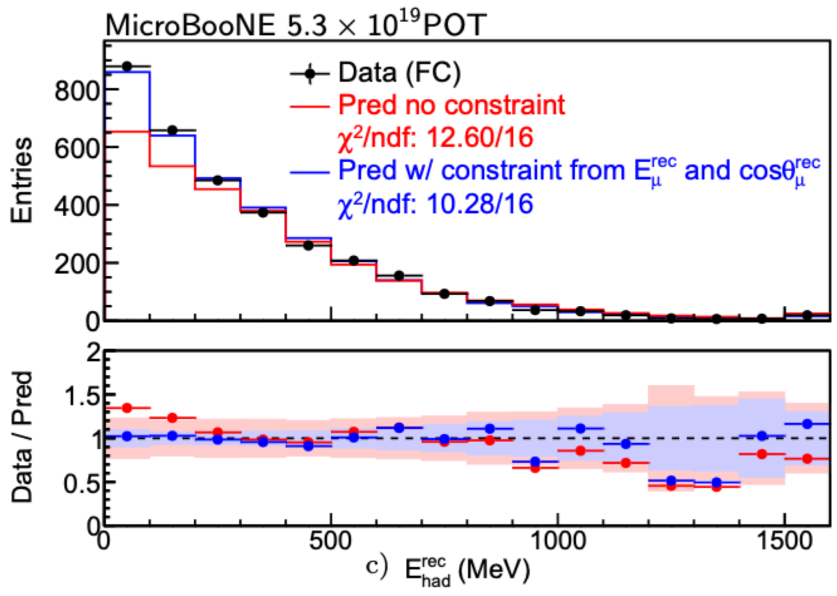

- A novel model validation for $\mathbf{D}(E_\nu \rightarrow E_{reco})$ using a conditional constraint is introduced

$\boldsymbol{\sigma(E_\nu)/\langle E_\nu \rangle}$

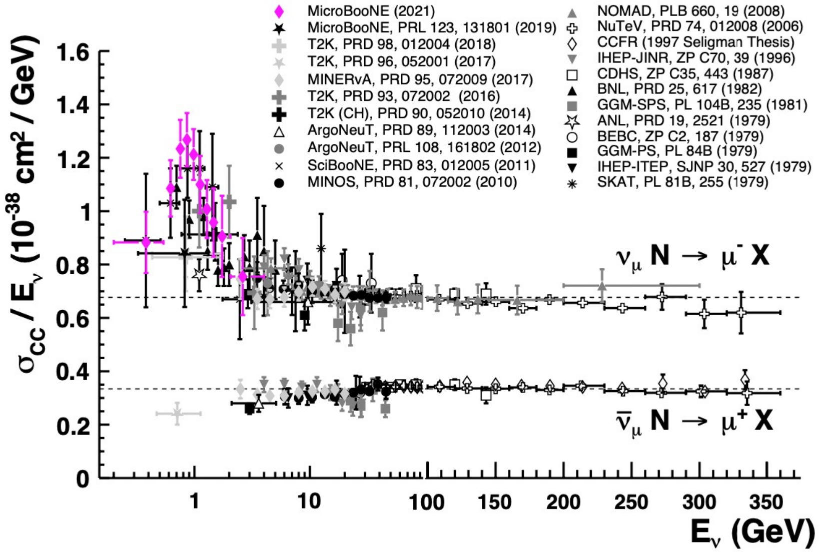

- A set of energy-dependent ν-Ar cross sections was extracted using Wiener-SVD unfolding procedure
  - Good separation power of model predictions from different generators

Evolved cross section extraction method

- Forward-folding

$$\left(\frac{d\sigma}{dp_\mu}\right)_i = \frac{N_i - B_i}{\tilde{\epsilon}_i \cdot N_{\text{target}} \cdot \Phi_{\nu_\mu} \cdot (\Delta p_\mu)_i}$$

N_i (B_i): # of candidate (bkgd) in reco bin i
N_{target} : # of argon nuclei
Φ_{ν_μ}: integrated neutrino flux
$(\Delta p_\mu)_i$: width for reco bin i
$\tilde{\epsilon}_i$: effective efficiency for reco bin i

- (Wiener-SVD) unfolding

$$\boldsymbol{M_i = \sum_j R_{ij} \cdot S_j + B_i}$$

M_i (B_i): # of candidate (bkgd) in reco bin i
R_{ij}: response (smearing) matrix
S_j: cross section to be extracted in **true bin j**

➥ Flux shape uncertainty properly treated ‡

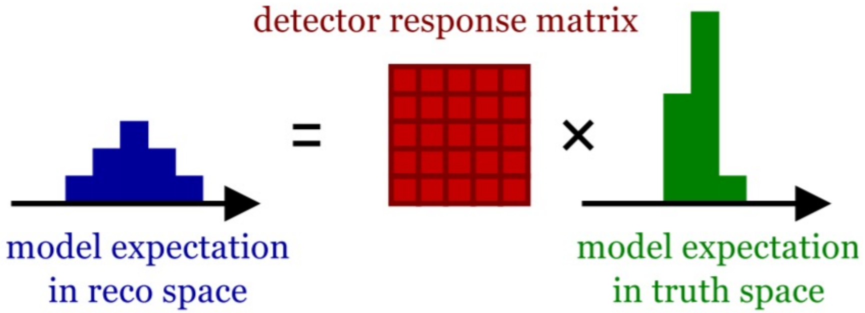

Wiener-SVD: JINST 12 (2017) 10, P10002

‡ : Phys. Rev. D 102 (2020) 113012

Fake Data: GENIE v2

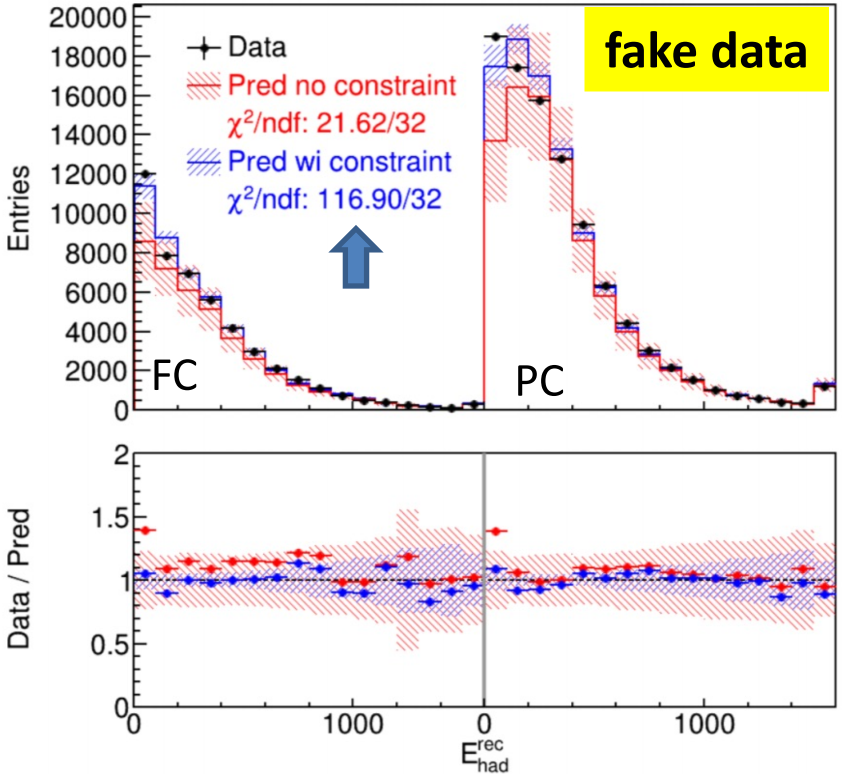

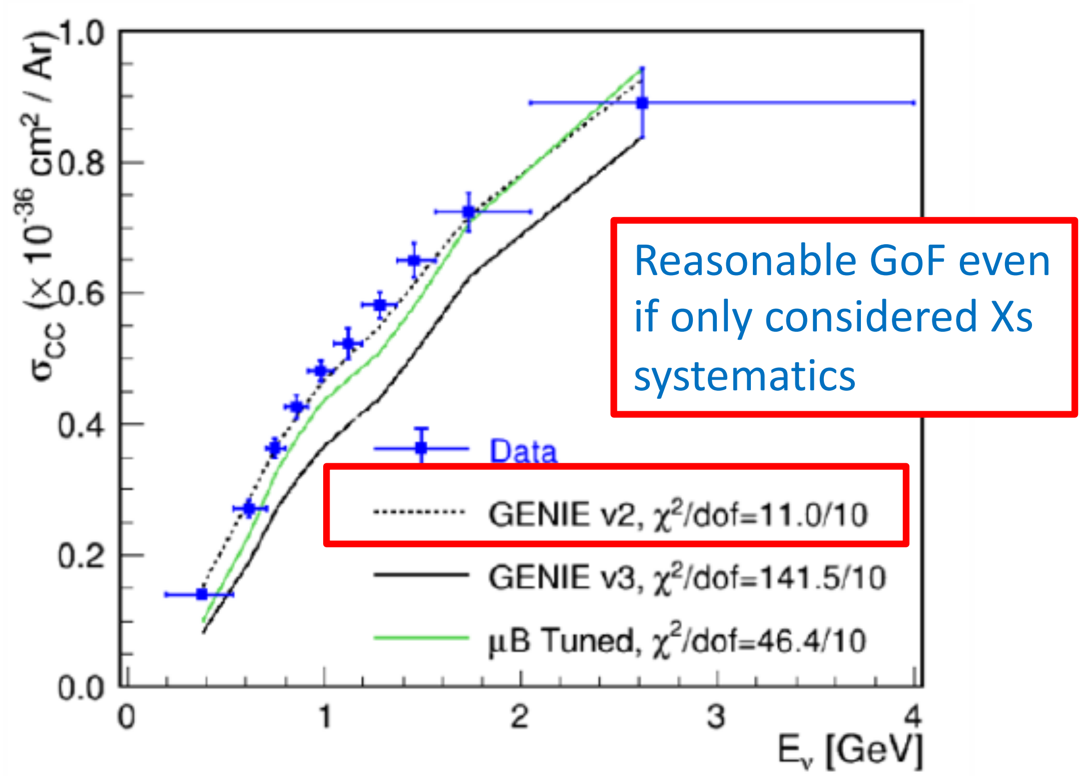

- Fake data (GENIE v2) shows a very poor χ^2/ndf for $E_{\rm had}^{\rm rec}$ after constraint to muon kinematics

- Model validation procedure is much more sensitive (stringent) to the model defects than the extraction of energy-dependent Xs

Fake Data: Enhance Missing Hadronic Energy

E_p^{rec} scaling factor	FC events (ndf=16)	PC events (ndf=16)	FC+PC (ndf=32)
0.95	2.55 (1.00)	4.08 (1.00)	5.34 (1.00)
0.90	8.90 (0.92)	17.13 (0.38)	21.05 (0.93)
0.85	18.66 (0.29)	39.45 (0.00)	47.01 (0.04)
0.80	32.95 (0.01)	67.88 (0.00)	80.60 (0.00)

χ^2 P-value

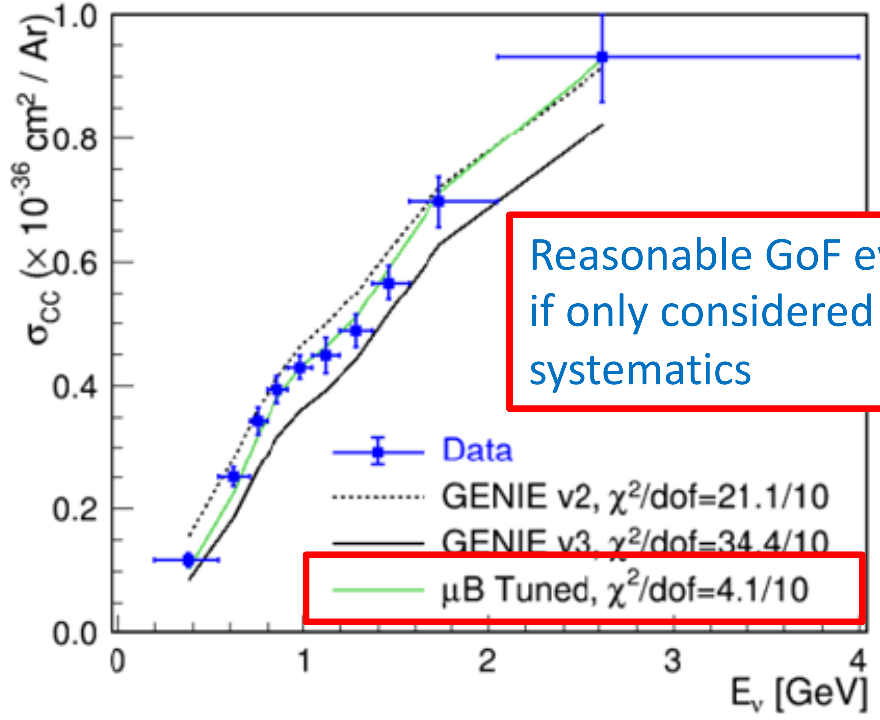

Reasonable GoF even if only considered Xs systematics

- χ^2/ndf has a significant increase with a shift of ~15% in the hadronic energy fraction allocated to protons (mimicking a variation of the proton-inelastic cross section)

- Model validation procedure is much more sensitive (stringent) to the model defects than the extraction of energy-dependent Xs

Largest Sample of neutrino interactions on argon in the world

2015-10-15 first beam

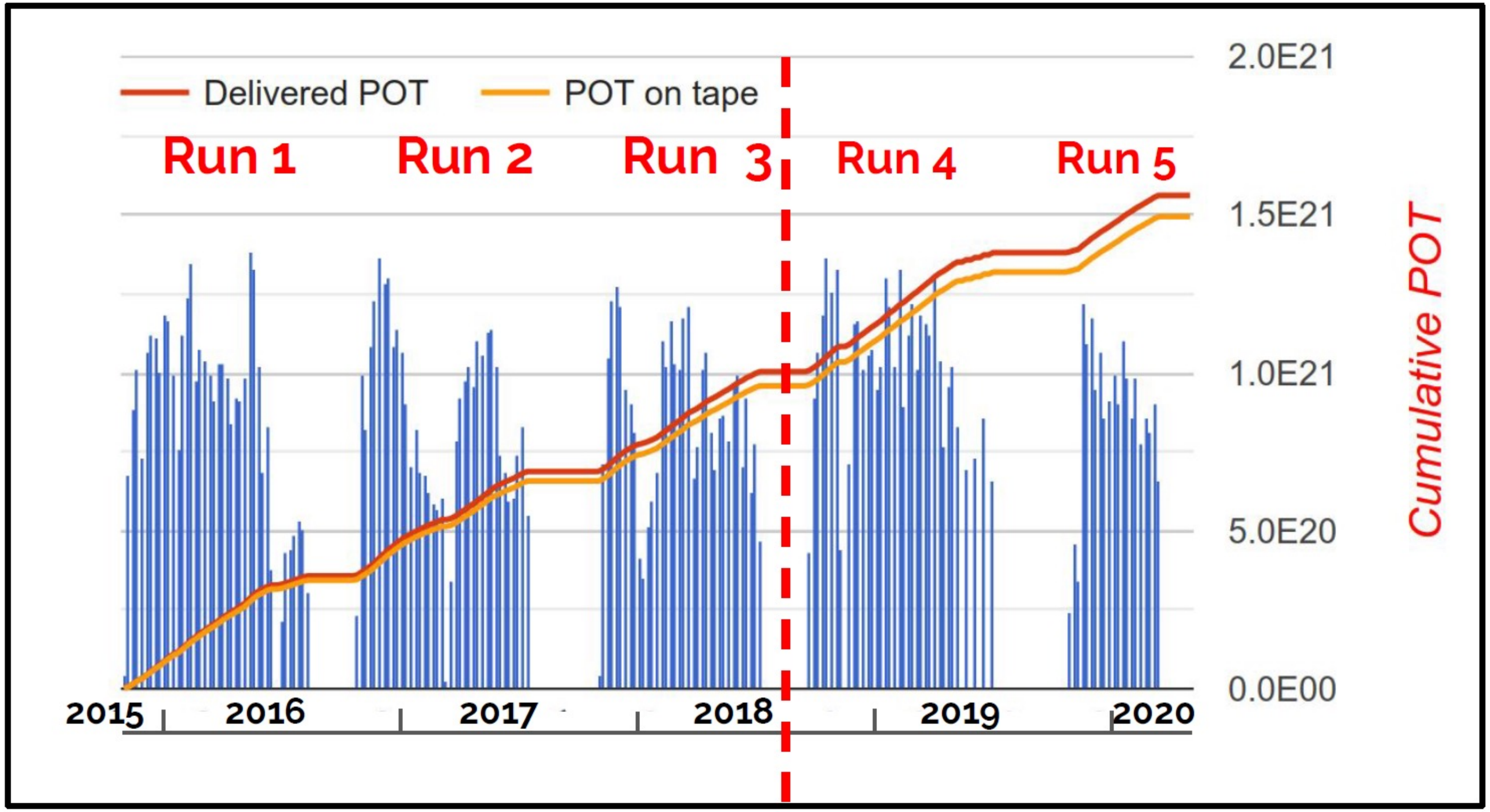

Recent physics results are based on ~7e20 protons-on-target from run 1 - 3

Searching for LEE

- ν_e analyses
  - restricting to quasi-elastic kinematics (Deep Learning , 1e1p)
  - MiniBooNE-like final state (Pandora, 1eNp0π, 1e0p0π)
  - all ν_e final states (Wire-Cell, 1eX)
- single photon analysis
  - targeting Delta radiative decay hypothesis (Pandora, 1γ1p, 1γ0p)

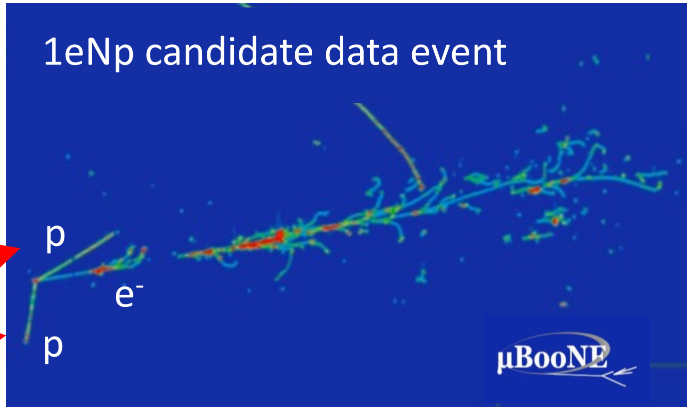

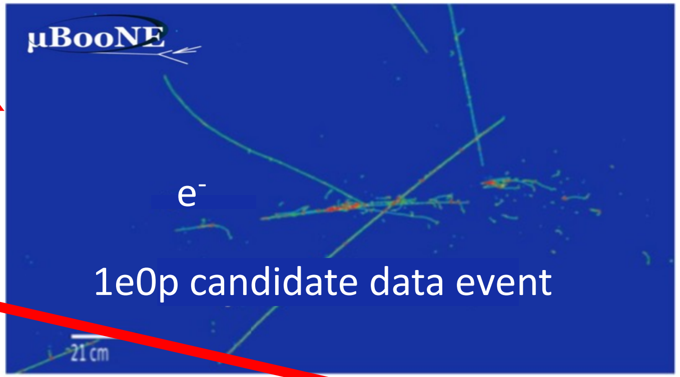

- 4 analyses, 6 final states

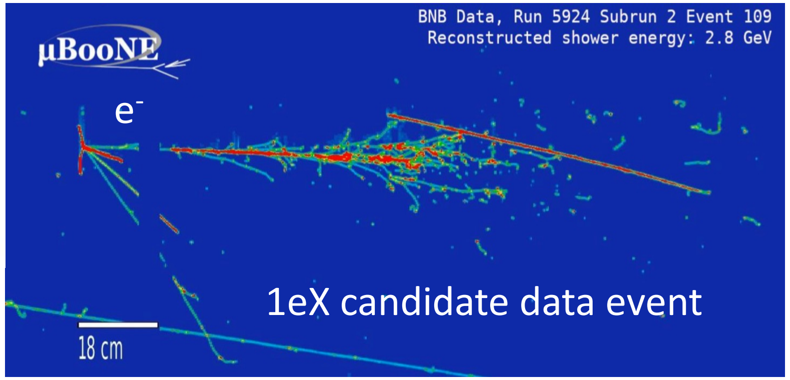

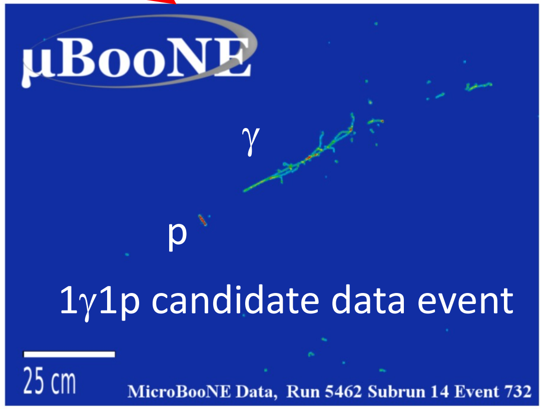

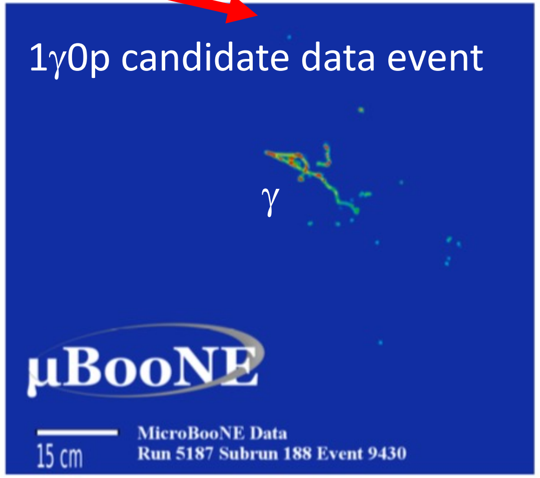

Search for Low-Energy Excess in ν_eCC

Channels	Reconstruction	Efficiency	Purity	Data Events
CCQE 1e1p	Deep Learning	6.6%	75%	25
1e0p0π	Pandora	9%	43%	34
1eNp0π	Pandora	15%	80%	64
Inclusive 1eX	Wire-Cell	46%	82%	606

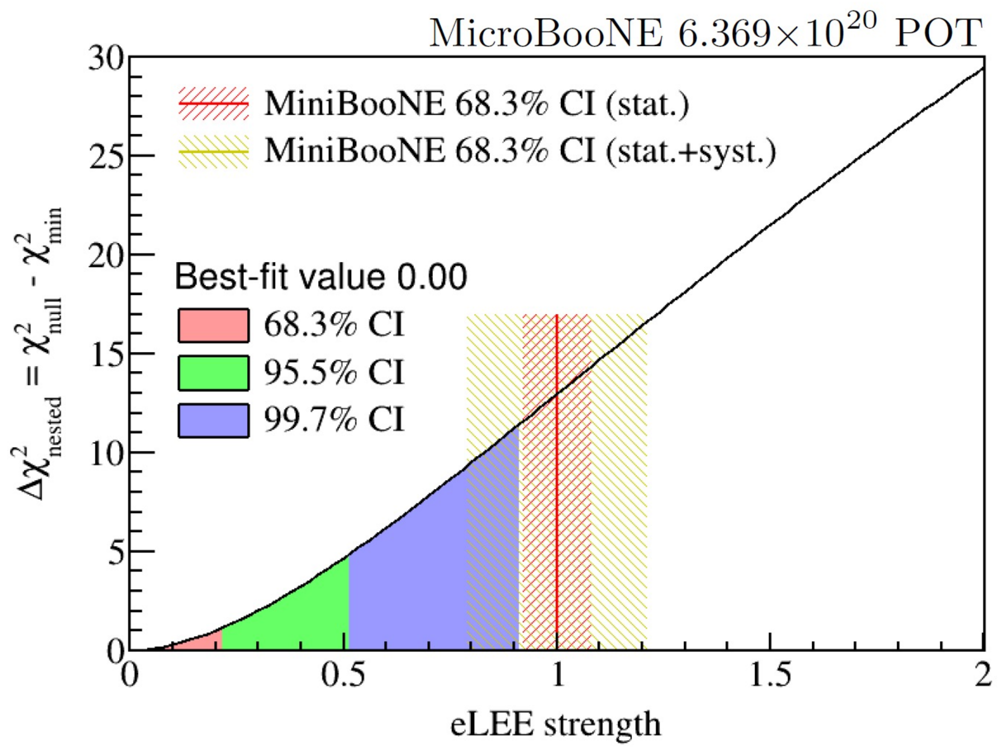

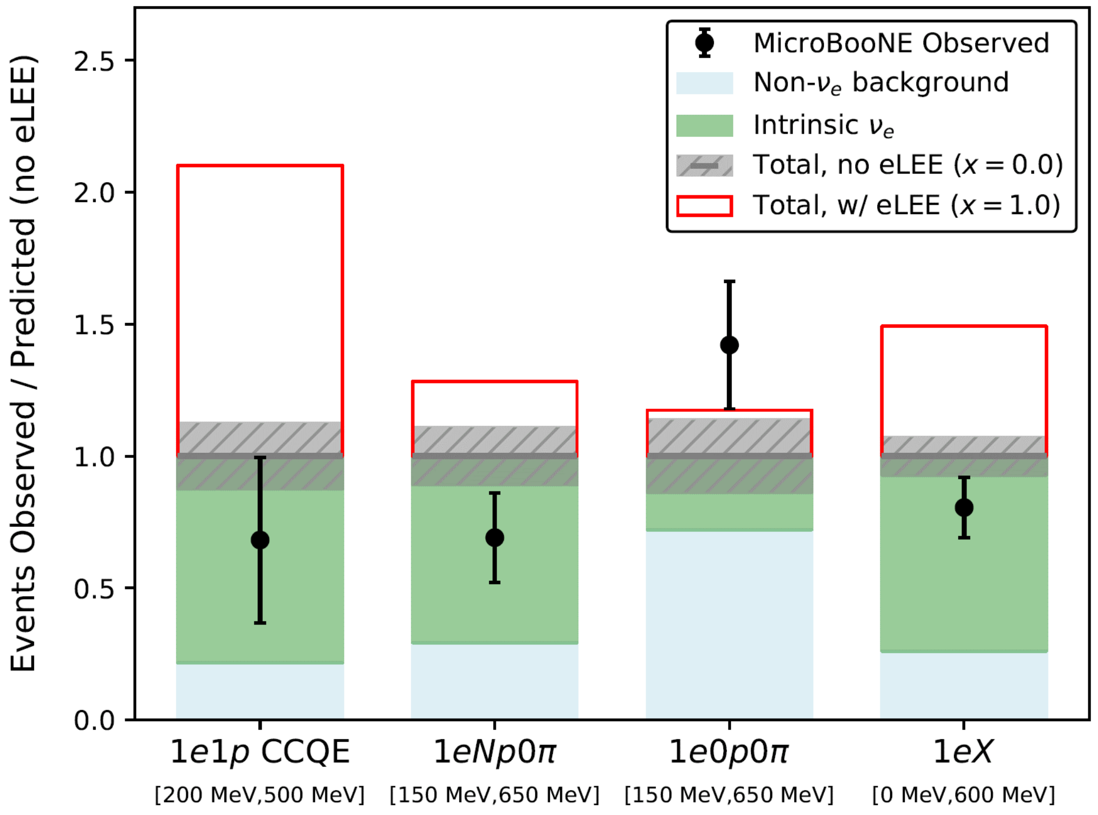

arXiv:2110.14054

ν_e cannot be the sole explanation of MiniBooNE excess!

Search LEE in Neutral-Current (NC) Δ→Nγ

- No LEE observed in NC Δ→Nγ
- Best-fit LEE strength at zero
- 90% CL limit on the branching ratio is 1.38%
  - Consistent with the expectation of 0.6%
- x50 fold improvement over the world's best limit at O(1 GeV) region

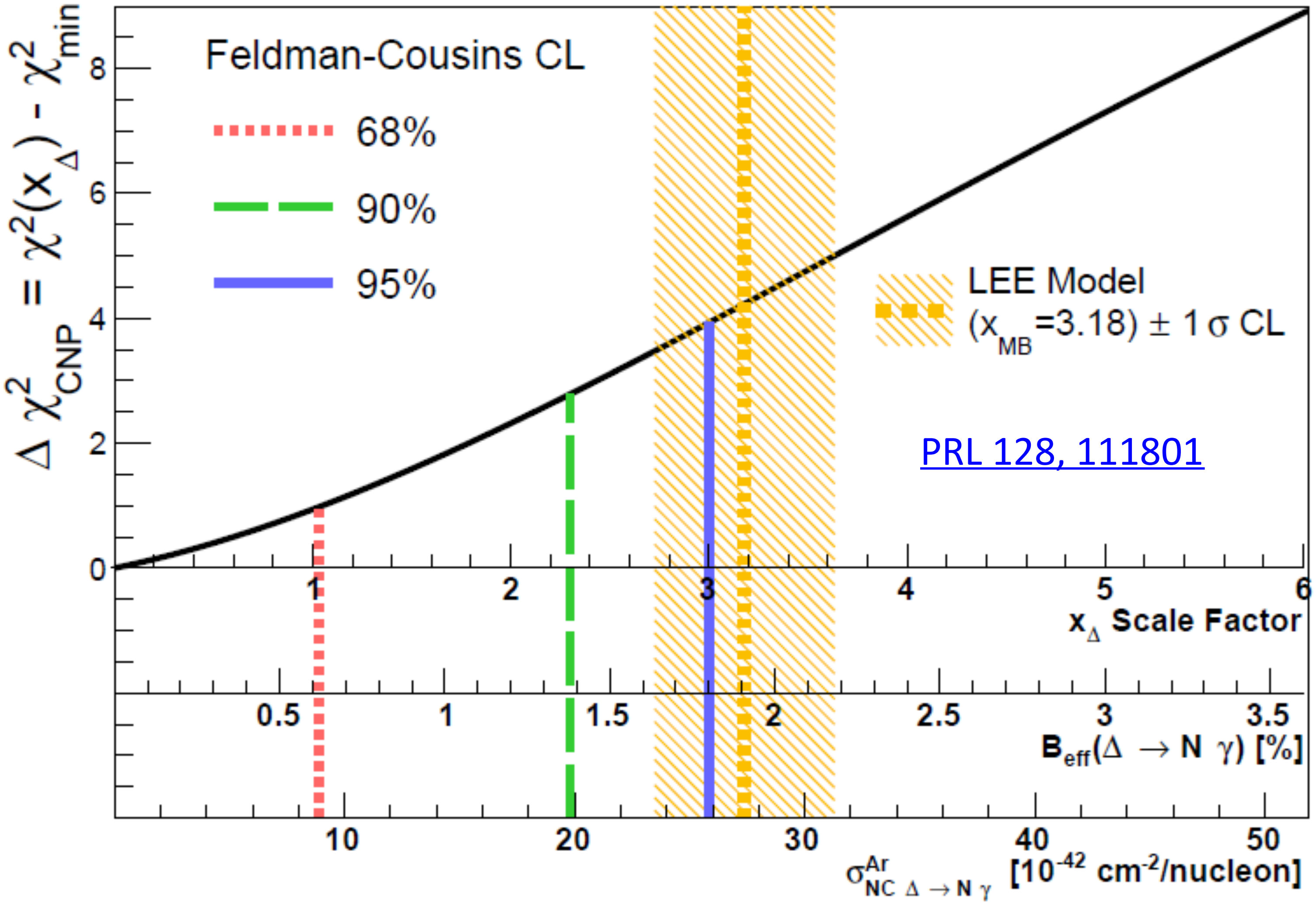

PRL 128, 111801

MicroBooNE pioneered the Usage of Cold Electronics in LArTPCs

Long-term stability of CE

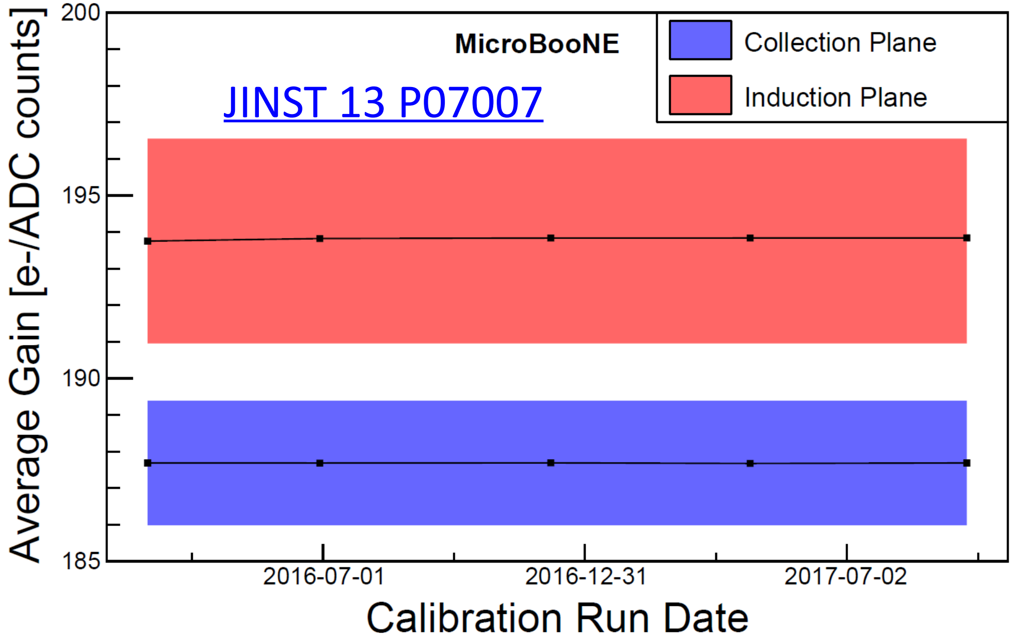

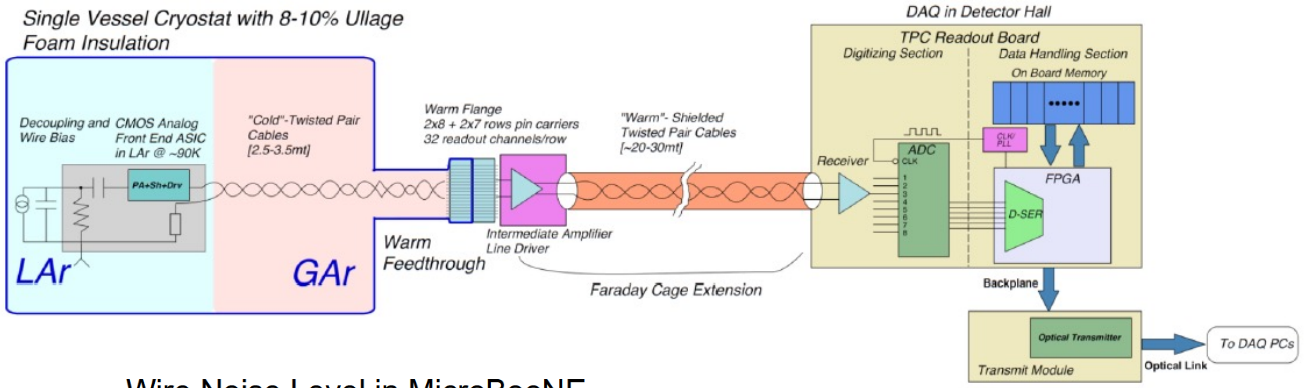

Wire Noise Level in MicroBooNE

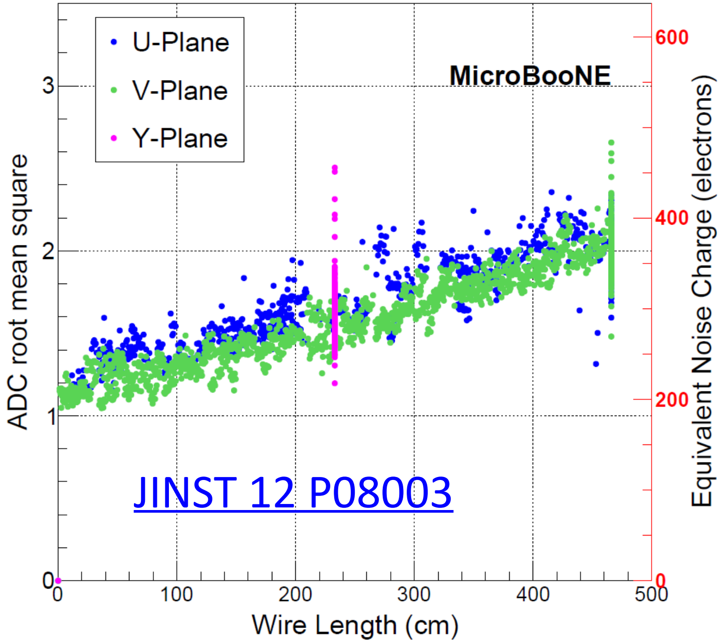

V. Radeka et al. "Cold electronics for 'Giant' Liquid Argon Time Projection Chambers", https://inspirehep.net/literature/922710

- Placing the preamplifier inside LAr significantly reduced electronics noise -- 5-6 times better than that of past warm electronics → an enabling technology
  - Foundation of technology advancements in signal processing (e.g. 2D deconvolution) and event reconstruction

LAr Purity in MicroBooNE

- MicroBooNE is the first TPC using passive insulation & filling without evacuation
  - "Piston-purge" and recirculation before cool down, procedure pioneered in LAPD
  - In-situ regenerable impurity filters

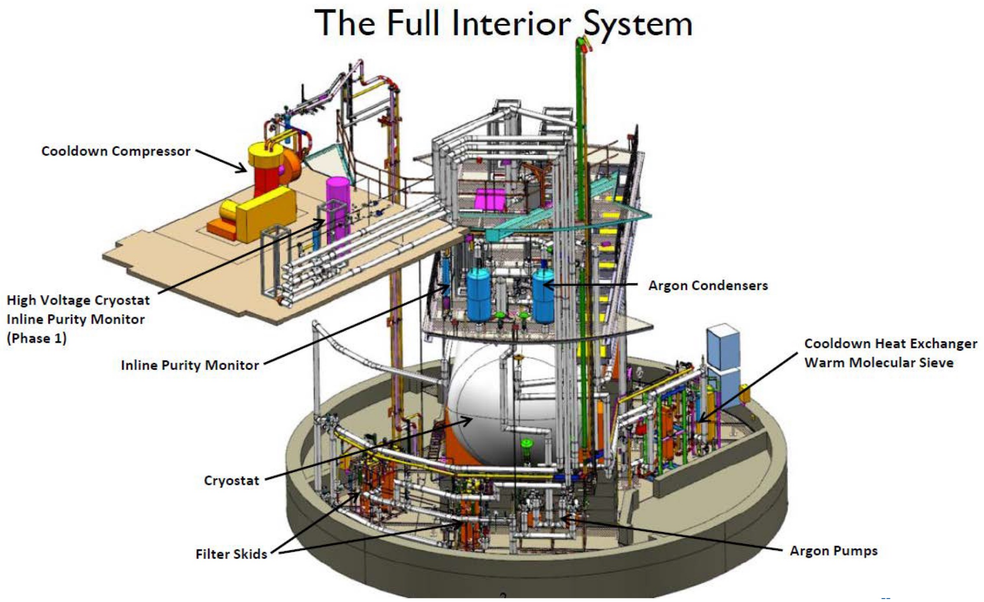

- x6 better than the design goal
- Stable over 6 years data taking

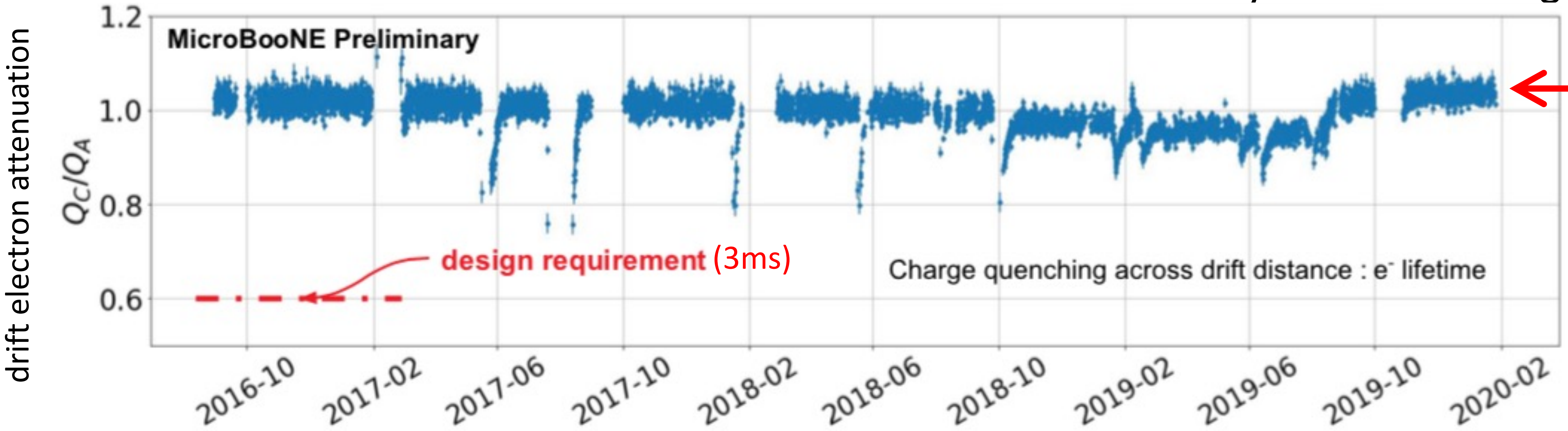

> 18 ms

(< 17 ppt O_2 contamination

MicroBooNE public note #1026

Improved TPC Signal Processing, Detector Simulation, and Improved Evaluation of Detector Systematics

- 2D deconvolution algorithm allows to accurately recover the ionization electrons from recorded original signals
- Improved 2D detector simulation, modeling both the long-range induction and the position-dependent effects lead to much better data/MC consistency

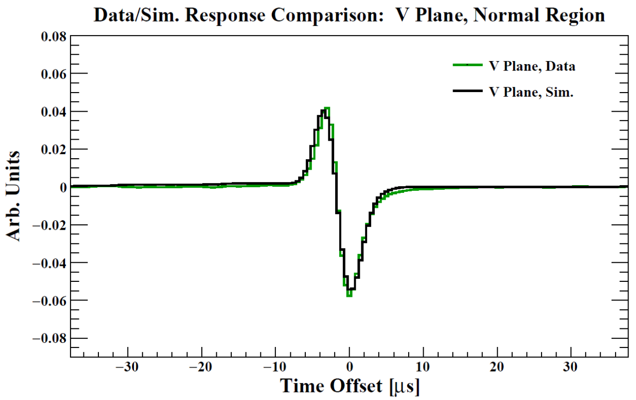

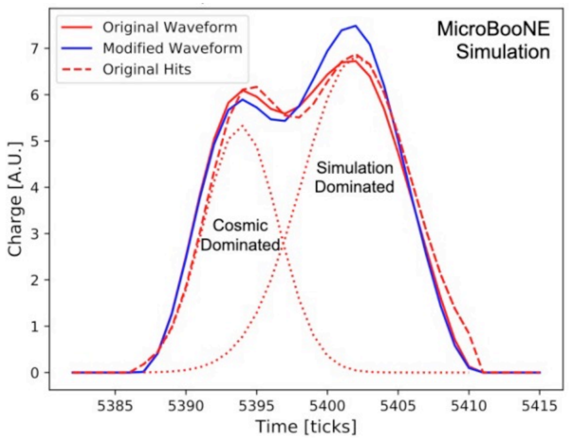

arXiv:2111.03556

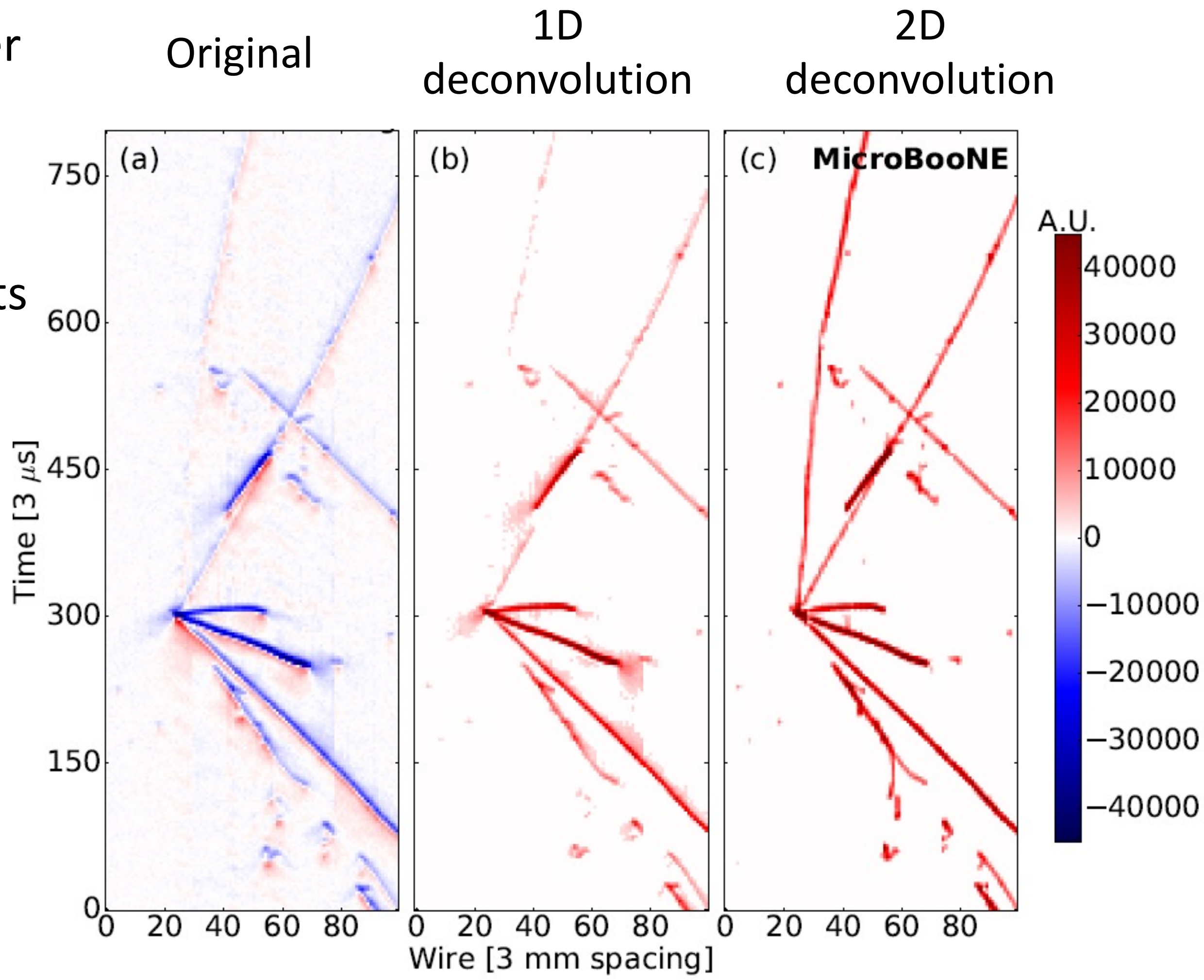

JINST 13 P07006/7

- Improved evaluation of detector systematic uncertainties with changes to detector modeling

nuPRISM

- nuPRISM: a technique to obtain effective mono-energetic neutrino flux with a series of off-axis beams
  - An in-situ calibration with the same beamline for FD
  - A direct calibration of the energy modeling $\mathbf{D}(E_\nu \rightarrow E_{reco})$ with mono-energetic beam
- Practical constraints likely require neutrino cross section models

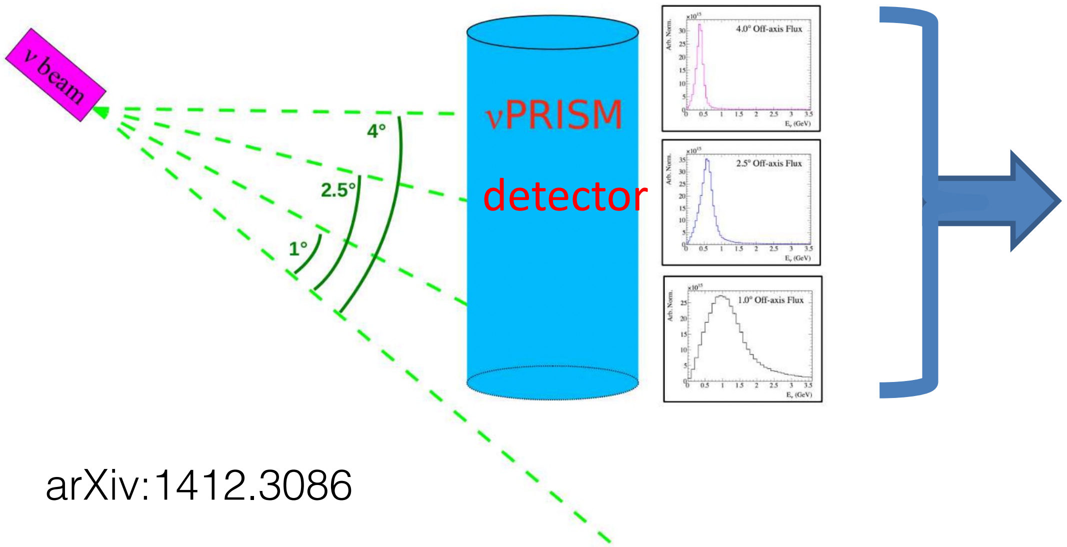

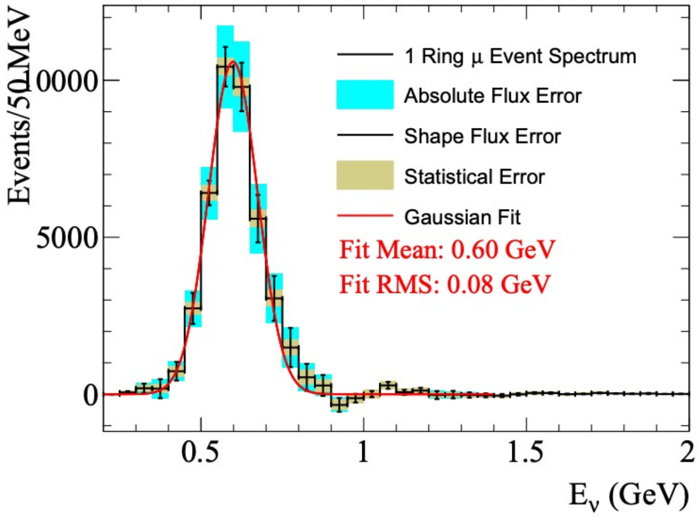

arXiv:1412.3086

Difficulties from (broadband) beam

- The precision of $\sigma(E_\nu)$ measurement is limited by large beam flux uncertainty
- Broadband beam flux ⇒ no mono-energetic beam to calibrate detector response $\mathbf{D}(E_\nu \rightarrow E_{reco})$

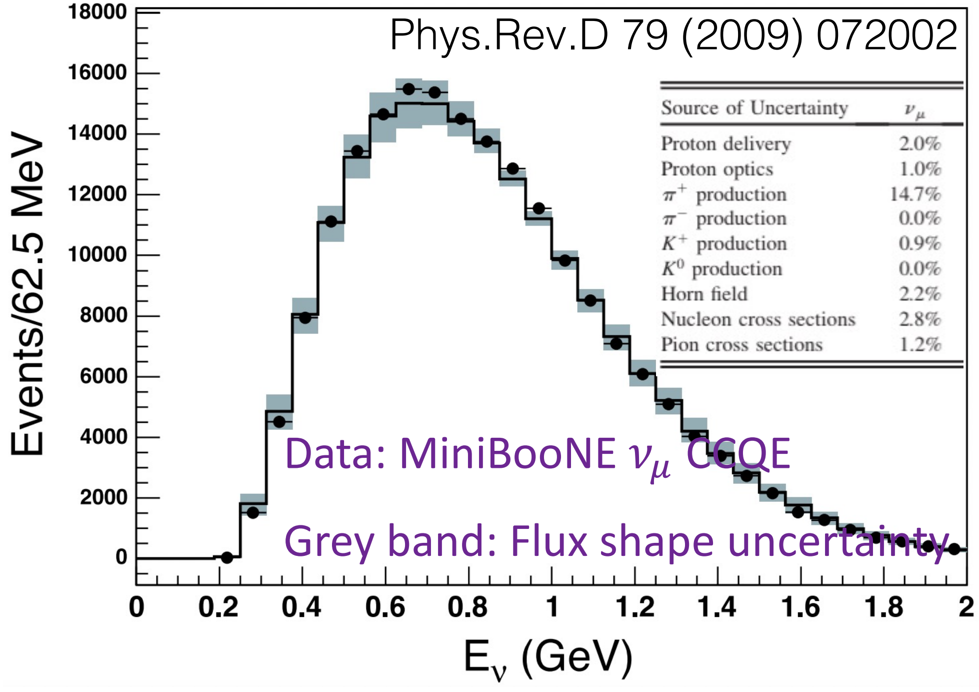

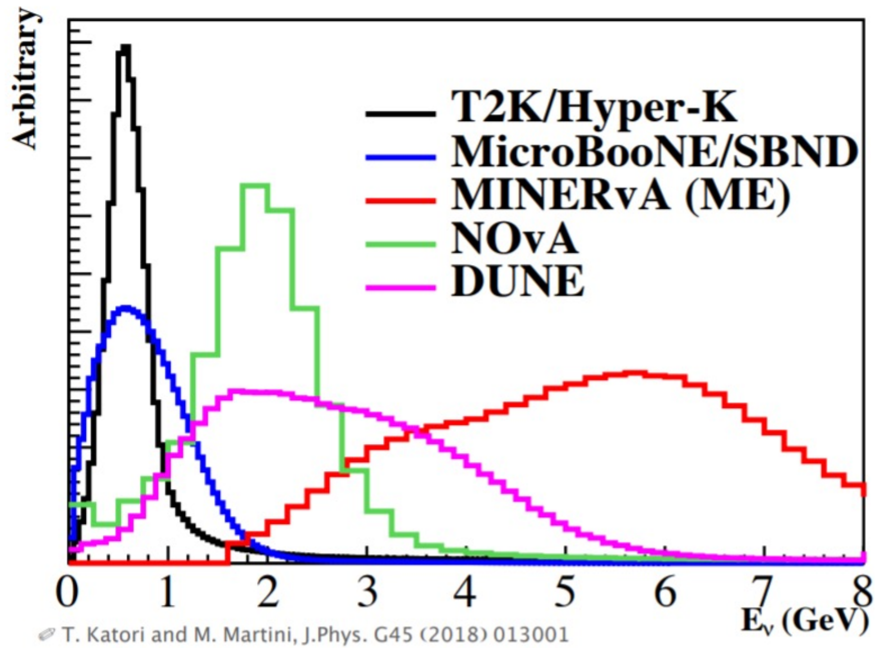

Cross-section measurements are important

- The energy-dependent cross section is desired: $\sigma(E_\nu)$ and $\mathrm{d}\sigma/\mathrm{d}\nu$
- Improvement of the cross-section model, an effective description, is a long-term process

JINST 12 (2017) 01, P01016

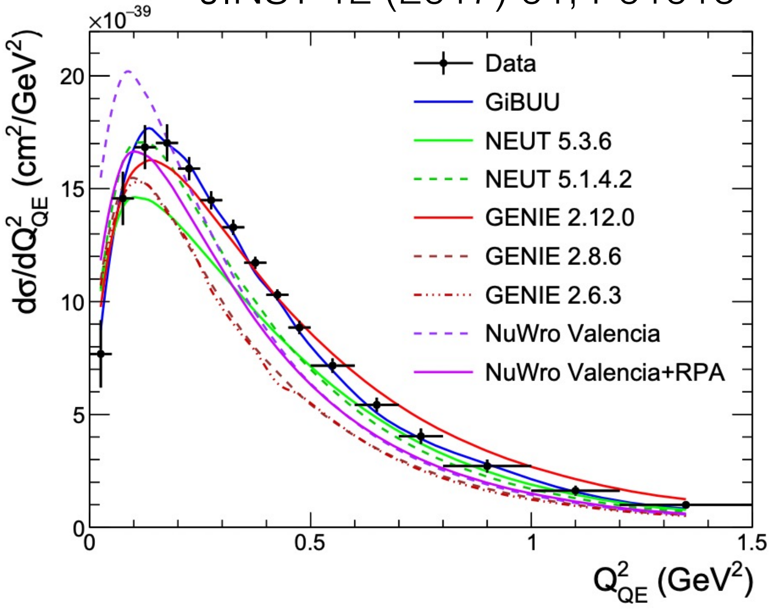

(a) MiniBooNE ν–CH_2 CCQE

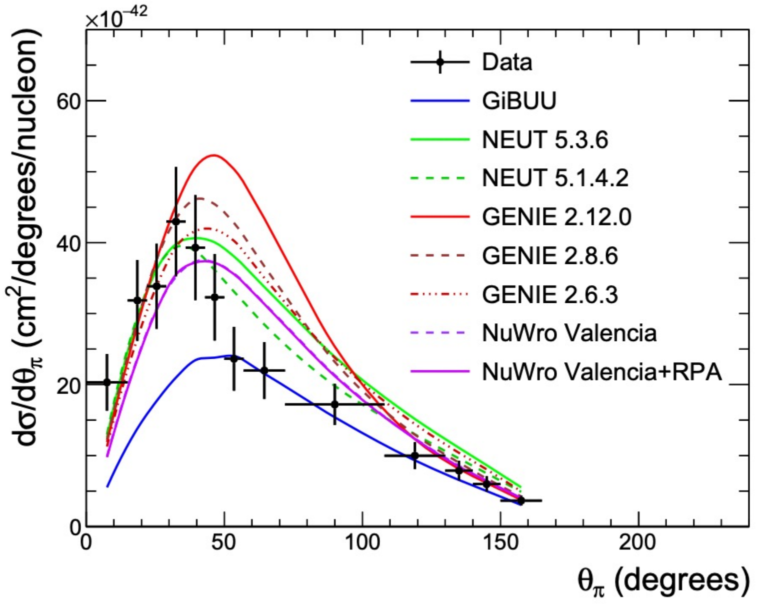

(b) MINERvA ν–CH CC$1\pi^\pm$

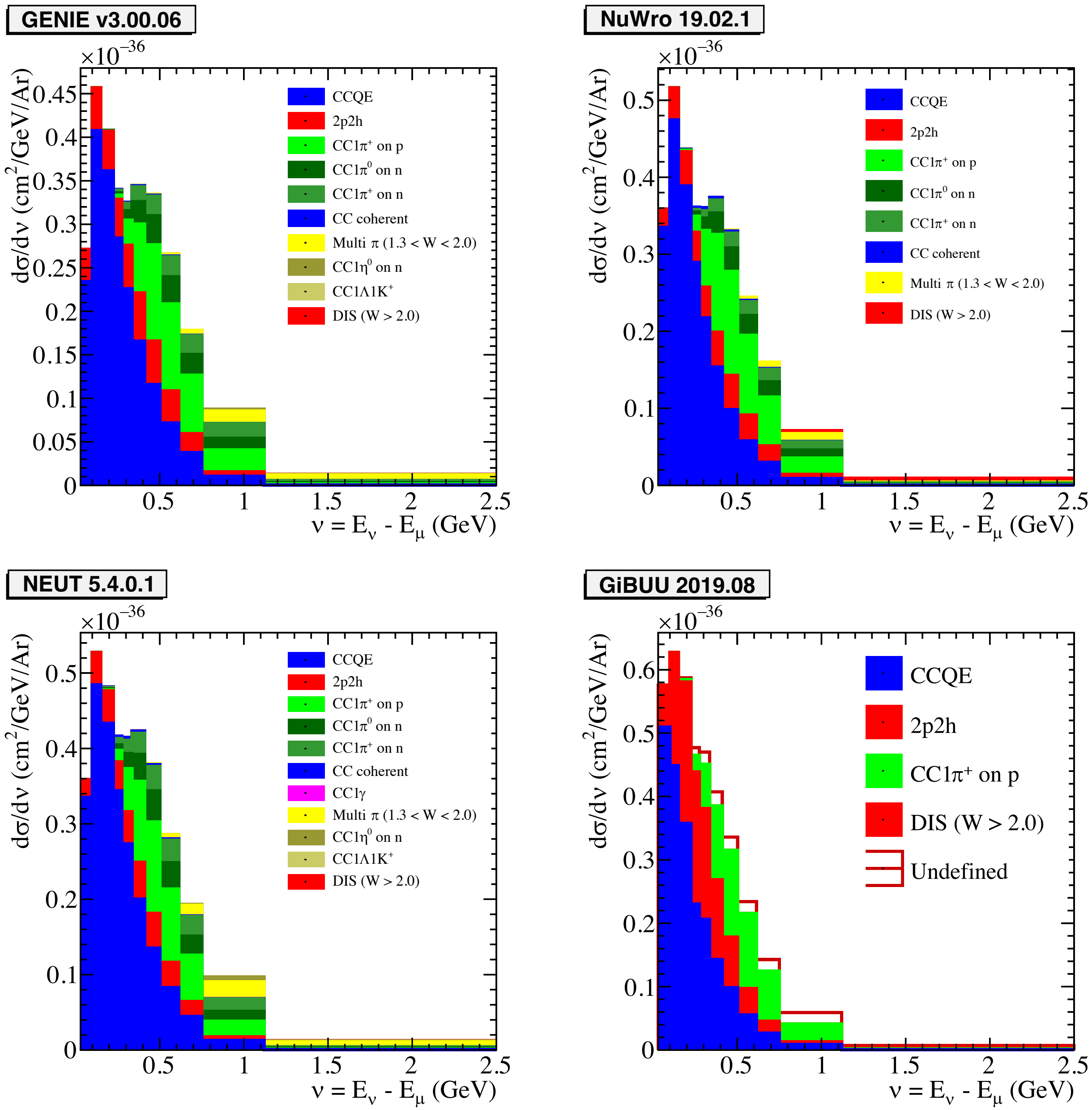
GENIE v3.00.06
NuWro 19.02.1
NEUT 5.4.0.1
GiBUU 2019.08
$\times 10^{-36}$
$d\sigma/d\nu$ (cm^2/GeV/Ar)
$\nu = E_\nu - E_\mu$ (GeV)
CCQE
2p2h
CC1π^+ on p
CC1π^0 on n
CC1π^+ on n
CC coherent
CC1γ
Multi π (1.3 < W < 2.0)
CC1η^0 on n
CC1Λ1K$^+$
DIS (W > 2.0)
Undefined

How to estimate systematic uncertainties?

- Full systematic covariance

$$\Sigma^{\text{syst}} = \Sigma^{\text{flux}} + \Sigma^{\text{xsec}} + \Sigma^{\text{det}} + \cdots$$

	Multisim	Unisim
# of parameter variation at a time	Many	One
Parameter(s) variation	Random	Exactly 1σ
# of MC run	One	Many (one per parameter)
Technical treatment	Event reweighting	Bootstrapping

Flux and cross section systematics: multisim

- Standard reweighting approach, each event has different weights from the randomization of the underlying model parameters.

Tuning parameter name	Parameter type
π^+ hadron production	FLUX
π^- hadron production	FLUX
K^+ hadron production	FLUX
K^- hadron production	FLUX
K_L^0 hadron production	FLUX
horn current distribution	FLUX
horn current calibration	FLUX
nucleon total scattering Xs	FLUX
nucleon inelastic scattering Xs	FLUX
nucleon quasi-elastic scattering Xs	FLUX
pion total scattering Xs	FLUX
pion inelastic scattering Xs	FLUX
pion quasi-elastic scattering Xs	FLUX
MicroBooNE GENIE All	GENIE Xs (μB tune)
Strength of the CCQE RPA correction	GENIE Xs (μB tune)
Parameterization of the CCQE nucleon axial form factor	GENIE Xs
Parameterization of the CCQE nucleon vector form factors	GENIE Xs
Changes angular distribution of nucleon cluster in MEC	GENIE Xs (μB tune)
CCMEC Cross-section Shape	GENIE Xs (μB tune)
Angular distribution for RES $\Delta \to N + \pi$	GENIE Xs
Angular distribution for RES $\Delta \to N + \gamma$	GENIE Xs (μB tune)
Scaling factor for CC coherent π production	GENIE Xs (μB tune)
Scaling factor for NC coherent π production	GENIE Xs (μB tune)
Second-class vector current	Xs
Second-class axial current	Xs
π^- interactions	GEANT4
π^+ interactions	GEANT4
proton interactions	GEANT4

Neutrino flux

Neutrino-argon cross section

Final-state hadron-argon interaction

Geant4Reweight: JINST 16 (2021) 08, P08042

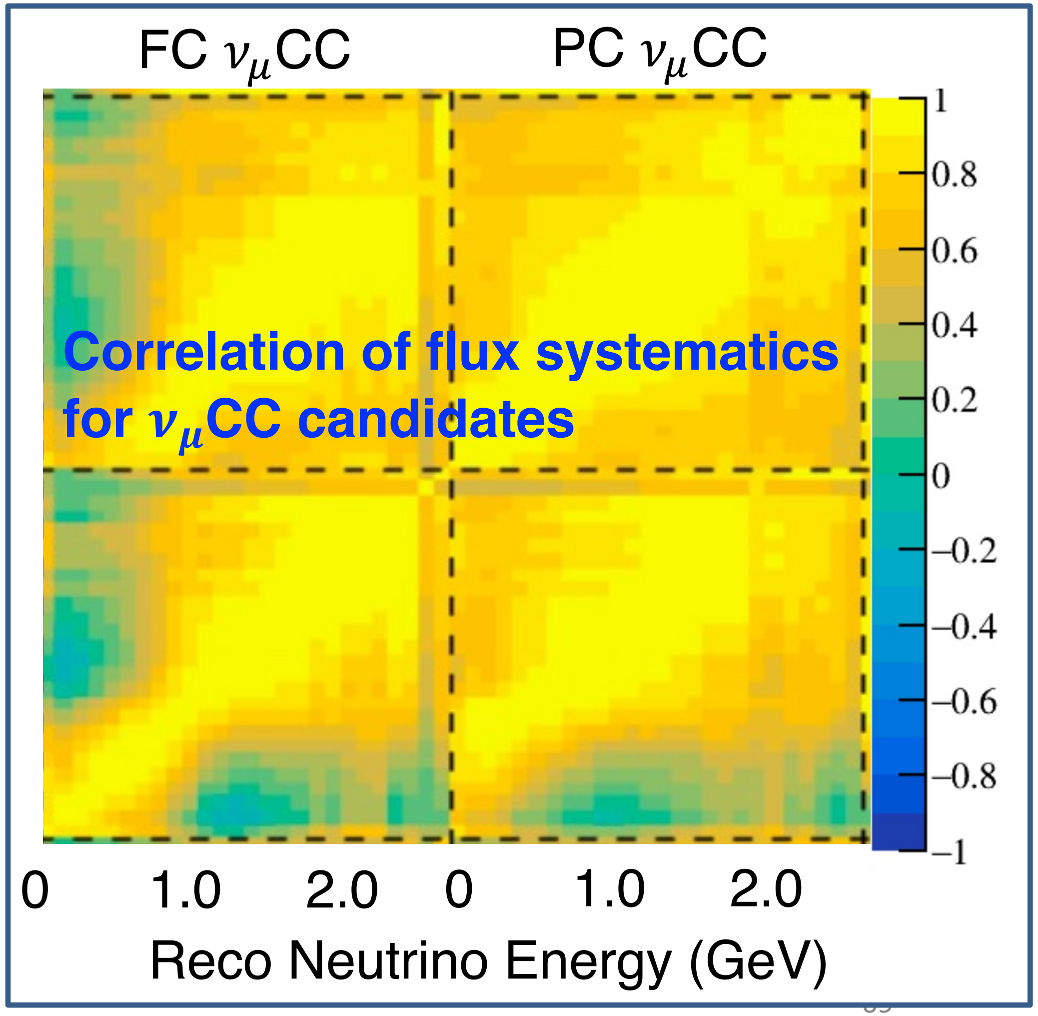

Detector systematics: unisim

- Four major categories
  1) Light yield and propagation
  2) Charge readout detector response
  3) Recombination model ($\frac{dE}{dx}$ to $\frac{dQ}{dx}$ conversion)
  4) Space charge effect (impacts on E-field)

- For each source of the systematic uncertainty, <u>the same set of MC simulation events are re-simulated</u> with a change to the detector modeling parameter of interest. In total, we have two samples
  1) One sample with nominal value of all parameters: <u>CV sample</u>
  2) One sample with changed value of interested par: <u>1σ sample</u>

Can not calculate the covariance matrix by the two samples in traditional way, which needs many samples with different pars values:

$$COV_{ij} = EXP\left((X_i - \bar{X})(X_j - \bar{X})\right)$$

Detector systematics: bootstrapping method

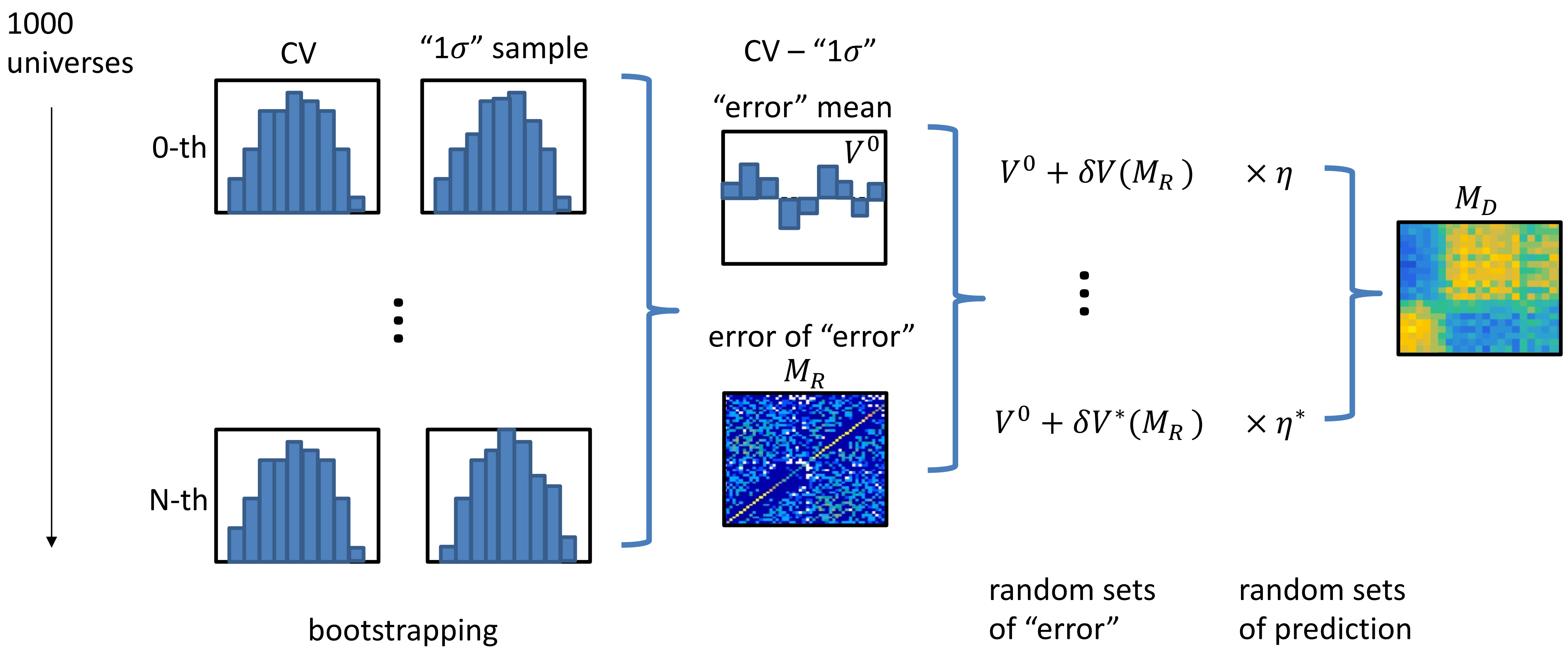

Detector systematics: bootstrapping method

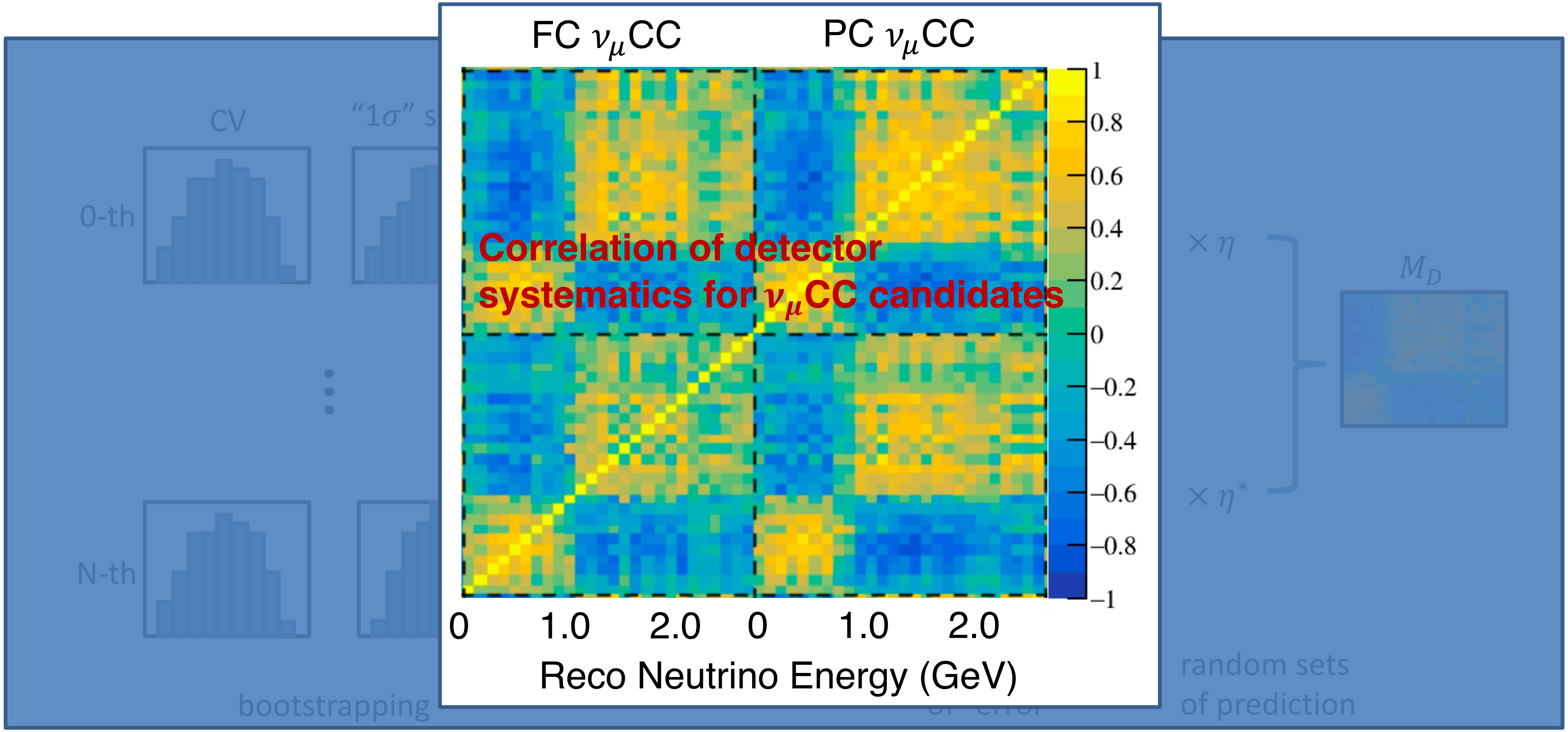

Inclusive ν_μCC measurements

- Modern accelerator-based neutrino experiments:

Experiment	Target	References
ArgoNeuT	Ar	Phys. Rev. Lett. 108 161802 Phys. Rev. D 89 112003
MicroBooNE	Ar	Phys. Rev. Lett. 123 131801
MINERvA	CH, C/CH, Fe/CH, Pb/CH	Phys. Rev. Lett. 112, 231801 Phys. Rev. D94, 112007 Phys. Rev. Lett. 116
MINOS	Fe	Phys. Rev. D81, 072002
NOMAD	C	Phys. Lett. B660, 19
SciBooNE	CH	Phys. Rev. D83, 12005
T2K	CH, H_2O, Fe	Phys. Rev. D87, 092003 Phys. Rev. D90, 052010 Phys. Rev. D93, 072002

$\langle E_\nu \rangle = 9.6$ GeV

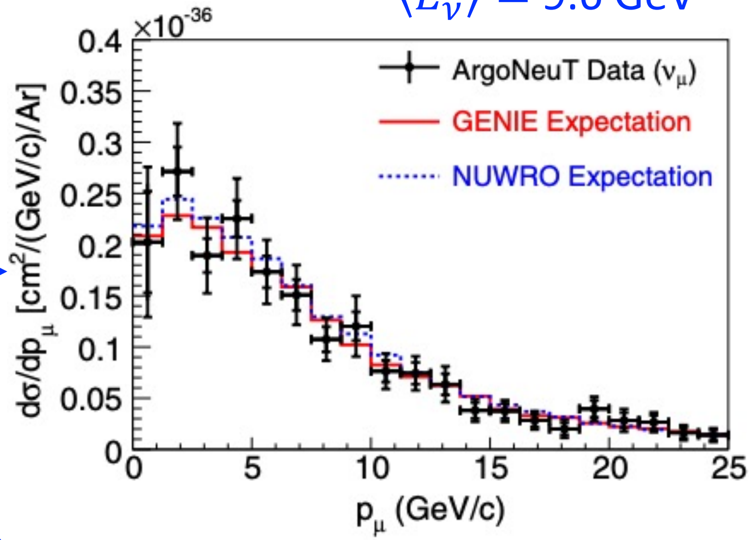

$\langle E_\nu \rangle = 0.8$ GeV

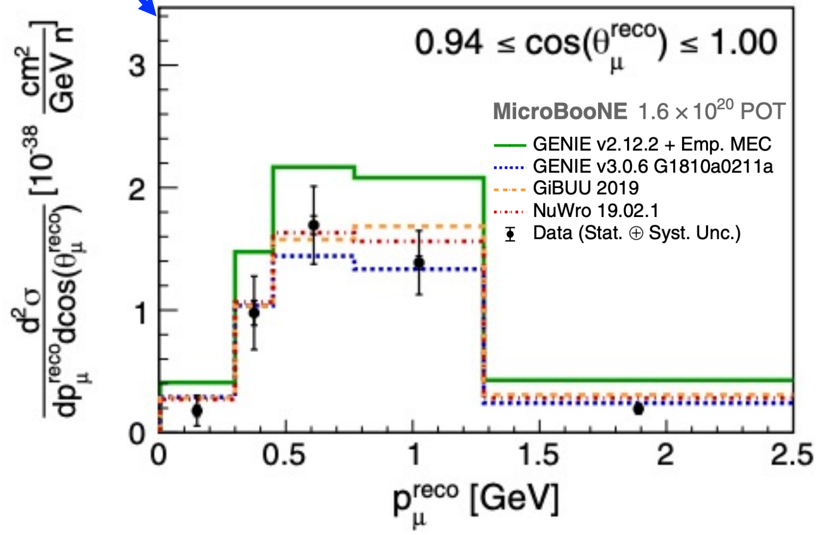

Inclusive ν_μCC measurements

Experiment	Target	References	Efficiency (%) $\nu_\mu(\bar{\nu}_\mu)$	Purity (%) $\nu_\mu(\bar{\nu}_\mu)$
ArgoNeuT	Ar	Phys. Rev. Lett. 108 161802 Phys. Rev. D 89 112003	49.5 42.0 (59.0)	95 95.2 (91.2)
MicroBooNE	Ar	Phys. Rev. Lett. 123 131801 Phys. Rev. Lett. **128**, 151801	57.2 68	50.4 92
MINERvA	CH, C/CH, Fe/CH, Pb/CH	Phys. Rev. Lett. 112, 231801 Phys. Rev. D94, 112007 Phys. Rev. Lett. 116	24 ~ 50	60 ~ 80
MINOS	Fe	Phys. Rev. D81, 072002		
NOMAD	C	Phys. Lett. B660, 19	40.9 ~ 73.3	99.3
SciBooNE	CH	Phys. Rev. D83, 12005	34.5	~90
T2K	CH, H_2O, Fe	Phys. Rev. D87, 092003 Phys. Rev. D90, 052010 Phys. Rev. D93, 072002	~50 41.2 ~50 @1GeV	~86 89.4 ~97

Improvement w.r.t previous work

Scaled to 5.3E19 POT

	Phys. Rev. Lett. 123, 131801 (2019)	This work
Expected # of true ν_μ CC	4541	10605
Efficiency*	57.2%	68%
Purity	50.4%	92%

*: definition of efficiency is slightly different

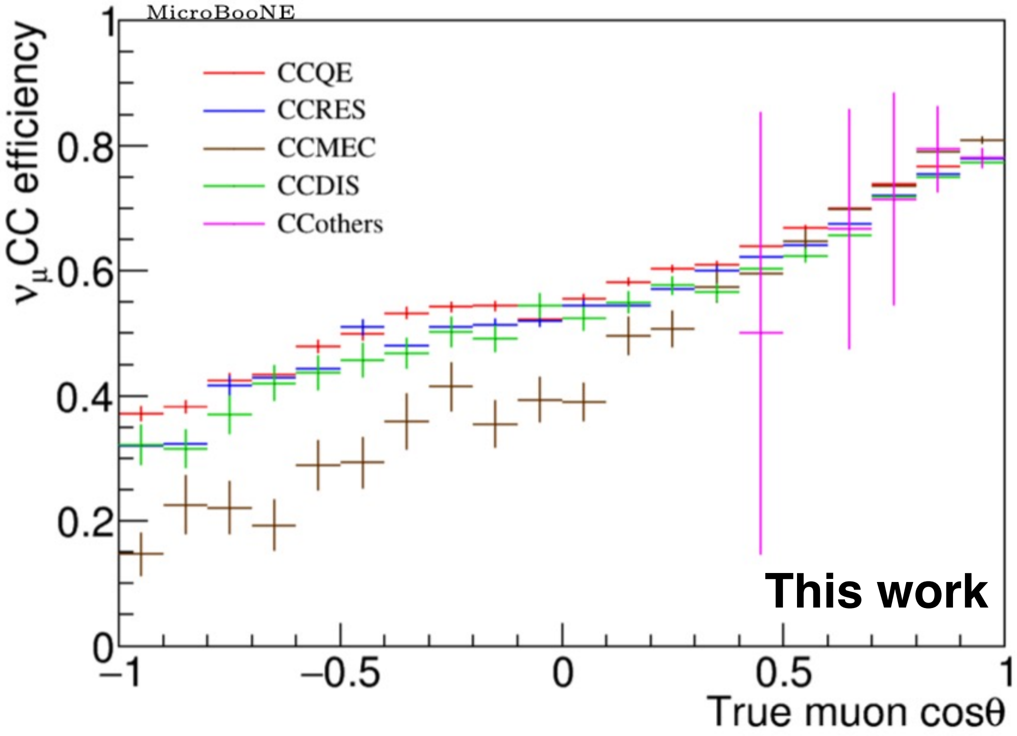

- muon polar angle: key variable for background rejection
  ⇒ confirms inclusive ν_μCC selection

Equation For Unfolding

$$M_i - B_i = \sum_j R_{ij} \cdot S_j$$

⟺

$$\chi^2 = (\boldsymbol{M} - \boldsymbol{B} - \boldsymbol{R} \cdot \boldsymbol{S})^T \cdot \boldsymbol{V}^{-1} \cdot (\boldsymbol{M} - \boldsymbol{B} - \boldsymbol{R} \cdot \boldsymbol{S})$$

$$R_{ij} = \tilde{\Delta}_{ij} \cdot \tilde{F}_j$$

$$\tilde{\Delta}_{ij} = \frac{POT \cdot T \cdot \int_j F\left(E_{\nu\,\mathrm{j}}\right) \cdot \sigma\left(E_{\nu\,\mathrm{j}}\right) \cdot D\left(E_{\nu\,\mathrm{j}}, E_{rec\,i}\right) \cdot \varepsilon\left(E_{\nu\,\mathrm{j}}, E_{rec\,i}\right) \cdot dE_{\nu\,\mathrm{j}}}{POT \cdot T \cdot \int_j \overline{F}\left(E_{\nu\,\mathrm{j}}\right) \cdot \sigma\left(E_{\nu\,\mathrm{j}}\right) \cdot dE_{\nu\,\mathrm{j}}}$$

➥ a MC ratio, less sensitive to Xs uncertainty

$$\tilde{F}_j = POT \cdot T \cdot \int_j \overline{F}\left(E_{\nu\,\mathrm{j}}\right) \cdot dE_{\nu\,\mathrm{j}}$$

$$S_j = \frac{\int_j \overline{F}\left(E_{\nu\,\mathrm{j}}\right) \cdot \sigma\left(E_{\nu\,\mathrm{j}}\right) \cdot dE_{\nu\,\mathrm{j}}}{\int_j \overline{F}\left(E_{\nu\,\mathrm{j}}\right) \cdot dE_{\nu\,\mathrm{j}}}$$

} Not subject to prior knowledge of the Xs uncertainty

- ***V*** is the covariance matrix encoding:
  - Data statistical uncertainty: **M**
  - Flux uncertainty: **B, R (F)**
  - Cross-section (Xs) uncertainty: **B, R (*σ*)**
  - GEANT4 hadron interaction uncertainty: **B, R (D, ε)**
  - Detector-model uncertainty: **B, R (D, ε)**
  - "Dirt" uncertainty: **B**
  - POT uncertainty (2%): **M**
  - MC statistical uncertainty: **M**
- The unfolded cross section S_j is defined based on the nominal flux $\overline{F}$
  - Easy for model comparisons
  - Simple for uncertainty calculation

PRD 102 (2020) 113012

	GENIE 3.0.6	NEUT 5.4.0.1	NuWro 19.2.1	GiBUU 2019.08
Nuclear Model	LFG	LFG	LFG	LFG
QE	Valencia	Nieves	Lwlyn-Smith	standard
MEC	Valencia	Nieves	Nieves	empirical
Resonant	KLN-BS	Berger-Sehgal	Adler-Rarita-Schwinger	MAID (Spin-dependent)
Coherent	Berger-Sehgal	Rein-Sehgal	Berger-Sehgal	
FSI	hA2018 cascade	cascade	cascade	BUU transport model

Benefit Of the S_j Definition

- Define the flux-averaged cross section using the nominal flux $\overline{F}$, thus can be easily compared with any model prediction based on the nominal flux

$$S_j = \frac{\int_j \overline{F}\left(E_{\nu\,\mathrm{j}}\right) \cdot \sigma\left(E_{\nu\,\mathrm{j}}\right) \cdot dE_{\nu\,\mathrm{j}}}{\int_j \overline{F}\left(E_{\nu\,\mathrm{j}}\right) \cdot dE_{\nu\,\mathrm{j}}}$$

- Simplify the uncertainty calculation
  - Switch $\overline{F}$ *to F* would bring up complicated systematic correlation
  - Proper treatment of flux shape uncertainty: PRD **102** 113012

$$M_i - B_i = \sum_j R_{ij} \cdot S_j \quad \Longleftrightarrow \quad \chi^2 = (\boldsymbol{M} - \boldsymbol{B} - \boldsymbol{R} \cdot \boldsymbol{S})^T \cdot \boldsymbol{V}^{-1} \cdot (\boldsymbol{M} - \boldsymbol{B} - \boldsymbol{R} \cdot \boldsymbol{S})$$

V is the covariance matrix encoding:

- Data statistical uncertainty: **M**
- Flux uncertainty: **B, R (F)**
- Cross-section (Xs) uncertainty: **B, R (*σ*)**
- GEANT4 hadron interaction uncertainty: **B, R (D, ε)**
- Detector-model uncertainty: **B, R (D, ε)**
- “Dirt” uncertainty: **B**
- POT uncertainty (2%): **M**
- MC statistical uncertainty: **M**